INFORMATION TO USERS

This material was produced from a microfilm copy of the original document. While the most advanced technological means to photograph and reproduce this document have been used, the quality is heavily dependent upon the quality of the original submitted.

The following explanation of techniques is provided to help you understand markings or patterns which may appear on this reproduction.

1. The sign or "target" for pages apparently lacking from the document photographed is "Missing Page(s)". If it was possible to obtain the missing page(s) or section, they are spliced into the film along with adjacent pages. This may have necessitated cutting thru an image and duplicating adjacent pages to insure you complete continuity.

2. When an image on the film is obliterated with a large round black mark, it is an indication that the photographer suspected that the copy may have moved during exposure and thus cause a blurred image. You will find a good image of the page in the adjacent frame.

3. When a map, drawing or chart, etc., was part of the material being photographed the photographer followed a definite method in "sectioning" the material. It is customary to begin photoing at the upper left hand corner of a large sheet and to continue photoing from left to right in equal sections with a small overlap. If necessary, sectioning is continued again – beginning below the first row and continuing on until complete.

4. The majority of users indicate that the textual content is of greatest value, however, a somewhat higher quality reproduction could be made from "photographs" if essential to the understanding of the dissertation. Silver prints of "photographs" may be ordered at additional charge by writing the Order Department, giving the catalog number, title, author and specific pages you wish reproduced.

5. PLEASE NOTE: Some pages may have indistinct print. Filmed as received.

Xerox University Microfilms
300 North Zeeb Road
Ann Arbor, Michigan 48106

Downloaded from SHAREOK. Persistent Handle URL: https://hdl.handle.net/11244/3913

75-15,261

LEU, Jin-chian, 1942-
MODELING OF THE PYROLYSIS AND IGNITION OF WOOD.

The University of Oklahoma, Ph.D., 1975
Engineering, chemical

Xerox University Microfilms, Ann Arbor, Michigan 48106

THIS DISSERTATION HAS BEEN MICROFILMED EXACTLY AS RECEIVED.

THE UNIVERSITY OF OKLAHOMA

GRADUATE COLLEGE

MODELING OF THE PYROLYSIS AND IGNITION OF WOOD

A DISSERTATION

SUBMITTED TO THE GRADUATE FACULTY

in partial fulfillment of the requirements for the

degree of

DOCTOR OF PHILOSOPHY

BY

JIN CHIAN LEU

Norman, Oklahoma

1975

MODELING OF THE PYROLYSIS AND IGNITION OF WOOD

APPROVED BY

C. M. Sliepcevich

J. Reddy Heller

F. M. Townsend

K. E. Starling

R. C. Gerner

DISSERTATION COMMITTEE

ABSTRACT

The weight and energy changes associated with thermal decomposition of spruce and redwood were studied. Quantitative data were obtained describing the chemical kinetics of pyrolysis and the energy of pyrolysis.

The overall chemical kinetics of pyrolyzing wood were investigated in a nitrogen atmosphere at heating rates of 10°, 20°, 40°, 80° and 160°C/min. Arrhenius parameters were obtained from these data.

The total energy changes were measured in a nitrogen atmosphere at 20°, 40° and 80°C/min using differential scanning calorimetry. Lumped sensible and pyrolysis heat effects were obtained by this method.

It was demonstrated that both the kinetic parameters and total energy changes are reasonably independent of heating rate.

Ignition criteria were proposed, and ignition times were predicted by incorporating extrapolated kinetic and energy data into a mathematical model based on heat transport phenomena. The predicted results obtained in the present study were compared with the available experimental ignition data for spruce and redwood.

ACKNOWLEDGMENTS

I would like to express my gratitude and appreciation to a number of persons who have contributed to this research effort.

Dr. C. M. Sliepcevich, George Lynn Cross Research Professor of Engineering, for his direction and support.

Dr. J. R. Welker, Associate Director of the Flame Dynamics Laboratory, for his invaluable guidance and untiring assistance throughout the program.

Dr. L. E. Brown and Dr. W. M. Woodard for their help in many areas.

Dr. K. E. Starling, Dr. R. C. Jerner and Dr. F. M. Townsend for their service on my graduate committee.

Ms. Bobbie Everidge for her assistance in preparation of this manuscript.

I am grateful to the National Science Foundation and Naval Weapons Center for providing financial support.

Finally, I would also like to acknowledge my parents. wife and friends for their constant encouragement and support.

Jin-chian Leu

TABLE OF CONTENTS

		Page
LIST OF TABLES		vi
LIST OF ILLUSTRATIONS		vii
Chapter		
I.	INTRODUCTION	1
II.	REVIEW OF PREVIOUS WORK	3
	Ignition Process	3
	Ignition Criteria	5
	Surface Temperature Studies	10
	Reaction Kinetics	12
	Absorptivity	17
	Effect of Moisture Content	19
	Effect of Pilot Position	19
	Ignition Tests	20
	Ignition Models	23
III.	EXPERIMENTAL STUDIES AND RESULTS	31
	Measurements of Weight Loss and Rate of Weight Loss of Wood as a Function of Temperature Using Thermal Gravimetric Analysis	32
	Analysis of Data	50
	Measurement of "Energy Capacity" Versus Temperature Relationship of Wood Using Differential Scanning Calorimetry	59
IV.	MATHEMATICAL MODEL	75
V.	DISCUSSION OF RESULTS	95
VI.	CONCLUSIONS	104
BIBLIOGRAPHY		105

LIST OF TABLES

Table		Page
II-1.	Different Methods Used for Radiative Heating of Material	21
III-1.	Magnetic Standards for TGS-1B Furnace Calibration	35
III-2.	Kinetic Parameters for Pyrolysis of Spruce and Redwood	56
V-1.	T_{peak} versus Heating Rate for Spruce and Redwood	104

LIST OF ILLUSTRATIONS

Figure		Page
II- 1.	Effect of Rate of Heating on Kinetics of Weight Loss of Dry Pine Wood in Nitrogen Atmosphere	16
III- 1.	Perkin-Elmer TGS-1 Thermobalance and UU-1 Temperature Controller	33
III- 2.	Schematic of Perkin-Elmer TGS-1 Furnace and Weight Assembly	34
III- 3.	TGS-1 Temperature Calibration Curve, Heating Rate 80°C/min	36
III- 4.	TG and DTG Curves for Spruce at a Nominal Heating Rate of 10°C/min	38
III- 5.	TG and DTG Curves for Spruce at a Nominal Heating Rate of 20°C/min	39
III- 6.	TG and DTG Curves for Spruce at a Nominal Heating Rate of 40°C/min	40
III- 7.	TG and DTG Curves for Spruce at a Nominal Heating Rate of 80°C/min	41
III- 8.	TG and DTG Curves for Spruce at a Nominal Heating Rate of 160°C/min	42
III- 9.	Summary of TG Curves for Spruce in a Nitrogen Atmosphere	43
III-10.	TG and DTG Curves for Redwood at a Nominal Heating Rate of 10°C/min	44
III-11.	TG and DTG Curves for Redwood at a Nominal Heating Rate of 20°C/min	45
III-12.	TG and DTG Curves for Redwood at a Nominal Heating Rate of 40°C/min	46

LIST OF ILLUSTRATIONS--Continued

Figure		Page
III-13.	TG and DTG Curves for Redwood at a Nominal Heating Rate of 80°C/min	47
III-14.	TG and DTG Curves for Redwood at a Nominal Heating Rate of 160°C/min	48
III-15.	Summary of TG Curve for Redwood in a Nitrogen Atmosphere	49
III-16.	Plot to Obtain Activation Energy for Spruce at Various Values of Conversion	52
III-17.	Plot to Obtain Activation Energy for Redwood at Various Values of Conversion	53
III-18.	Variation of Activation Energy with Conversion for the Weight Loss of Spruce	54
III-19.	Variation of Activation Energy with Conversion for the Weight Loss of Redwood	55
III-20.	Determination of the Order of Reaction and Frequency Factor for Spruce	57
III-21.	Determination of the Order of Reaction and Frequency Factor for Redwood	58
III-22.	Perkin-Elmer DSC-1B	60
III-23.	Relation Between Programmed and Actual Temperatures in Perkin-Elmer DSC-1B Instrument	66
III-24.	Energy Capacity of Redwood as a Function of Temperature at a Nominal Heating Rate of 20°C/min	68
III-25.	Energy Capacity of Redwood as a Function of Temperature at a Nominal Heating Rate of 40°C/min	69

LIST OF ILLUSTRATIONS--Continued

Figure		Page
III-26.	Energy Capacity of Redwood as a Function of Temperature at a Nominal Heating Rate of 80°C/min	70
III-27.	Energy Capacity of Spruce as a Function of Temperature at a Nominal Heating Rate of 20°C/min	71
III-28.	Energy Capacity of Spruce as a Function of Temperature at a Nominal Heating Rate of 40°C/min	72
III-29.	Energy Capacity of Spruce as a Function of Temperature at a Nominal Heating Rate of 80°C/min	73
IV- 1.	A Mesh Region (i,j) and Its Adjacent Mesh Points	80
IV- 2.	Thermal Conductivity of White Pine as a Function of Temperature	88
IV- 3.	Estimate of Effect of Heating Rate on Heat of Pyrolysis for Spruce	90
IV- 4.	Estimate of Effect of Heating Rate on Heat of Pyrolysis for Redwood	91
IV- 5.	Relation Between T_{peak} and Heating Rate for Spruce and Redwood	94
V- 1.	Surface Temperature History of Spruce at H_i = 1.08 cal/cm^2-sec	98
V- 2.	Surface Temperature History of Redwood at H_i = 0.88 cal/cm^2-sec	99
V- 3.	Ignition Time of Spruce versus Incident Irradiance	102
V- 4.	Ignition Time of Redwood versus Incident Irradiance	103

CHAPTER I

INTRODUCTION

The study of ignition phenomena is a fundamental aspect of fire research. The objectives of the ignition studies are to develop a reliable procedure for predicting whether ignition will occur under a given set of conditions and whether burning will be sustained once ignition has occurred. A fundamental mathematical model describing the transient transport and chemical processes that precede ignition and combustion would be of value in evaluating fire retardants, fire hazards, and fire prevention systems. Different investigators have used different techniques and mathematical approaches in order to arrive at ignition criteria to explain their data. Due to the lack of data on the chemical kinetics of the degradation process, the usefulness of the proposed models is limited.

Since 1966, the Flame Dynamics Laboratory at the University of Oklahoma has been concerned with the investigation of fundamental thermal, physical and chemical properties of pyrolyzing wood. The data obtained have led to the development of a successful model describing the transient temperature

and density profiles of pyrolyzing wood (7, 18). This work is now to be extended to include the prediction of ignition times for pyrolyzing wood.

The objectives of this study are to:

1. Measure experimentally the energy changes associated with wood pyrolysis and the effect of heating rate on these energy changes.
2. Determine the actual kinetics of the thermal decomposition process, the weight loss and rates of weight loss, and the effect of heating rate on these processes.
3. Incorporate these findings and a set of proposed criteria for ignition into a mathematical model to predict the piloted ignition times for wood.

A further objective is to test the validity of the mathematical model by comparing computed and experimental piloted ignition times for wood.

CHAPTER II

REVIEW OF PREVIOUS WORK

The ignition of cellulosic materials by external heating has been a subject of extensive studies for many years. The main objectives of these ignition studies were to develop a reliable method for predicting whether ignition will occur under given conditions and whether burning will continue once the ignition has taken place. In this chapter the ignition process, the different criteria proposed for ignition, the various mathematical models for the ignition process and the effects of the dominant parameters on ignition will be reviewed.

Ignition Process

It was Brown (6) who first concluded that if a combustible material is heated gradually in the presence of sufficient air, a very slow reaction between the material and oxygen occurs. The reaction becomes faster as the temperature increases, and the heat produced further increases the rate of reaction. At the same time there is heat loss from the material through conduction, radiation, and convection. At a certain temperature the rate of reaction is sufficiently

rapid that the resulting rate of heat production exceeds that of heat loss; consequently, the temperature of the material rises faster than it would because of the external heating alone. Thus, the reaction accelerates itself and very rapid heating follows. When this process continues, visible evidence of ignition, such as glow and flame, occurs. Brown lists the following requirements for ignition to take place:

1. A combustible material must be present.
2. A source of oxygen, such as air, must be available within certain concentrations relative to the combustible.
3. Heat must be evolved as a result of the reactions producing combustion.
4. The reaction must proceed more or less rapidly over a certain temperature range.
5. The reaction must be accelerated by a rise in temperature.
6. A supply of energy, sufficient to the point where the reaction becomes autogenous, is necessary.

It is generally accepted that the decomposition into different products depends on whether pyrolysis is slow or rapid. For very low heating the specimen may be completely charred without flaming, whereas at a high rate of heating, glowing or flaming occurs. Wesson (45) lists the following two separate and distinct processes for ignition of flammable solids:

1. The thermal decomposition of a solid phase into volatile products and a residue.

2. Gas phase oxidation reactions of volatiles near the surface.

Alvares, et al. (3) classified the factors influencing the ignition process of materials into the external and internal. Thermal properties, pyrolysis characteristics, the absorptivity of the irradiated surface, diathermancy, size of the irradiated area and moisture content of the solid are considered as internal factors which are mainly the properties of the solid. Factors such as irradiance, time of exposure, area of uniform energy flux, the type of ignition, draft and specimen preheating are recognized as external factors.

A detailed mathematical description of the ignition process of a solid requires that the internal and external factors be fully specified while the wood sample undergoes the entire range of state change. In the remainder of this chapter, previous studies of these thermal and chemical properties will be considered, and various mathematical models reported in the literature will be discussed.

Ignition Criteria

Hallman (16) described the ignition phenomena as a function of many variables:

$$Ig = F(T_z, \bar{T}, T_s, T_o, T_g, R, H_f, H_z, E_s, C_p, K, t, L, h, \rho, M, A, \varepsilon_\lambda, \nu_\lambda, \alpha_\lambda, H_i, \ldots) \quad \text{(II-1)}$$

where Ig = ignition criteria

T_g = gas film temperature

$\bar{T}$ = source temperature

T_z = pyrolysis temperature

T_s = surface temperature of the material

T_o = ambient temperature

R = universal gas constant

E_s = activation energy of the material

C_p = specific heat

K = thermal conductivity

t = time

L = thickness of the material

h = convective heat transfer coefficient

M = molecular weight

A = area of the material under test

ε_λ = emittance of surface for each wavelength involved

ν_λ = attenuation factor for each wavelength involved

α_λ = surface absorptance for each wavelength involved

λ = wavelength

ρ = density

H_i = incident irradiance

H_f = heat of fusion

H_z = heat of pyrolysis

The complexities of ignition phenomena can be realized from the above equation.

In his review of the literature, Martin (25) gave the necessary and sufficient conditions for the ignition of solid

fuels subjected to thermal radiation. These conditions were stated as:

1. The gaseous fuel evolving from the solid must have a high degree of reactivity either because of its chemical composition or its kinetic energy.
2. The relative concentration of fuel to oxygen must lie between two well defined limits.

Each of these conditions commonly exists at different levels above a decomposing solid, but until they occur simultaneously at the same location, ignition will not occur.

Bamford, et al. (4) simplified their one-dimensional slab model to the case of an opaque solid and neglected the energy transfer due to mass transfer through the sample. The heating of the wood slab was accomplished by direct contact with gas flames on both sides. One of the boundary conditions they used was the combined effect of radiative and convective heat transfer between the surface and the contacting flame. They ignored the details of the decomposition reactions of wood and used a single reaction with assumed constant activation energy and frequency factor. From interpretation of their calculated results for weight loss, they postulated a criterion of a critical rate of evolution of volatiles for ignition. Accordingly, they concluded that sustained ignition is possible when the weight loss at ignition is equal to or greater than 2.5×10^{-4} gm/cm^2-sec. However, the required rate of evolution of gases prior to ignition is not known for piloted ignition.

Akita (1) in his study on the mechanism of ignition of wood gave the ignition criterion for spontaneous and piloted ignition. For woods, Akita reported 500°C as the approximate surface ignition temperature.

Simms (30, 31, 32) has correlated ignition data for wet and dry woods. He also postulated constant surface temperature as the criterion for ignition. For spontaneous ignition of wood and other cellulosic materials he reported a correlating temperature of 525°C. In the case of piloted ignition of wood he reported that the correlating temperature depends upon the position of the pilot flame. For piloted ignition of wood he gave correlating temperatures between 300°C and 410°C depending on the position of the pilot flame. Alvares (2) measured the surface temperature of thermally irradiated α-cellulose. He gave a surface ignition temperature of 600°C for spontaneous ignition of α-cellulose.

Deverall and Lai (11) have predicted a criterion for ignition of cellulosic materials. The mathematical form is

$$H_i\Big|_{x=0} = 2\Delta H_f \dot{m}_f\Big|_{x=0} - K \frac{\partial T}{\partial x}\Big|_{x=0} \qquad \text{(II-2)}$$

where H_i = incident irradiance

ΔH_f = heat required for pyrolysis

$\dot{m}_f$ = fuel flux through the exposed surface

K = thermal conductivity of the fuel

T = temperature of the fuel

The above equation states that the threshold for ignition occurs when the irradiance is twice the heat flux required for pyrolysis less the heat conducted into the solid, where all are evaluated at the solid surface. The derived threshold criterion does not depend upon detailed information on gas phase kinetics. It provides a necessary condition but not a sufficient condition for ignition, and applies to sustained ignition.

Kanury (20) in his review lists the following conditions for ignition to occur:

1. Attainment of a fixed critical temperature T* by the exposed surface is an adequate criterion to predict transient flame ignition for radiative as well as convective heating. If ignition is spontaneous, the concept of critical exposed surface temperature is expected to be associated with some sort of a critical thermal phenomenon. If the ignition is piloted, attainment of the critical temperature by the exposed surface is expected to be a passive indication of attainment of a critical pyrolysis rate.
2. If the enthalpy content of the solid at the instant of termination of the external heating exceeds a critical lower limit enthalpy, persistent flaming is assumed. The critical lower limit enthalpy is roughly $2L\rho c\ (T_p - T_o)$ where ρc is the volumetric heat capacity of the solid, $2L$ is the thickness of the slab, T_p is a temperature

related to the pyrolysis kinetics (may be taken as approximately 320°C for cellulosic solids) and T_o is the initial temperature.

3. As the slab thickness becomes small, the thin slab limit is approached. In this limit, once ignition occurs, it is persistent. Therefore, for thin bodies, fulfillment of the T* criterion automatically fulfills the critical enthalpy content criterion.

Surface Temperature Studies

The surface temperature and temperature profile histories of a cellulosic material subjected to ignition have been of interest to previous investigators because of their importance in determining the course of pyrolysis. Wesson (45) discusses the different techniques that have been used to determine the irradiated surface temperatures.

1. The most common procedure is to place thermocouples in contact with the surface of the sample. Gardon used this technique in his measurements. He estimated his measurement would not be in error by more than 20°C. The shortcomings of this method are:
   a. An unknown portion of the recorded signal is due to the direct absorption of radiant energy by the thermocouple.
   b. The thermocouple bead may lose its intimate contact with the surface when char occurs.

2. A second method is to imbed thermocouples at various depths in the sample and extrapolate the interior measurements at the time of ignition to obtain the surface temperature. Due to the nature of contact, depth of energy penetration for extremely short exposure periods, the distance from the surface and the extrapolating technique, the results of these measurements are questionable.
3. The third method is by means of radiation pyrometers which allow remote measurements of the surface temperature. This method is classified into two groups.
   a. Optical pyrometers.
   b. Radiation pyrometers.

Alvares (2) used a radiation device to measure the surface temperature of α-cellulose at ignition. He concluded that the surface temperature at which spontaneous ignition occurred was between 600° and 650°C. Smith and Schilberg (37) used a radiometer sensitive to radiation in a narrow band. The wavelengths used for temperature measurements were longer than the wavelengths of the radiation incident on the sample surface in order to preclude effects of reflection of incident radiation to the temperature detector. They found piloted ignition temperatures from 340°C to 540°C and spontaneous ignition temperatures from 460°C to 540°C for pine blocks. Koohyar, et al. (21) used a radiometer sensitive to a wide wavelength band in their studies. The surface temperature varied widely for all the tests, and no discernible

trends were clearly established. The physical limitations imposed by using open flames as the radiation energy source contributed to the variation. Simms (30) did not measure the ignition temperature; he calculated it based on a simple heat transfer model. He estimated the piloted ignition temperature for wood samples to be about 360°C and the spontaneous ignition temperature to be about 525°C.

There is no doubt that the spontaneous ignition temperature is higher than the piloted ignition temperature. In the case of spontaneous ignition, either the sample surface must be heated to the point where it ignites the gases or the gases themselves must be heated to the ignition point. For piloted ignition to occur, the sample surface must rise only high enough to pyrolyze the sample, provided that pyrolysis is rapid enough to result in enough combustible pyrolysis gases to form a combustible mixture with the surrounding air at the pilot location.

Reaction Kinetics

Many investigators have studied the pyrolysis of wood and other materials. The composition and the yield of gases, vapors and char, and the relative proportion of flammable and non-flammable gases that are produced will vary according to the conditions of temperature, pressure, time, etc., under which pyrolysis of an organic material occurs. It is generally accepted that decomposition into different products depends

on whether pyrolysis is slow or rapid. Slow heating of cellulosic material produces much charcoal, little tar and less flammable gases. On the other hand, rapid heating produces little charcoal, but much tar and highly flammable gases. However, identification of the elementary chemical reactions which occur when wood thermally decomposes is virtually impossible due to the heterogeneous composition of wood and the complex decomposition scheme which the components in wood follow. Fortunately, the pyrolysis model requires only an expression which accurately describes the rate of weight loss and its dependence on temperature, composition and heating history.

Two types of experiments have been used in determining the kinetic parameters of wood pyrolysis, isothermal and temperature-programmed. Welker (44) has reviewed the work done by different investigators on the thermal decomposition of α-cellulose.

Using an increasing temperature technique is more realistic in measuring pyrolysis parameters, and it has several advantages over the isothermal method, such as

1. Kinetic data (weight versus time) over a broad temperature range can be obtained in only a few minutes.
2. The problem of decomposition before reaching the desired test temperature is not encountered in the dynamic method since the test may be initiated well below the incipient decomposition temperature.

3. Different heating rates may be studied.

Two types of experiments have been used to determine the kinetics of wood pyrolysis in a dynamic temperature environment.

Roberts and Clough (29) used the dynamic temperature technique studying the pyrolysis of beech cylinders. Small samples, on the order of 10 to 100 mg, were subjected to heating at a linear rate of temperature rise. The data were fitted to the first order kinetic expression given as:

$$-\frac{dW}{dt} = (W - W') \exp(-E/RT) \qquad \text{(II-3)}$$

where W = weight of specimen at time t (gm)

W' = final weight of specimen (gm)

Freeman and Carrol (13) discuss a technique for obtaining kinetic data from such measurements. Tang (38) used the procedure of Freeman and Carrol to obtain kinetic parameters of wood pyrolysis from thermogravimetric data. Heinrich and Kaesche-Krischer (19) used dynamic thermogravimetry to study weight loss kinetics of beech sawdust subjected to linearly increasing heating rates of 1°, 2°, 3°, 4° and 12°C/min in a vacuum. They found that weight loss occurred at lower temperatures for heating rates of 1°C/min than for 12°C/min. Such behavior may be due to thermal lag if the sample temperature does not follow the heater temperature at higher heating rates as discussed by Goldfarb, et al. (15). However, such

lags should not be appreciable at these lower heating rates. Brown (7) studied the pyrolysis of white pine and oak sawdust at heating rates of 20°, 40°, 80° and 160°C/min in an inert atmosphere. He found a similar shift in weight loss to higher temperatures with increasing heating rate. Figure II-1 shows typical data for multiple heating rates. Brown extracted kinetic parameters from his data and concluded that the overall chemistry of pyrolysis is independent of heating rate below 160°C/min.

The measurements of the heat of decomposition fall into two broad classes. In the first, the solution of a transient heat balance is used to estimate the heat effects. Values of the heat of decomposition reported by various investigators using this technique range from about 30 cal/gm to 300 cal/gm, all exothermic. The second technique used to measure heat effects is based on differential thermal analysis (DTA). Both Tang (38) and Broido (5) used the same DTA equipment to measure the heat effects for α-cellulose, yet obtained opposing results for heats of pyrolysis. Part of the problem is due to the sample sizes, which did not meet the assumption that there was no temperature gradient inside the sample, particularly if the heating rates are large. However, as Havens has pointed out, if samples of a few milligrams in size are used and if energy inputs rather than temperature differences are measured, the energy effects of pyrolysis can be measured. The resulting data can be used not only to

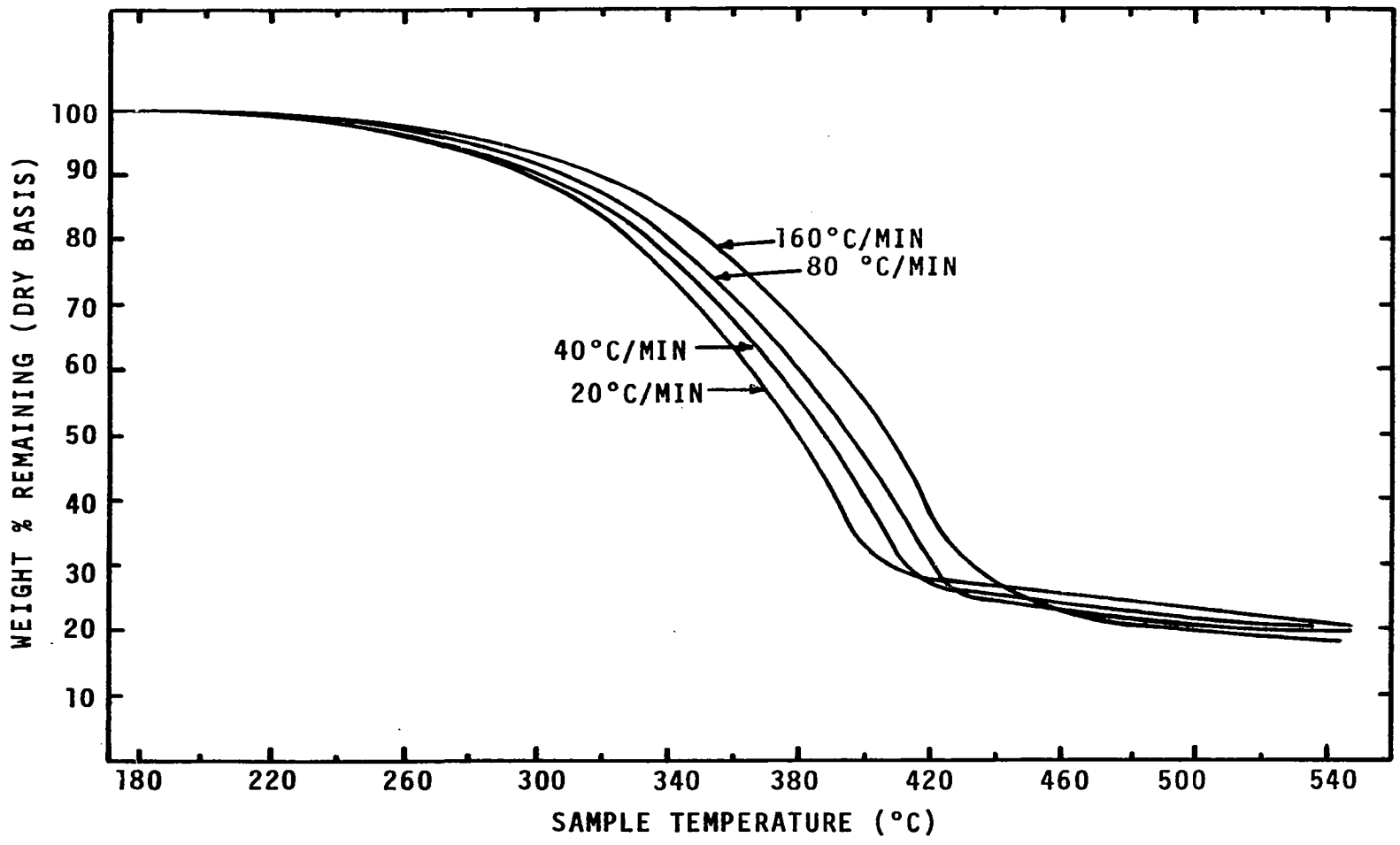

Figure II-1. Effect of Rate of Heating on Kinetics of Weight Loss of Dry Pine Wood in Nitrogen Atmosphere, Havens (18).

predict the temperature profile in a sample, but also to predict the weight loss rate. Brown (7) has further demonstrated this technique. He reported the heat of pyrolysis to be 43.2 cal/gm for white pine and 27 cal/gm for oak, both endothermic. The experimental DSC procedure developed by Havens (18) was also used in this study.

Absorptivity

Since the spectral distribution of energy is different for different radiation sources, the effects of surface absorptance have been considered in several papers. Smith (36) discusses absorptance effects and presents a technique for determining absorptance by means of transient surface temperature measurements. Welker, et al. (43) compared their white cotton ignition data using flame radiation with the data of Lee and Alvares (24), who used a tungsten filament lamp source operating at 2500°K. Welker, et al., observed that the flame source caused ignition in about 1/3 the time that was required for the tungsten source. They concluded that the ignition behavior of flammable materials is also dependent upon the spectral distribution of the incident radiation and the absorptance characteristics of the material being irradiated. Welker, et al., related the ignition behavior as a function of the net energy retained by defining

$$H_R = H_a - \text{energy losses}$$

where H_a = absorbed energy

H_R = retained energy

The energy losses term includes integrated transmitted energy losses over the applicable range of wavelengths and convective and reradiated energy losses from both front and rear surfaces of the target. For the emissive power of the flame source Welker used the data of Ryan, Penzias and Tourin (28). An average total absorptance for a given sample-radiation source configuration was defined as

$$\alpha_{av} = \frac{\int_{\lambda_1}^{\lambda_2} \alpha_\lambda e_\lambda \, d\lambda}{\int_{\lambda_1}^{\lambda_2} e_\lambda \, d\lambda} \qquad \text{(II-5)}$$

where α_{av} = average total absorptance for the sample-radiation source configuration under consideration

α_λ = absorptance of sample at wavelength

e_λ = emissive power of radiation source at wavelength λ

The integration limits λ_1 and λ_2 are those wavelengths that include all of the energy in the spectrum for the given radiation source. The approximation for Equation II-5 is

$$\alpha_{av} = \frac{\Sigma\ \alpha_\lambda e_\lambda \Delta\lambda}{\Sigma\ e_\lambda\ \Delta\lambda} \qquad \text{(II-6)}$$

Equation II-6 was used by Welker to obtain the values of α_{av} The absorbed irradiance was calculated as

$$H_a = \alpha_{av}\ H_i \qquad \text{(II-7)}$$

where H_i is the incident irradiance. Welker plotted the ignition time versus absorbed irradiance to prove the agreement among the different sets of data.

Effect of Moisture Content

As a result of a series of experiments to determine the effect of moisture content on ignition of wood, Fons (14) concluded that an increase in moisture content increased the time of ignition. Fons argued that the increase could be attributed to the presence of water vapor at the sample surface. The water vapor extended the time required for the concentration of flammable gases to build up for combustion to take place. Thomas, Simms and Law (39) concluded that moisture contents below 20 percent do not materially effect ignition times. However, Duvvuri (12) indicated a linear relationship between the piloted ignition time and percent moisture content from zero to 25 percent.

Effect of Pilot Position

Simms (33) studied the effect of pilot position on the piloted ignition of woods. He noted an increase in

piloted ignition time as the pilot was moved outward from the sample in a perpendicular direction. Piloted ignition ceased altogether if the pilot was just beyond 2 cm from the surface, which was about the visible thickness of the volatile stream. The flow of volatiles past the sample surface was laminar. Simms concluded that because of the laminar conditions, gradients in the concentration of the combustible volatiles would exist in the flow field which he thought would account for the variation in ignition time with pilot flame position. Muir (27) found that piloted ignition times increased significantly as the pilot flame was moved away from the sample in either the vertical or horizontal plane. Wesson (45) overcame the problem by having a heated coil as a pilot light, and the coil was large enough to prevent its location from being an important parameter in ignition time measurements.

Ignition Tests

Welker (44), in his literature review on the pyrolysis and ignition of cellulosic materials, has given an account of different techniques developed by different people investigating the ignition phenomena. A summary of the different methods used by different people for ignition tests is given in Table II-1.

TABLE II-1

DIFFERENT METHODS USED FOR RADIATIVE HEATING OF MATERIAL

Investigator	Radiant Source	Material Tested	Other Details
Lawson and Simms (23)	A surface combustion heater, burning a coal gas/air mixture	wood	Specimen, 5 cm square Radiating Temp, 1000°K Range, 0 to 1.5 cal/cm^2-sec
Varma and Steward (41)	A gas fired panel	wood shavings	Specimen, circular with 2 cm diameter
Buschmann (8)	A vertical gas fired refractory panel	wood	Specimen, 6 cm square Radiating Temp, 670°C
Alvares (2) and Martin (26)	Carbon arc image furnace	pure α-cellulose	Range, up to 100 cal/cm^2-sec
Simms (34)	Carbon arc-ellipsoidal mirror	wood, cotton, filter paper, etc.	Area covered, 3 cm^2 Radiating Temp, 4000°K Range, 1.5 to 12 cal/cm^2-sec
Simms (34)	Tungsten filament lamp	wood, cotton, filter paper, etc.	Area covered, 0.5 cm^2 Radiating Temp, 3000°K Range, 1 to 5 cal/cm^2-sec
Smith (35)	15 quartz tube lamps	wood, cardboard, marine uniform, etc.	Radiating Temp, 2500°K

TABLE II-1--Continued.

Investigator	Radiant Source	Material Tested	Other Details
Koohyar (22)	Vertical liquid hydrocarbon diffusion flames	wood	Range, 0 to 0.85 cal/cm^2-sec Specimen area, 100 cm^2
Wesson (45)	Vertical liquid hydrocarbon diffusion flames	wood	Range, 0 to 3.5 cal/cm^2-sec Specimen area, 100 cm^2
Wesson (45)	Tungsten filament lamps	wood	Range, 0 to 3.5 cal/cm^2-sec Specimen area, 100 cm^2

Ignition Models

Several mathematical models have been proposed for the process leading up to ignition. Because of the complexity of ignition phenomena, all of the treatments have been confined to one dimensional models. Each of the models has been made with several different simplifying assumptions. Koohyar (22) listed the assumptions made. Havens (18) proposed a mathematical model which considered the heat transfer aspects of the ignition problem as well as the kinetics of decomposition. Brown (7) has further demonstrated the applicability of the model proposed by Havens to predict transient temperature profiles in pyrolyzing wood using experimental data for wood char thermal conductivity. In the following discussion of ignition models, the basis suggested by Havens will be presented first and followed by several other techniques.

The model proposed by Havens is based on the following assumptions for cellulosic material in an ignition test:

1. Only one dimensional heat transfer is considered.
2. The sample surface is opaque to the incident radiation.
3. Heat transfer due to convection from gases moving through the porous interior of the material is neglected.
4. The material is locally isotropic, and the thermal conductivity is a function of temperature only and can be measured.
5. Average constant values can be used for optical properties of the sample.

6. Diathermancy can be ignored.

7. The dimensions of the solid remain constant.

The energy balance equation can be written for the material subjected to thermal radiation.

$$\frac{\partial}{\partial x}\left(k\,\frac{\partial T}{\partial x}\right) = \frac{\partial E_v}{\partial t} \qquad \text{(II-8)}$$

where T = sample temperature

E_v = volumetric energy content

k = thermal conductivity

t = time

x = distance into the material

Havens lumped the sensible heat and heat of decomposition together as the "energy capacity," E_v. If the sample is at uniform initial temperature and if it is thick enough that heat does not penetrate all the way through it, the initial condition is

$$T = T_o \text{ for } t \leq 0 \qquad \text{(II-9)}$$

and one boundary condition is

$$\frac{\partial T}{\partial x} = 0 \text{ for } x \to \infty \qquad \text{(II-10)}$$

The second boundary condition is written to cover heat transfer across the exposed surface of the sample and it is

$$-k\,\frac{\partial T}{\partial x} = \bar{\alpha} H_i - h(T - T_\infty) - \bar{\varepsilon}\sigma T^4 \quad \text{for } x = 0 \qquad \text{(II-11)}$$

where $\bar{\alpha}$ = average surface absorptance

H_i = incident irradiance

h = convection heat transfer coefficient

$\bar{\epsilon}$ = average surface emittance

σ = Stefan-Boltzmann constant

Welker (44) pointed out that Equation II-8 with its initial and boundary conditions is strictly applicable for thermally thick, opaque samples. However, $\partial E_v/\partial t$ had not been measured directly previous to Havens' work. Havens assumed that E_v is an explicit function of temperature only and defined

$$\frac{\partial E_v}{\partial t} = \left(\frac{\partial E_v}{\partial T}\right)\left(\frac{\partial T}{\partial t}\right) \qquad \text{(II-12)}$$

Havens measured values for $\partial E_v/\partial T$ from differential scanning calorimetry. He then solved Equation II-8 numerically, with boundary conditions of $-k\partial T/\partial r = C$ at $r = a$, and $-k\partial T/\partial r = h(T_s - T_a)$ at $r = b$ to predict temperature profile and weight loss for hollow cylindrical pine samples heated at the inside surface. The agreement between calculated and predicted values was very good. However, ignition times were not predicted because of the lack of a criterion for ignition. Brown (7) developed an experimental procedure to measure the thermal conductivity of the char phase. The thermal conductivity of white pine char was measured at temperatures ranging from 345°C to 650°C. Brown used the measured thermal conductivity in Havens' model to predict temperatures and weight

loss for pyrolyzing wood cylinders. The predicted results showed good agreement with the experimental data for pyrolyzing white pine cylinders. The applicability of the model proposed by Havens to predict the transient temperature profile in pyrolyzing wood was well established.

Equation II-8 has frequently been written in a less rigorous form by assuming constant values of specific heat, density, and thermal conductivity; a single first-order decomposition reaction; and a heat of decomposition.

$$k \frac{\partial^2 T}{\partial x^2} = \rho c \frac{\partial T}{\partial t} + wQk_o e^{-E/RT} \qquad \text{(II-13)}$$

where ρ = density

c = specific heat

w = weight of decomposable material per unit volume

Q = heat of decomposition

k_o = frequency factor

E = activation energy

R = gas law constant

Bamford, Crank, and Malan (4) solved Equation II-13 with the boundary condition

$$-k \frac{\partial T}{\partial x} = h(T_f - T_s) + \sigma(\varepsilon_f T_f^4 - T_s^4) \qquad \text{(II-14)}$$

for a slab of wood heated on both faces by a open flame. In Equation II-14, T_f = flame temperature and ε_f = flame emittance. The boundary condition in Equation II-14 is essentially

the same as Equation II-11 except that the sample was surrounded by flame. Weatherford, et al. presented correlations of their data on ignition by convective heating based on their solution of the first order decomposition model. They showed that a specified fuel generation rate was not an adequate criterion for ignition as had been proposed by Bamford, et al. However, they did suggest that a fixed fuel generation rate must be satisfied to achieve sustained piloted ignition in the presence of a heat source.

For an inert sample undergoing no decomposition, Equation II-13 is further simplified as

$$k \frac{\partial^2 T}{\partial x^2} = \rho c \frac{\partial T}{\partial t} \qquad \text{(II-15)}$$

If the front surface boundary condition is taken as

$$-k \frac{\partial T}{\partial x} = H_i \qquad \text{(II-16)}$$

and the rear surface boundary condition is

$$\frac{\partial T}{\partial x} = 0 \qquad \text{(II-17)}$$

for x = L, the sample thickness, the analytical solution can be found from Carslaw and Jaeger (10) and its dimensionless form is

$$\frac{\Delta T_s \rho c L}{H_i t} = 1 + \frac{1}{F}\left[\frac{1}{3} - \frac{2}{\pi^2} \sum_{n=1}^{\infty} \frac{1}{n^2} e^{-n^2 \pi^2 F}\right] \qquad \text{(II-18)}$$

where ΔT_s = surface temperature rise at ignition

F = Fourier number, $\alpha t/L^2$

α = thermal diffusivity, $k/\rho c$

Based on Equation II-18 for $\sqrt{F} < 0.6$, a criterion for which a slab heated on one side can be considered as a semi-infinite sample, Butler, et al. (9) estimated the surface temperature of cellulosic materials for the case of spontaneous ignition to be in the range of 700° to 800°C. Simms (29, 30, 31) used Equation II-14 as his basic equation for heat transfer, but included convective cooling losses at the front surface in the boundary equation. Thus, at the exposed surface of the sample,

$$-k \frac{\partial T}{\partial x} = H_i - h(T - T_\infty) \qquad \text{(II-19)}$$

The analytical solution of Equation II-15 corresponding to the case of Equation II-19 was given by Simms as

$$\frac{H_i \sqrt{t}}{\Delta T_s \sqrt{k\rho c}} = \frac{\beta}{1 - \text{erfc } \beta \exp \beta^2} \qquad \text{(II-20)}$$

where $\beta = [h^2 t/k\rho c]^{1/2}$. β is called the cooling modulus and ΔT_x is the surface temperature rise. If β^2 is small, the surface heat losses may be also neglected. The energy modulus therefore would be constant if the thermal properties and heat transfer coefficient are constant. Simms then plotted the energy modulus versus the cooling modulus, $h\sqrt{t}/\sqrt{k\rho c}$, and applied a constant ignition temperature such that the

theoretical curve gave the best fit through the experimental data (within 30 percent). Simms concluded that a fixed surface temperature is a reasonable criterion for the attainment of ignition.

Buschman (8), using his data and the solution of the conduction equation for opaque, inert solids, calculated the piloted ignition temperature. The tabulated results show a relatively constant value for surface temperature of each species of wood at ignition. The reported ignition temperatures varied for different kinds of wood ranging from 298°C for tempered hard board to 391°C for balsa.

Vyas (42), based on the constant surface temperature assumption, correlated his test data on an initially absorbed irradiance basis ($\bar{\alpha}H_i$), neglecting the irradiated surface losses due to convection and reradiation, and concluded that the time of ignition of wood is directly proportional to the product of thermal conductivity and density. The samples which Vyas tested were oriented in such a manner that the direction of heat flow was parallel to the grain structure. Since the time of ignition is strongly dependent upon the direction of heat flow, the time of ignition which Vyas measured is approximately twice as long as for heat flow perpendicular to the grain.

It is quite obvious from the previous work on ignition and pyrolysis of wood that an inert model cannot represent wood ignition exactly, particularly when no criterion or

set of criteria have been established which will allow prediction of ignition, even if the models were exact.

CHAPTER III

EXPERIMENTAL STUDIES AND RESULTS

The experimental portion of this study was designed to provide the data needed to solve the mathematical model. Experiments were undertaken to obtain the kinetic parameters of wood pyrolysis and to measure the energies of pyrolysis at different heating rates. Brown (7) stated that at heating rates up to 160°C/min the pyrolysis mechanism for polymeric materials is usually independent of heating rate. The piloted wood ignition studies of Koohyar (22) and Wesson (45) have shown that a minimum surface heating rate of 30° to 40°C/min is required for piloted ignition of wood. Surface heating rates in real fires of up to 1500°C/min are not uncommon. One of the objectives of the experimental portion of this study was to demonstrate the independence of pyrolysis kinetics on heating rates by measuring "energy capacity" data obtained at heating rates higher than 20°C/min, which was the highest heating rate in the literature before Brown's study.

Measurements of Weight Loss and Rate of Weight Loss of Wood as a Function of Temperature using Thermal Gravimetric Analysis

Weight loss data required for kinetic analysis were obtained using the Perkin-Elmer TGS-1 Thermobalance and UU-1 Temperature Control Unit shown in Figure III-1. A Texas Instrument Servowriter-II was used to record the output from the Thermobalance. The Perkin-Elmer TGS-1 sample holder, furnace, and weighing assemblies are shown schematically in Figure III-2. The weighing mechanism in the TGS-1 is a Cahn RG Electrobalance. The Electrobalance is of the null-counter balance type and is designed for measurements from 0.1 to 200 mg. The Electrobalance generates a continuous signal proportional to weight during a test run which can be recorded as weight or can be internally differentiated with respect to time and then recorded. The Thermobalance has the capacity of detecting weight changes of 10^{-6} grams.

The temperature calibration of the instrument was carried out using the Curie point ferromagnetic standards which were supplied by the manufacturer in wire form. The Curie point temperatures shown in Table III-1 are those originally published by Perkin-Elmer for the metals shown. Based upon careful reexamination of the magnetic transition temperature for these metals, Perkin-Elmer published a revised set of Curie point temperatures which they entitled magnetic transition temperatures.

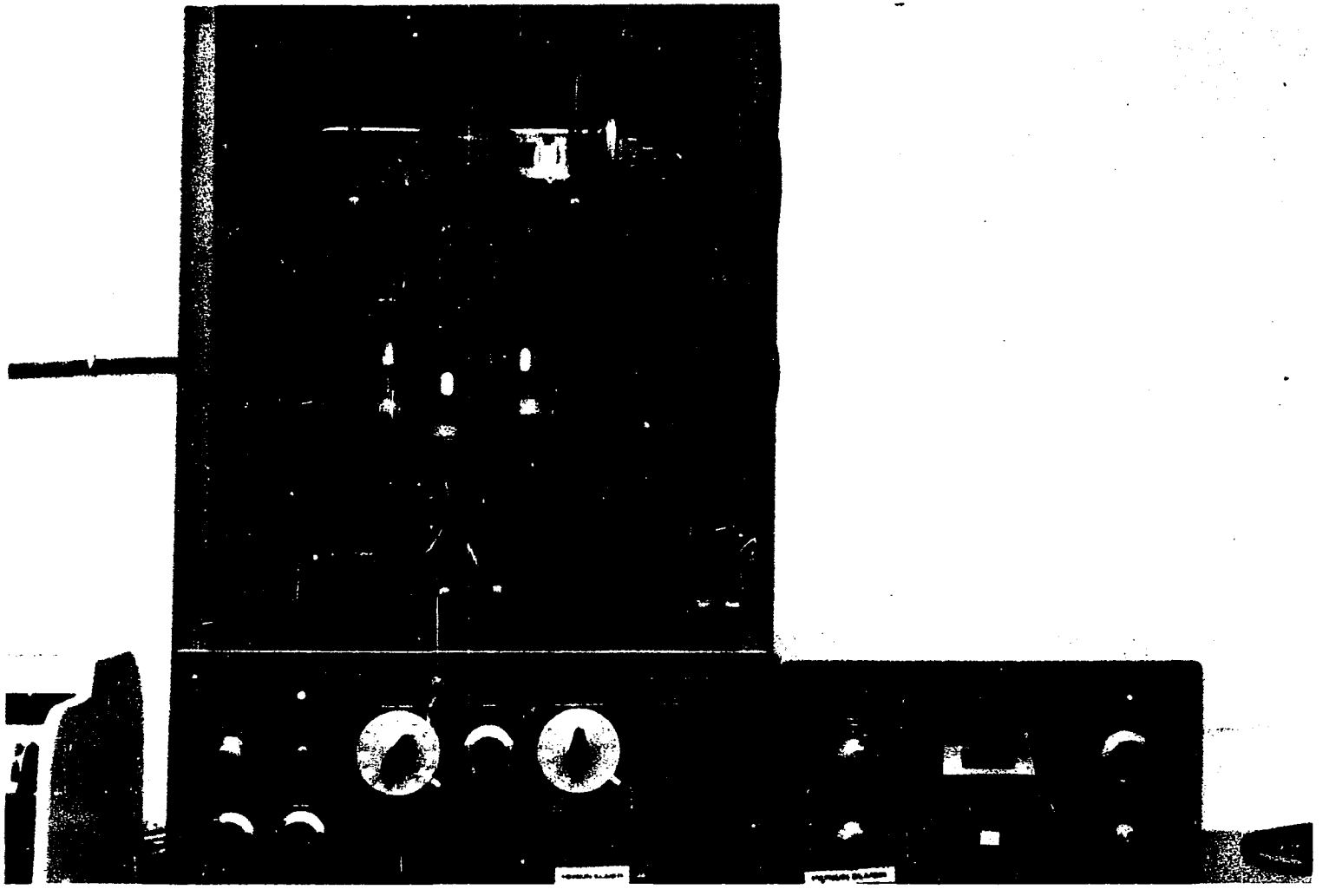

Figure III-1. Perkin-Elmer TGS-1 Thermobalance and UU-1 Temperature Controller.

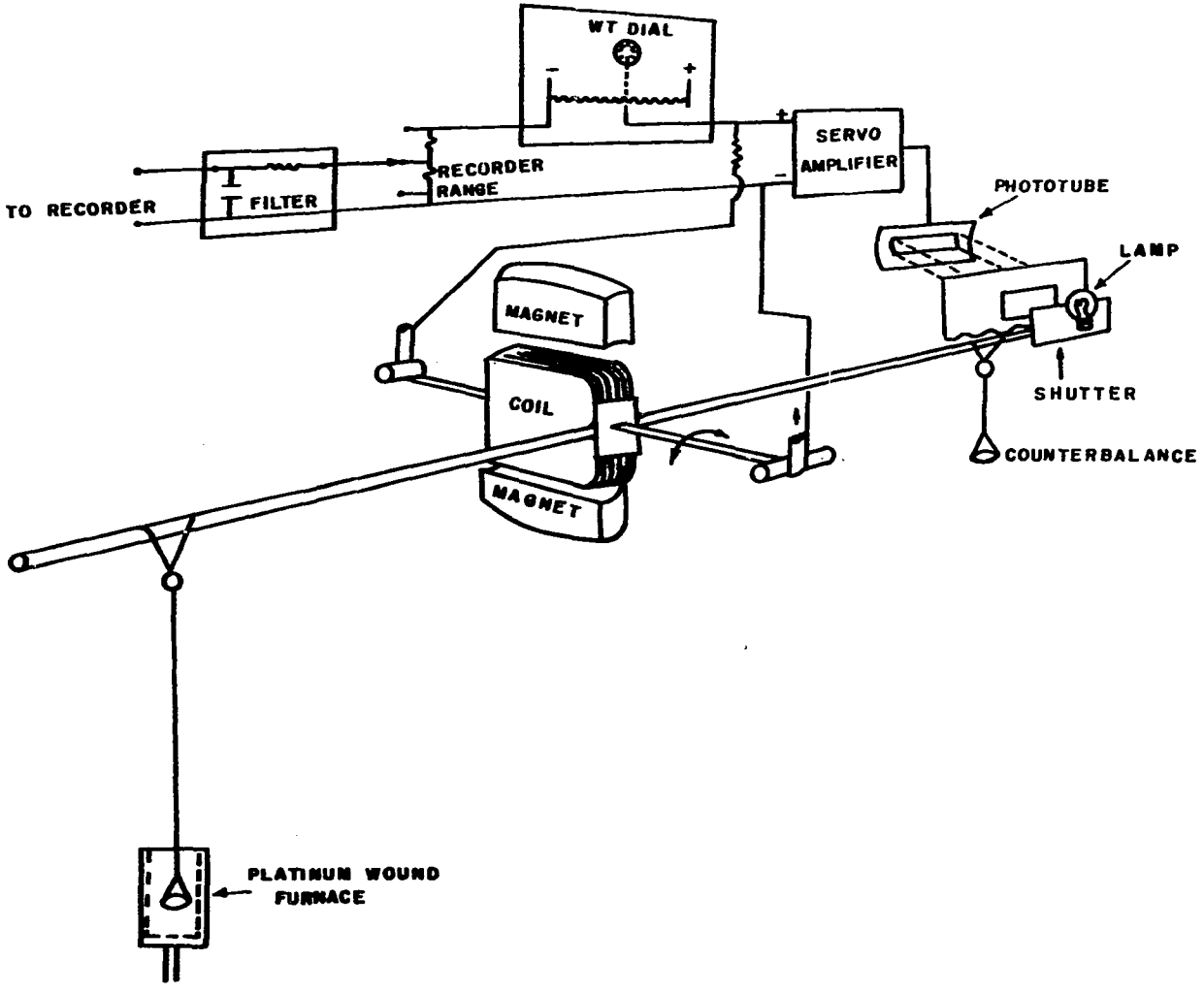

Figure III-2. Schematic of Perkin-Elmer TGS-1 Furnace and Weigh Assembly.

TABLE III-1

MAGNETIC STANDARDS FOR TGS-1B FURNACE CALIBRATION

Metal	Curie Point Temperature, °C	Magnetic Transition Temperature, °C
Monel	65	65
Alumel	158	163
Nickel	358	354
Numetal	390	393
Nicoseal	445	438
Perkalloy	598	596
Iron	786	780
Hi-Sat 50	994	1000

The temperature calibration of the Thermobalance involves determination of a calibration curve relating the digital readout on the UU-1 Temperature Control Unit with the known transition temperatures. Ideally the TGS-1 calibration should be linear over the range from 25°C to 1000°C. In this study an individual calibration was done at each heating rate investigated; calibration was checked several times during the use of that heating rate to guarantee the reproducibility of the calibration. A typical temperature calibration curve is shown in Figure III-3.

A Cahn No. 3100 Time Derivative Computer was connected directly to the TGS-1 enabling the weight loss and derivative weight loss to be measured from a single run. The time derivative computer was essentially calibrated for each sample run. The integrated area under the dw/dt curve given by the computer represents the total weight lost by the sample during its

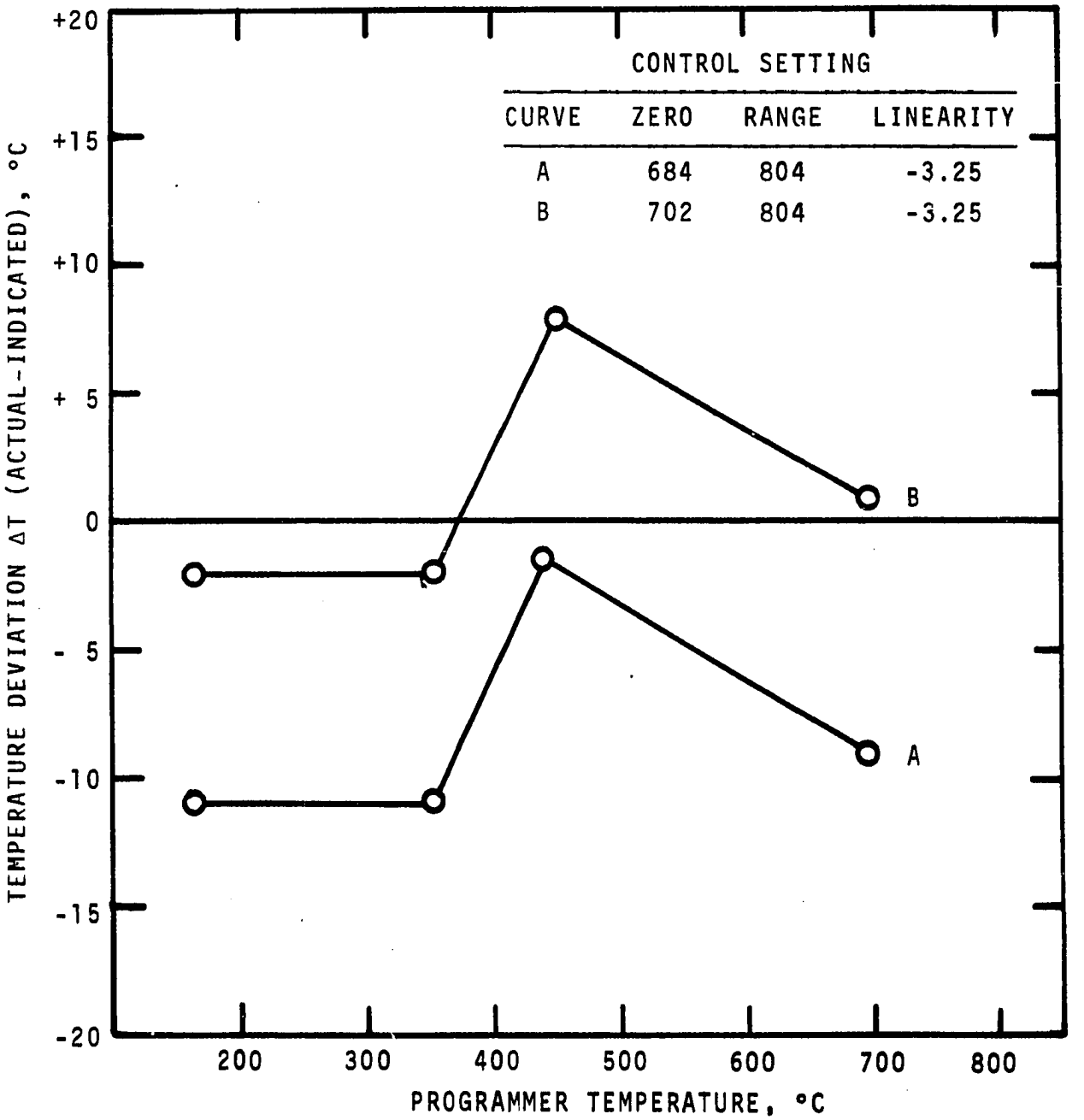

Figure III-3. TGS-1 Temperature Calibration Curve, Heating Rate 80°C/min.

decomposition. For each sample run, the proper ordinate values may be obtained from

$$\underset{(mg/sec\text{-}cm)}{\text{ordinate}} = \frac{\text{weight loss (mg)} \times \text{chart speed (cm/sec)}}{\text{area (cm)}^2} \qquad \text{(III-1)}$$

Experimental Results

The weight loss kinetics of spruce and redwood were studied in a flowing nitrogen atmosphere at heating rates of 10°, 20°, 40°, 80° and 160°C/min. A nitrogen flow rate of 40 ml/min Was used. The samples used were cut from knot-free boards and were milled and passed through a 40 mesh screen before being pyrolyzed. Three runs of each sample were made at each heating rate. The weight loss and rate of weight loss for spruce are shown in Figures III-4 through III-9 and for redwood in Figures III-10 through III-15. The form of the data is nearly identical to that obtained by Havens and Brown (7, 18).

Figures III-9 and III-15 show that as the heating rate is increased, the weight loss curves shift toward higher temperatures. The reason for this shift may be seen by investigating the equation used to describe the weight loss kinetics

$$-\frac{1}{W_o - W_f}\frac{dW}{dt} = Ae^{-E/RT}(W)^n \qquad \text{(III-2)}$$

Equation III-2 may be integrated in terms of temperature by dividing both sides by the heating rate $\beta = dT/dt$. The result is

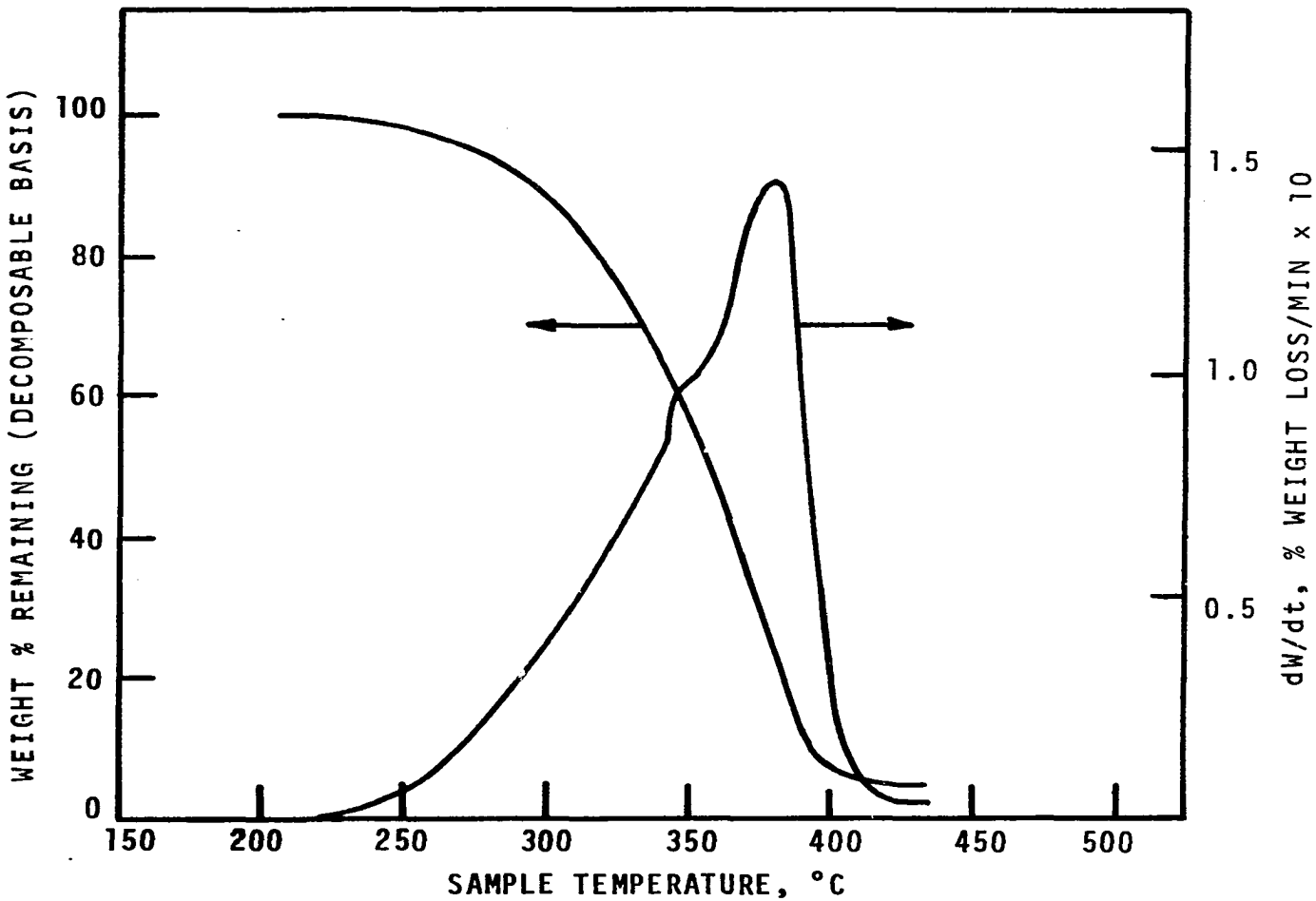

Figure III-4. TG and DTG Curves for Spruce at a Nominal Heating Rate of 10°C/min.

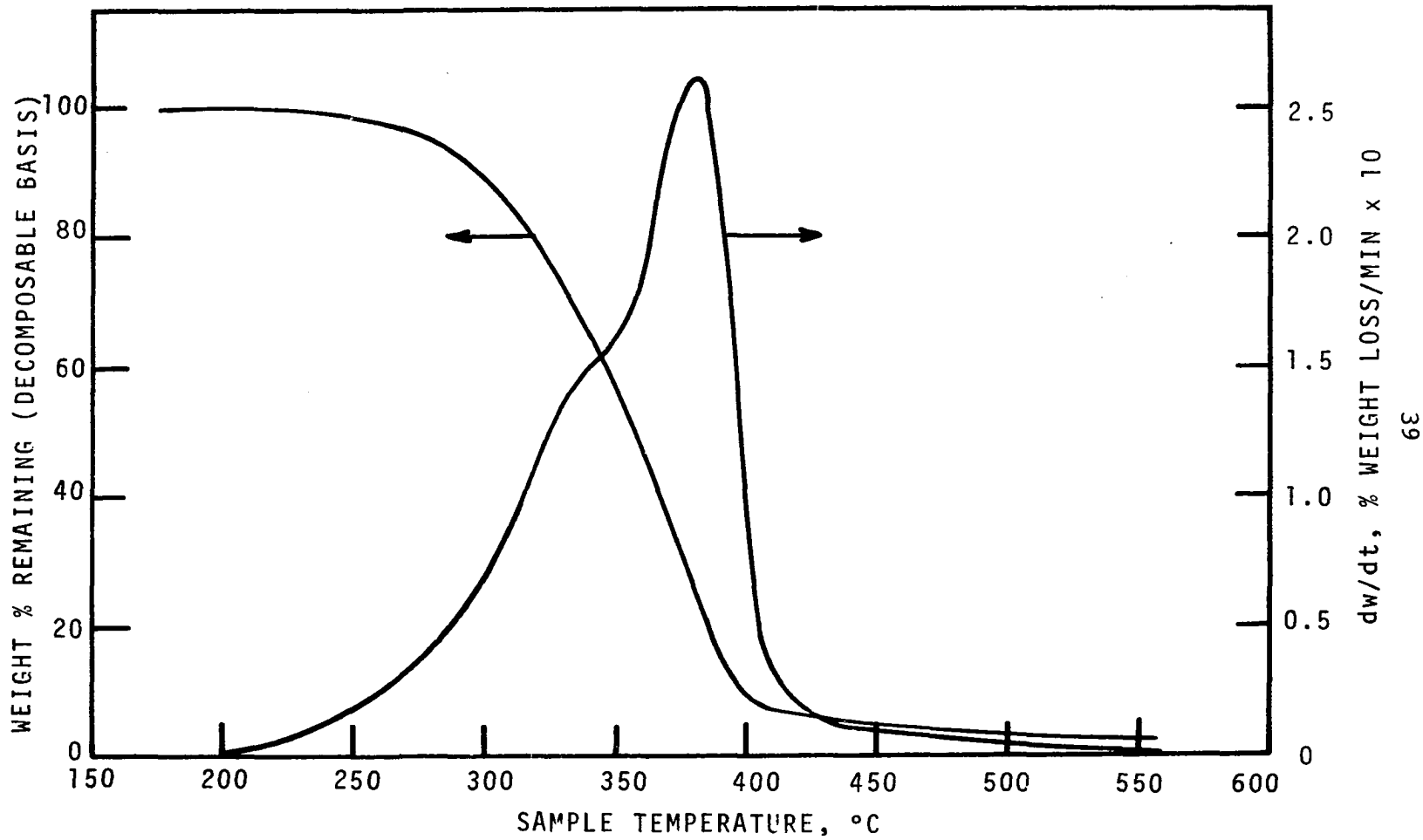

Figure III-5. TG and DTG Curves for Spruce at a Nominal Heating Rate of 20°C/min.

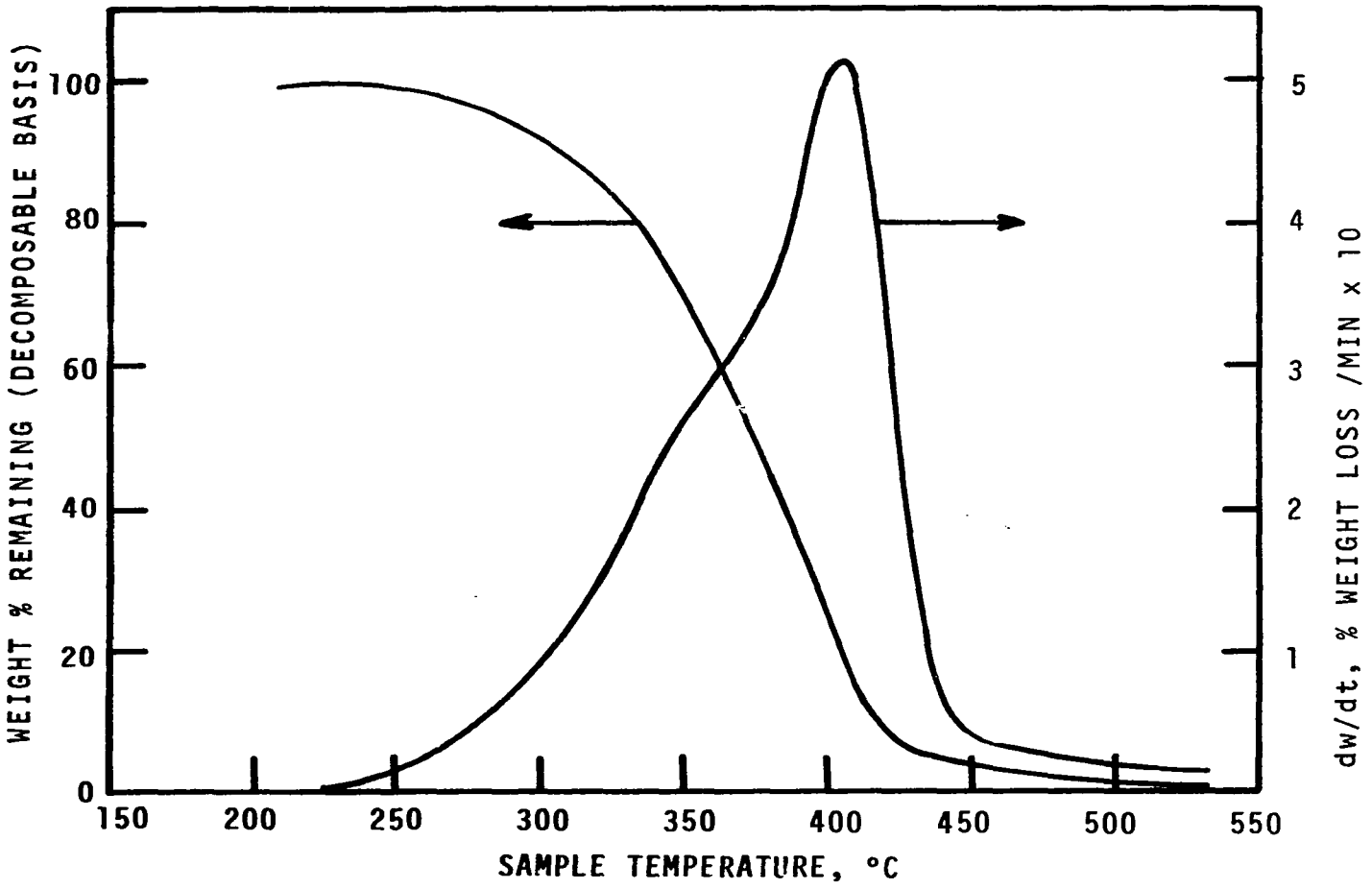

Figure III-6. TG and DTG Curves for Spruce at a Nominal Heating Rate of 40°C/min.

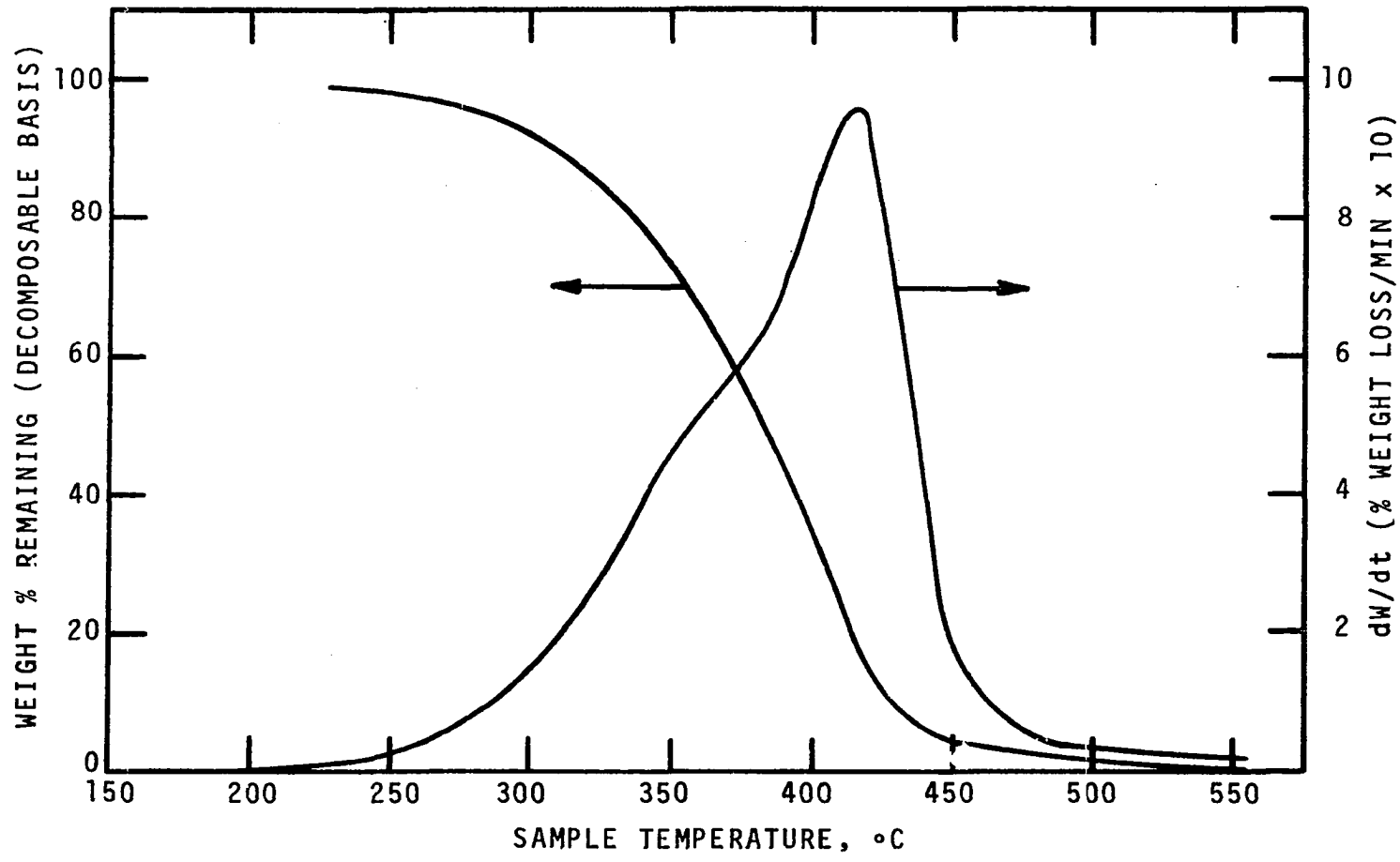

Figure III-7. TG and DTG Curves for Spruce at a Nominal Heating Rate of 80°C/min.

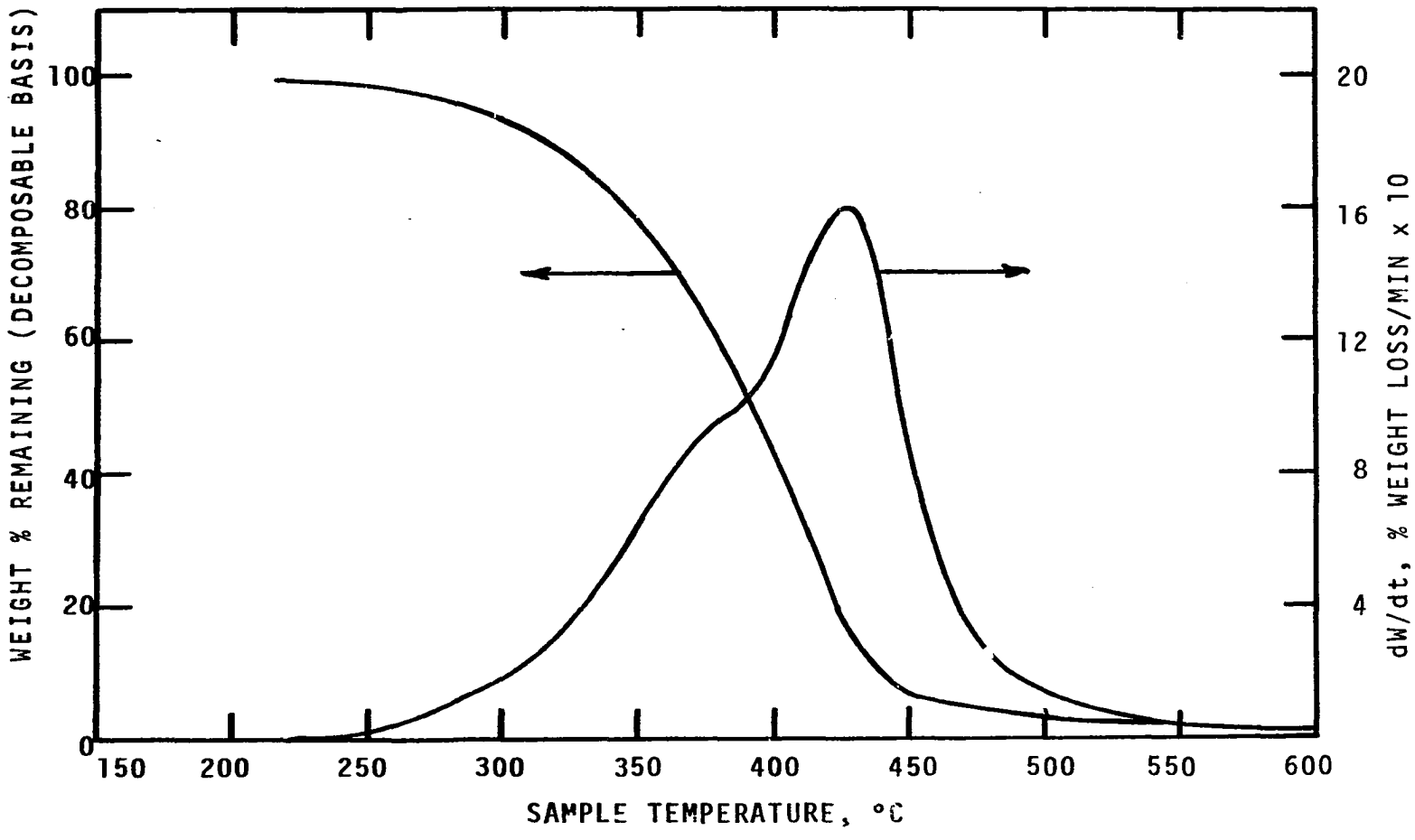

Figure III-8. TG and DTG Curves for Spruce at a Nominal Heating Rate of 160°C/min.

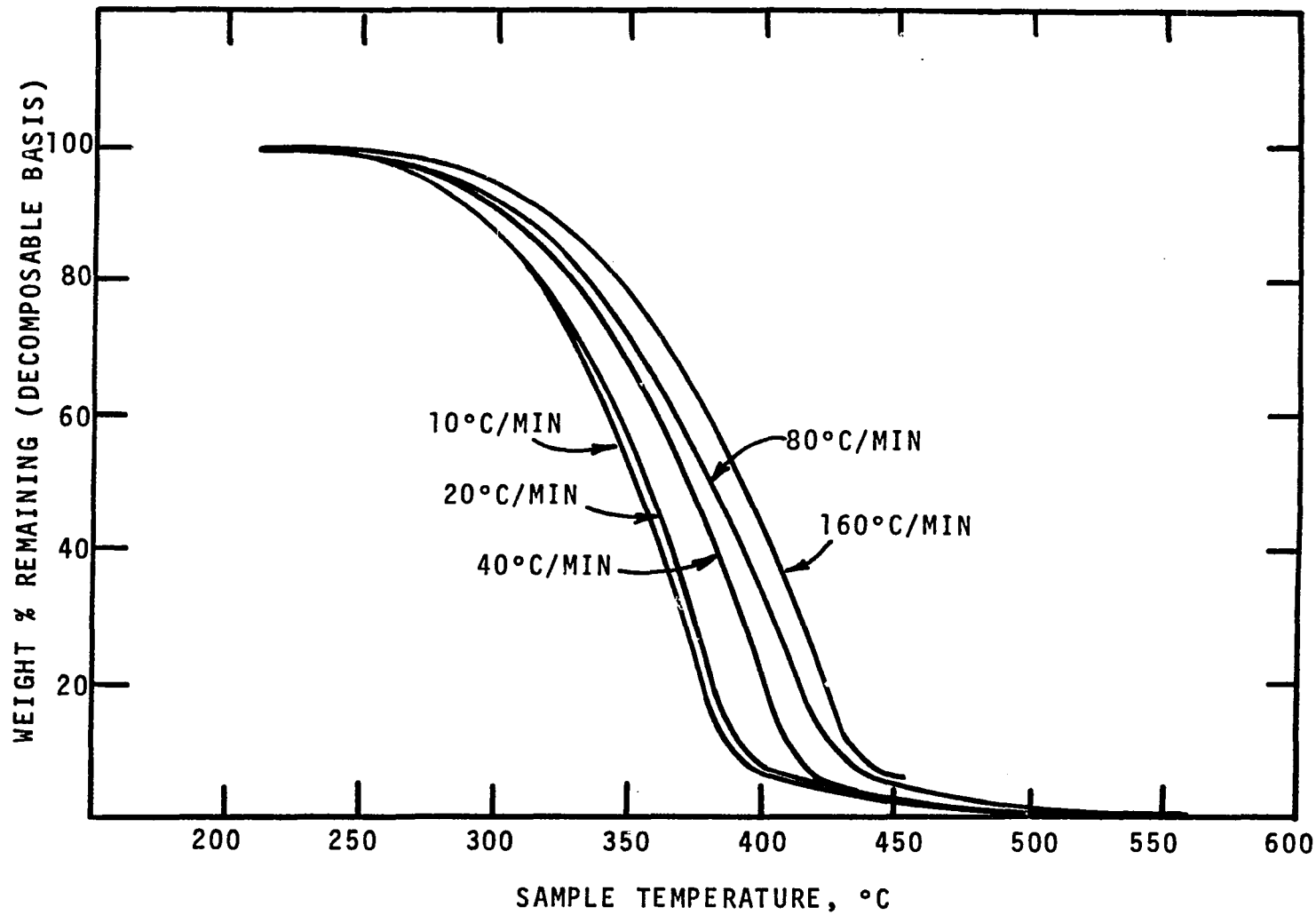

Figure III-9. Summary of TG Curve for Spruce in a Nitrogen Atmosphere.

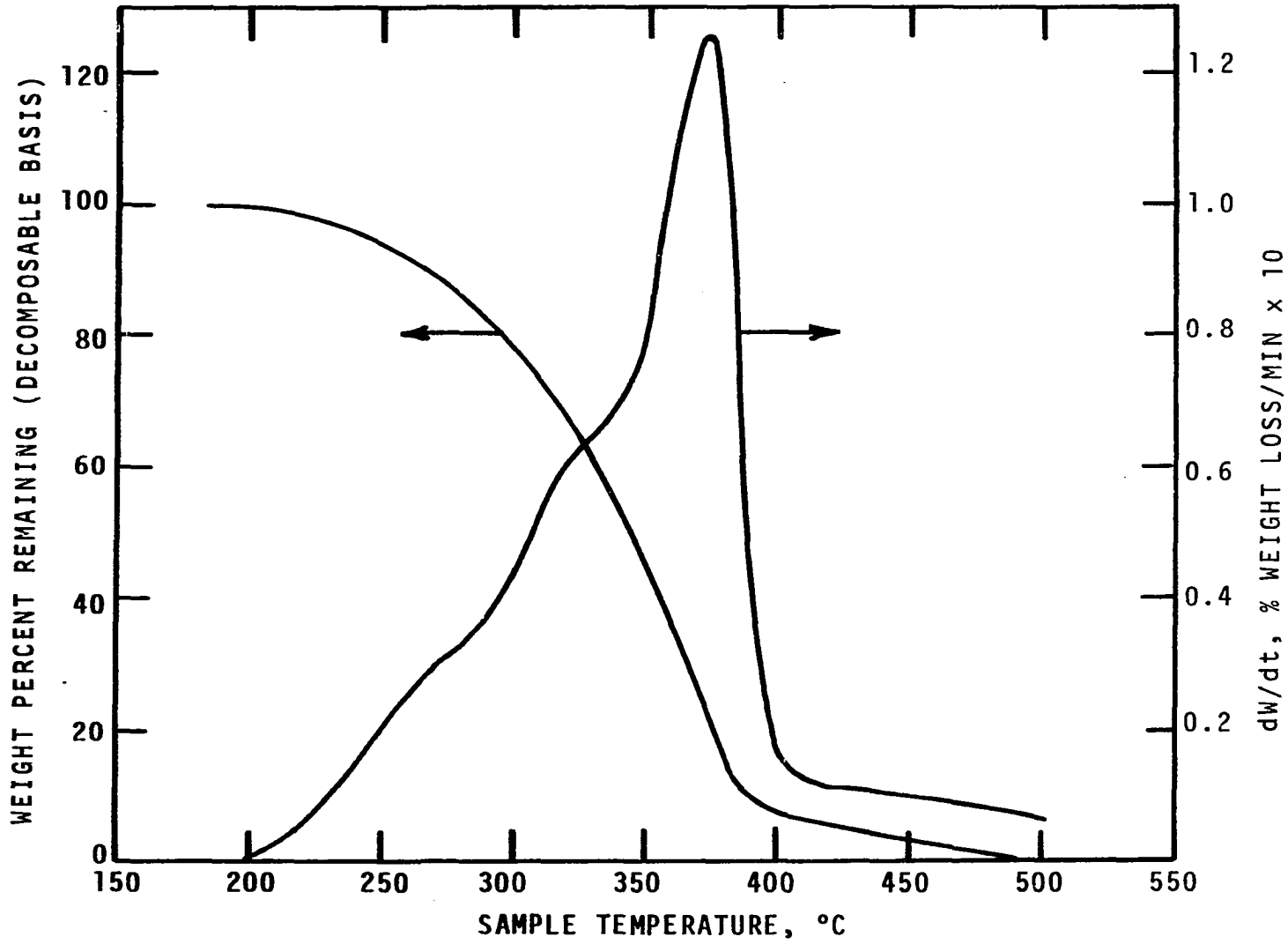

Figure III-10. TG and DTG Curves for Redwood at a Nominal Heating Heating Rate of 10°C/min.

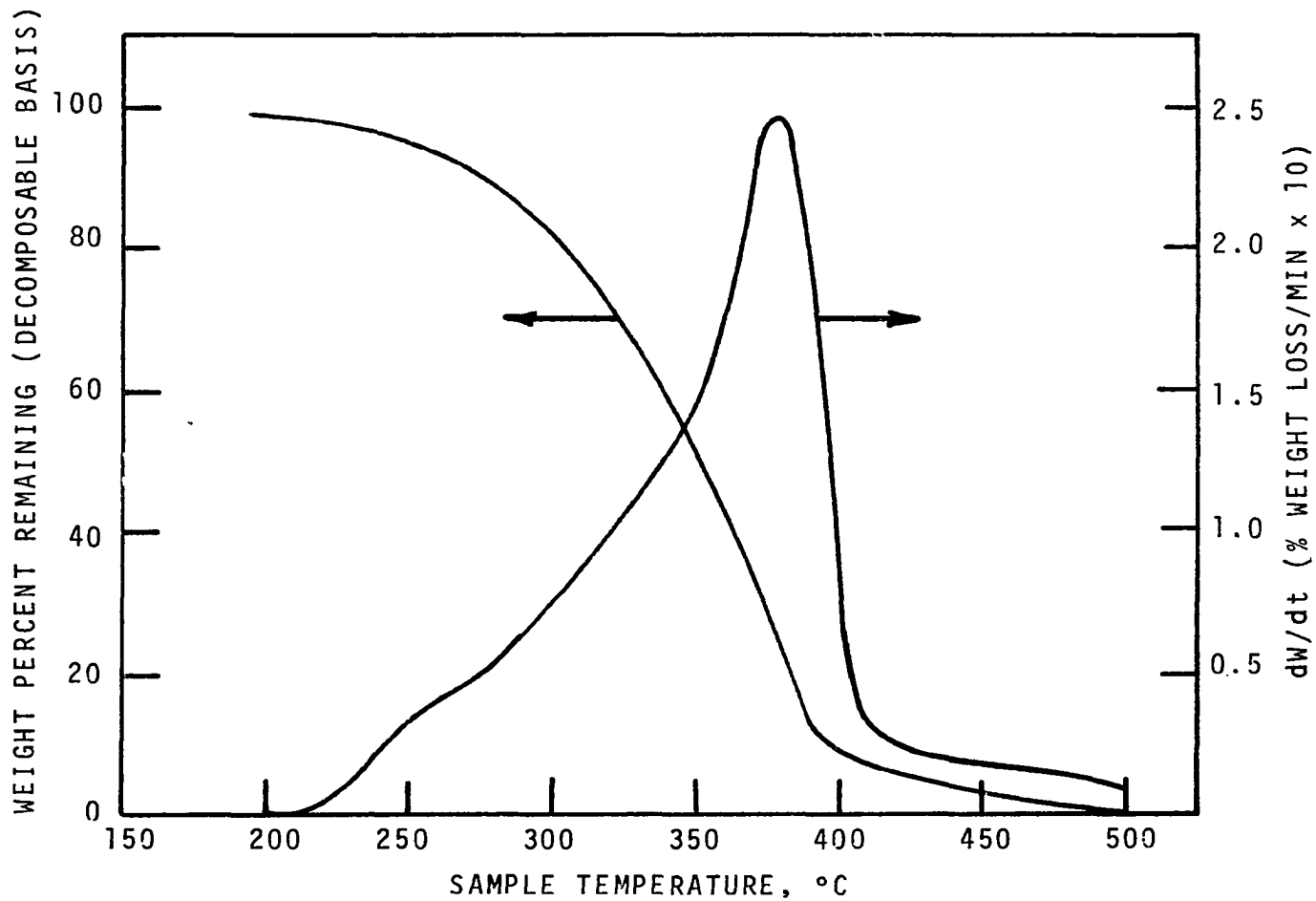

Figure III-11. TG and DTG Curves for Redwood at a Nominal Heating Rate of 20°C/min.

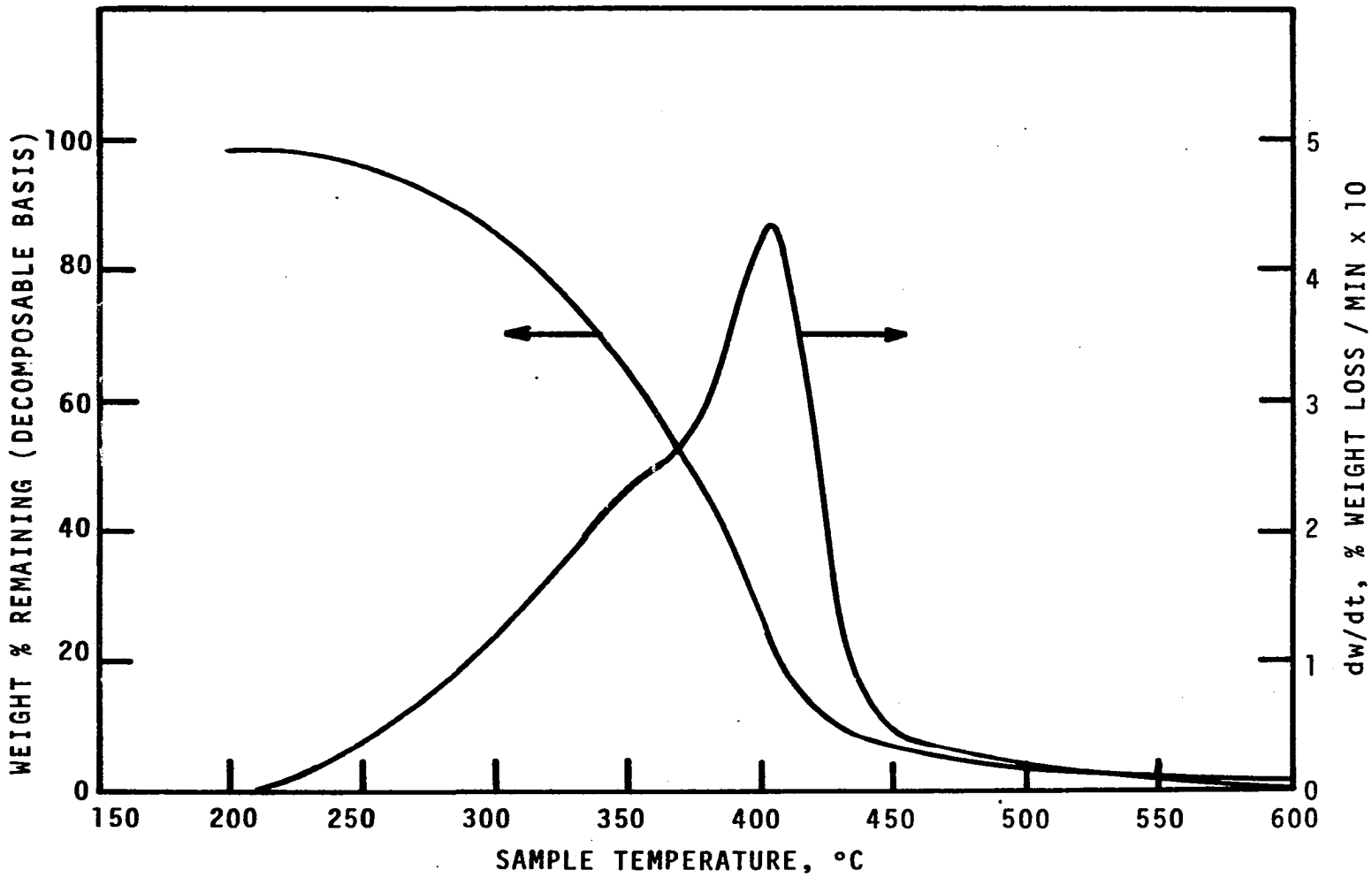

Figure III-12. TG and DTG Curves for Redwood at a Nominal Heating Rate of 40°C/min.

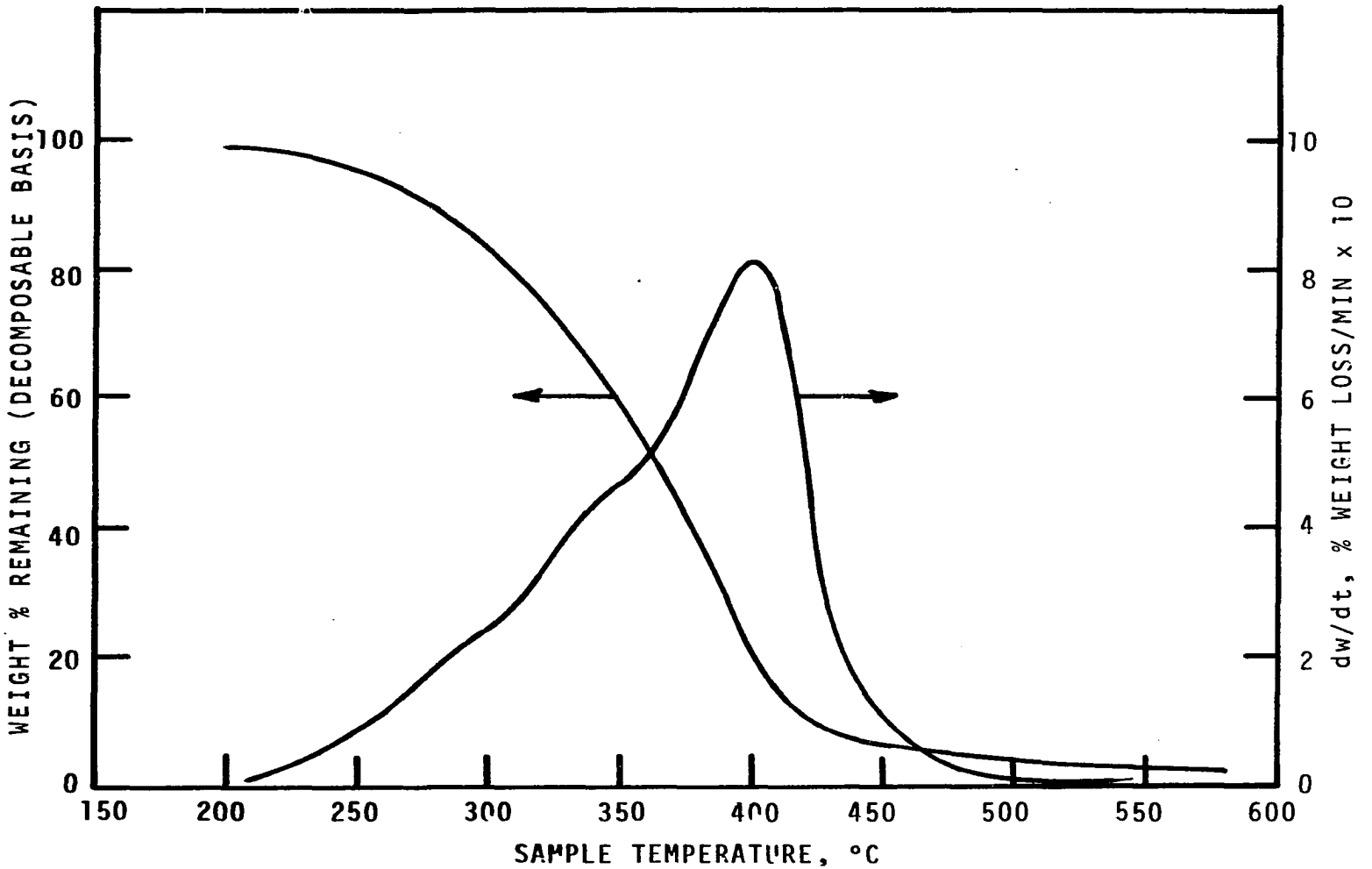

Figure III-13. TG and DTG Curves for Redwood at a Nominal Heating Rate of 80°C/min.

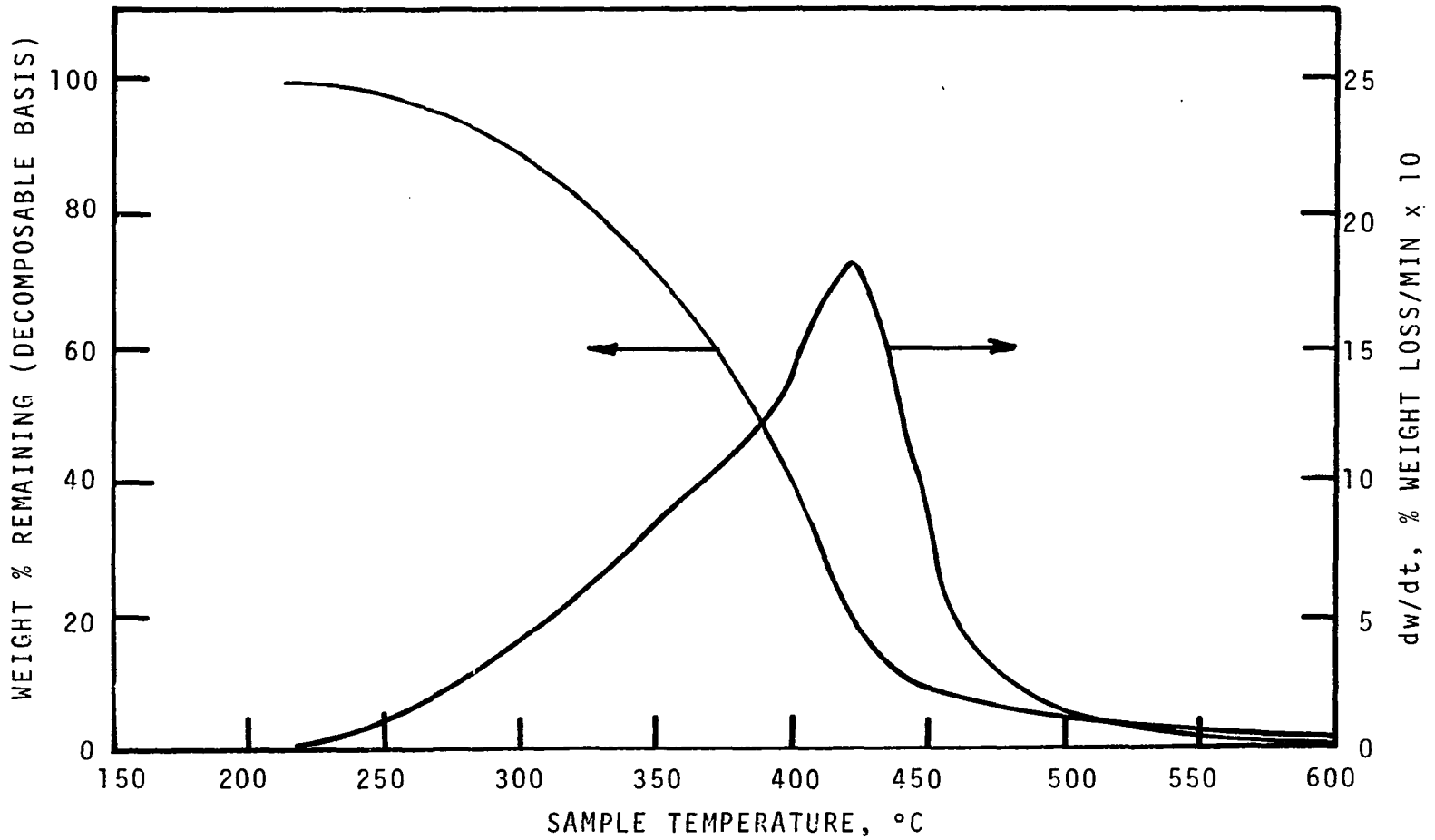

Figure III-14. TG and DTG Curves for Redwood at a Nominal Heating Rate for 160°C/min.

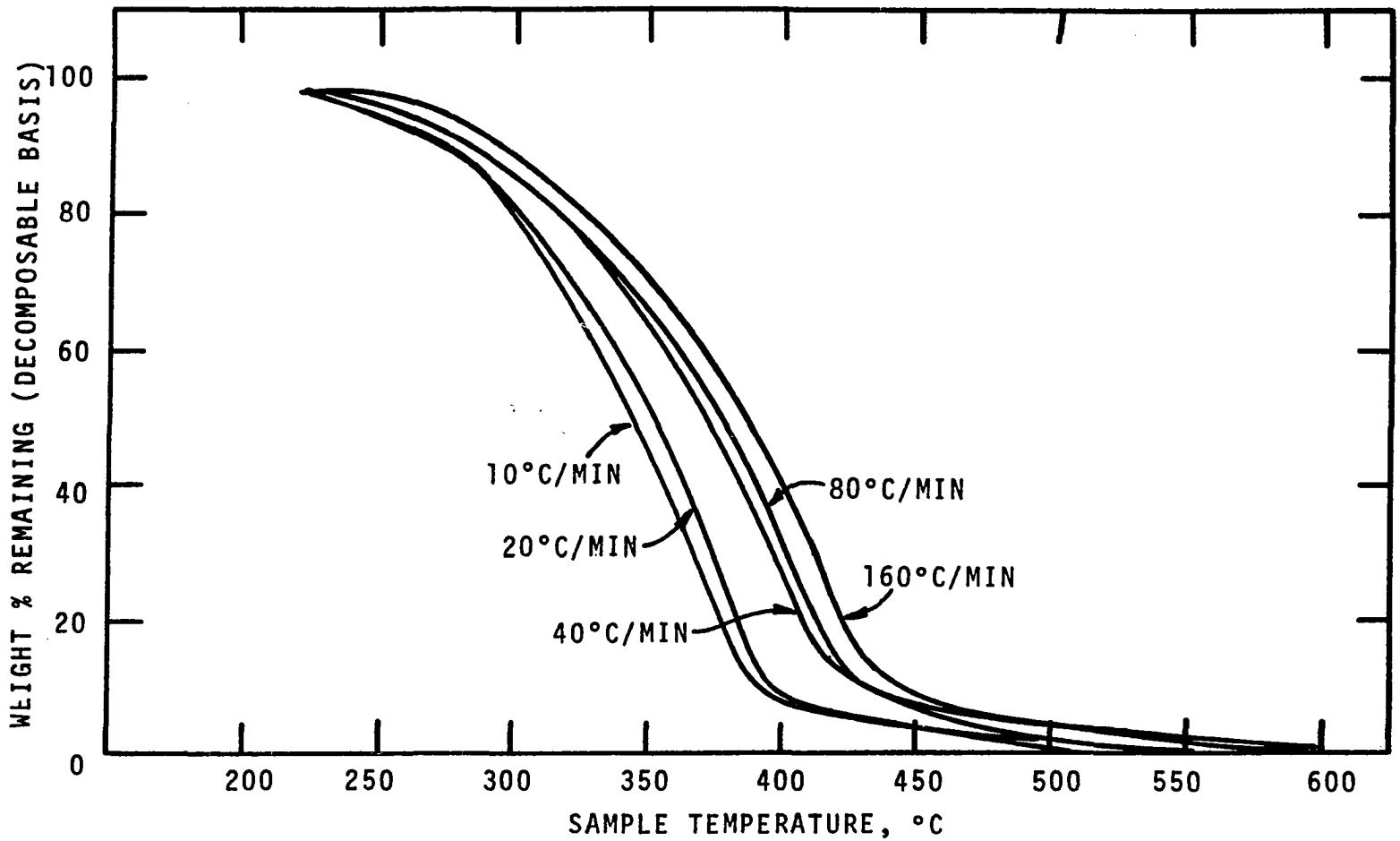

Figure III-15. Summary of TG Curve for Redwood in a Nitrogen Atmosphere.

$$\frac{-1}{W_o - W_f} \int_{1.0}^{W} \frac{dW}{W^n} = A/\beta \int_{T_o}^{T} e^{-E/RT}\, dT \qquad \text{(III-3)}$$

The term A/β will decrease with increasing heating rate β. Thus a higher temperature is required to compensate for the value of A/β to achieve any specified weight loss, W.

Analysis of Data

In reviewing the literature on kinetic methods for programmed TGA, it is found that the technique of Goldfarb, McGuchan and Meeks (15) can offer an adequate, meaningful method of modeling the degradation. The postulated rate expression based on weight terms is given by

$$\frac{-1}{W_o - W_f} \frac{dW}{dt} = k_o e^{-E/RT} F(W) \qquad \text{(III-4)}$$

where W = sample weight (mg)

W_o = initial sample weight (mg)

W_f = final sample weight (mg)

t = time (sec)

k_o = frequency factor (sec^{-1})

E = activation energy (cal/g-mole)

R = gas constant (1.986 cal/g-mole-°K)

T = temperature (°K)

F(W) = an undefined function of weight

The logarithmic expression of Equation III-4 at any specified heating rate is

$$\log \left[\frac{-1}{W_o - W_f} \frac{dW}{dt}\right]_H = \log k_o + \log F(W) - \frac{E}{2.303\ R\ T_H} \qquad \text{(III-5)}$$

The equation above denotes that both the rate and temperature corresponding to any specific value of F(W) are dependent on the heating rate employed. If the chemistry of pyrolysis is independent of heating rate, then F(W) will be constant at any weight loss regardless of heating rate. Thus, by plotting log (rate) versus reciprocal temperature with parameters of constant conversion (at different heating rates) the activation energy can be obtained for any conversion. Figure III-16 and Figure III-17 show the plots of log $[-1/(W_o-W_f) \times dW/dt]_H$ versus $1/T_H$ for spruce and redwood, respectively. The activation energy may be obtained from the slope of the line and log $[k_o F(W)]$ from the intercept for each value of conversion. The variation in activation energy with conversion thus calculated may be examined for the two samples in Figures III-18 and III-19. It is seen that the activation energy does not vary much over the entire range, except there is a small amount of scatter at the ends. Average values of activation energy are then calculated over the entire degradation range. For spruce the average E is 51.9 kcal/g-mole and for redwood the average E is 44.2 kcal/g-mole. The average activation energy is then used to calculate log $k_o F(W)$ values at each conversion for the various heating rates. By rearranging Equation III-5

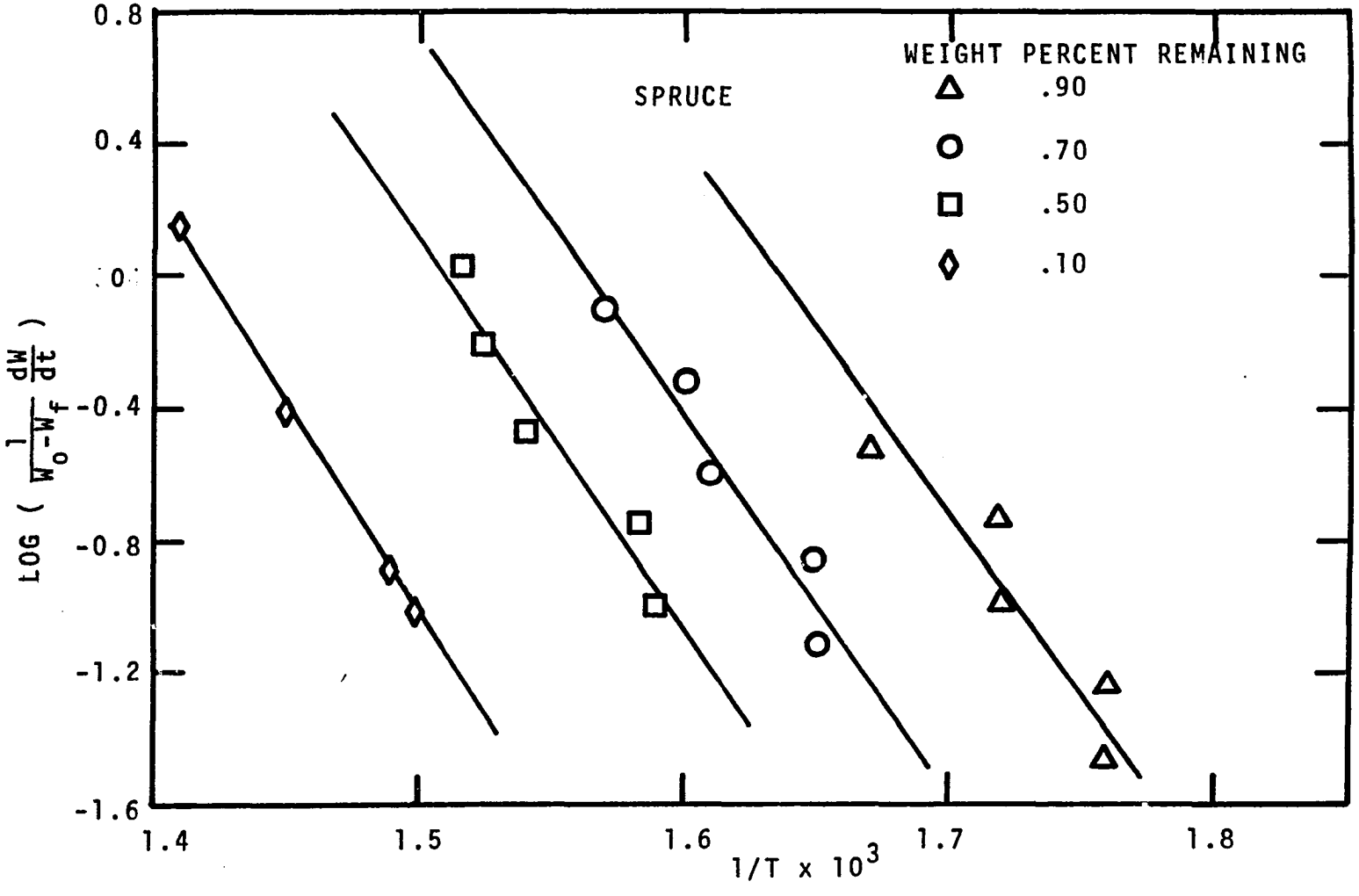

Figure III-16. Plot to Obtain Activation Energy for Spruce at Various Values of Conversion, Method of Friedman.

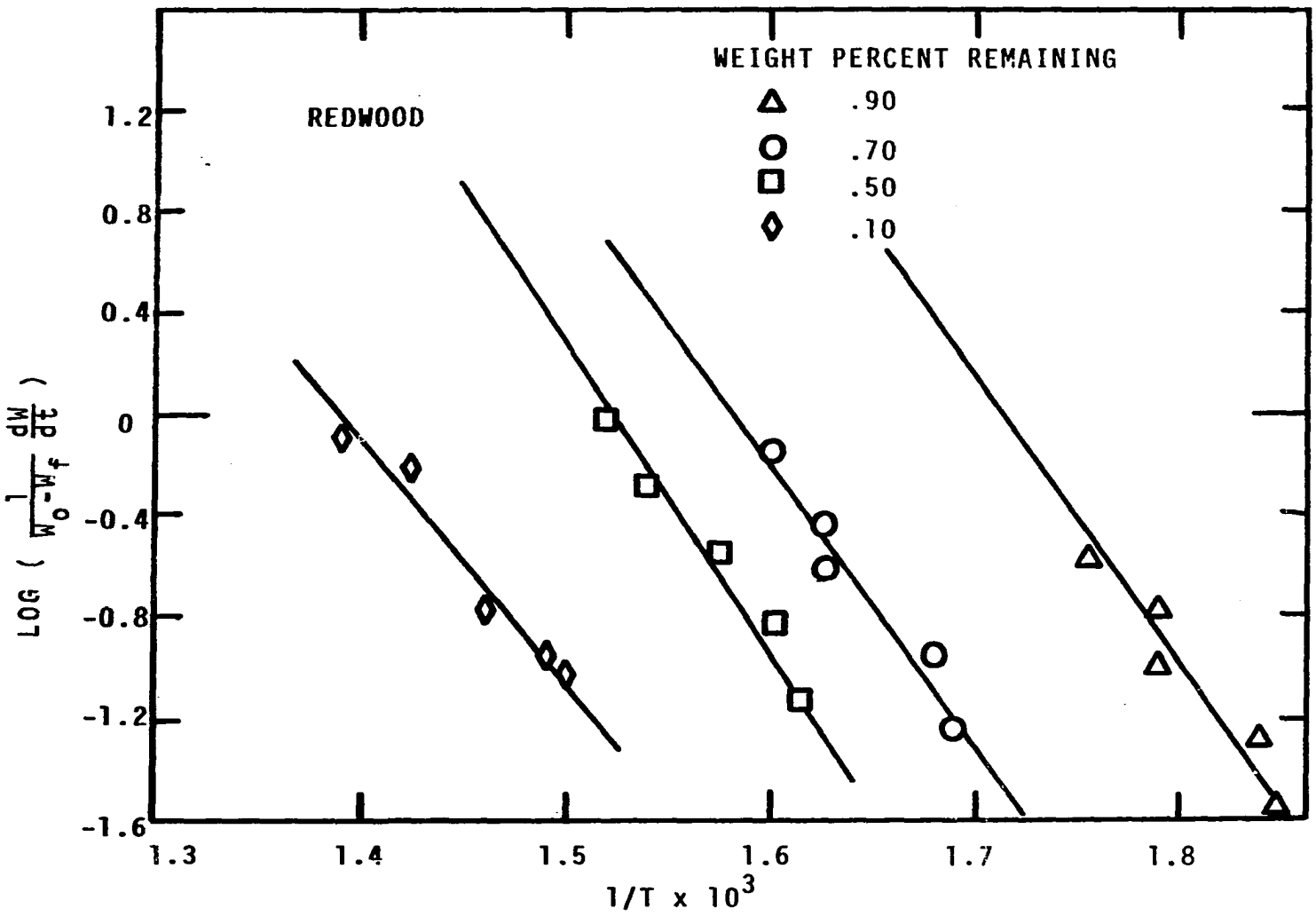

Figure III-17. Plot to Obtain Activation Energy at Various Values of Conversion for Redwood.

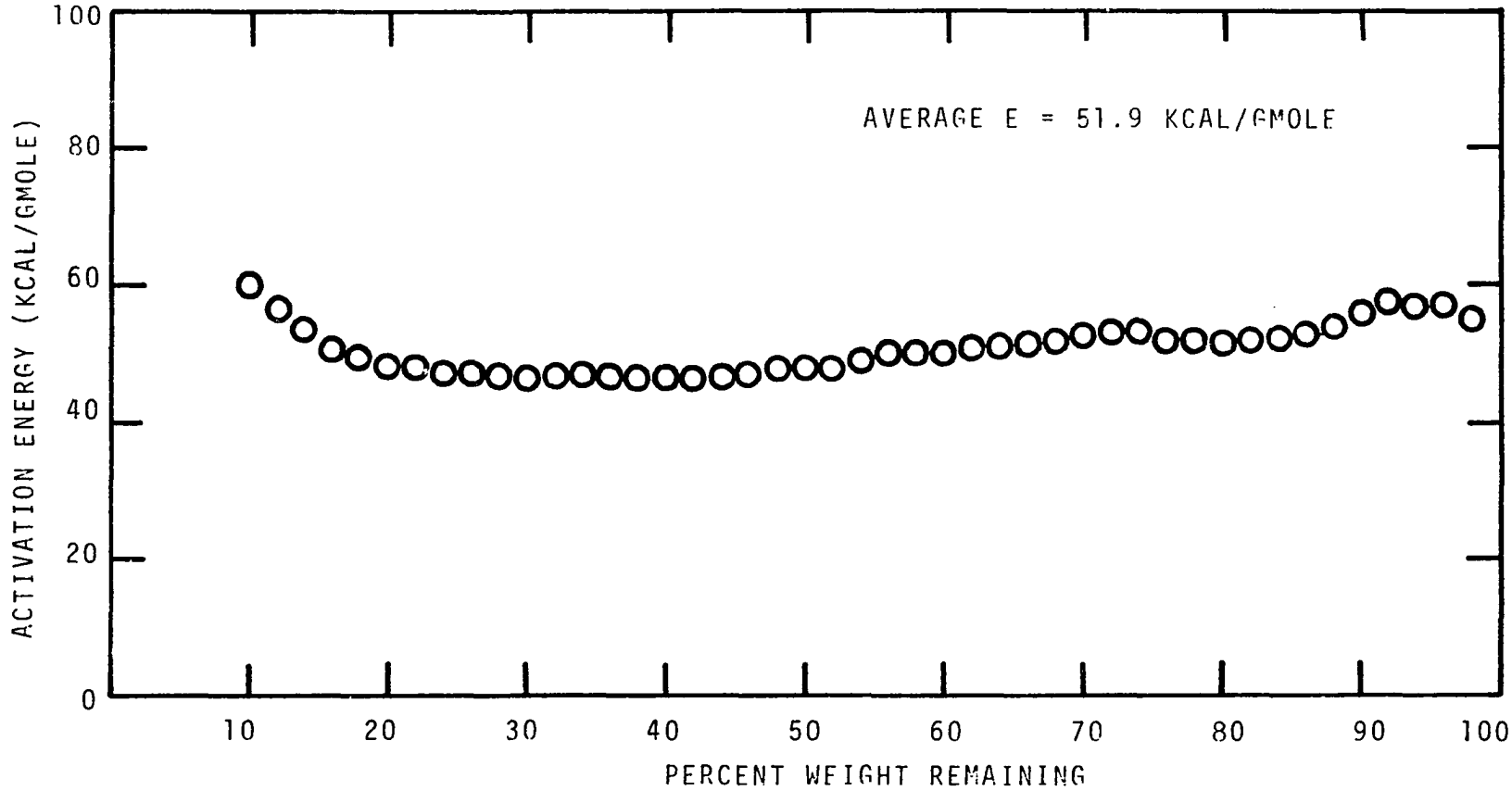

Figure III-18. Variation of Activation Energy with Conversion for the Weight Loss of Spruce.

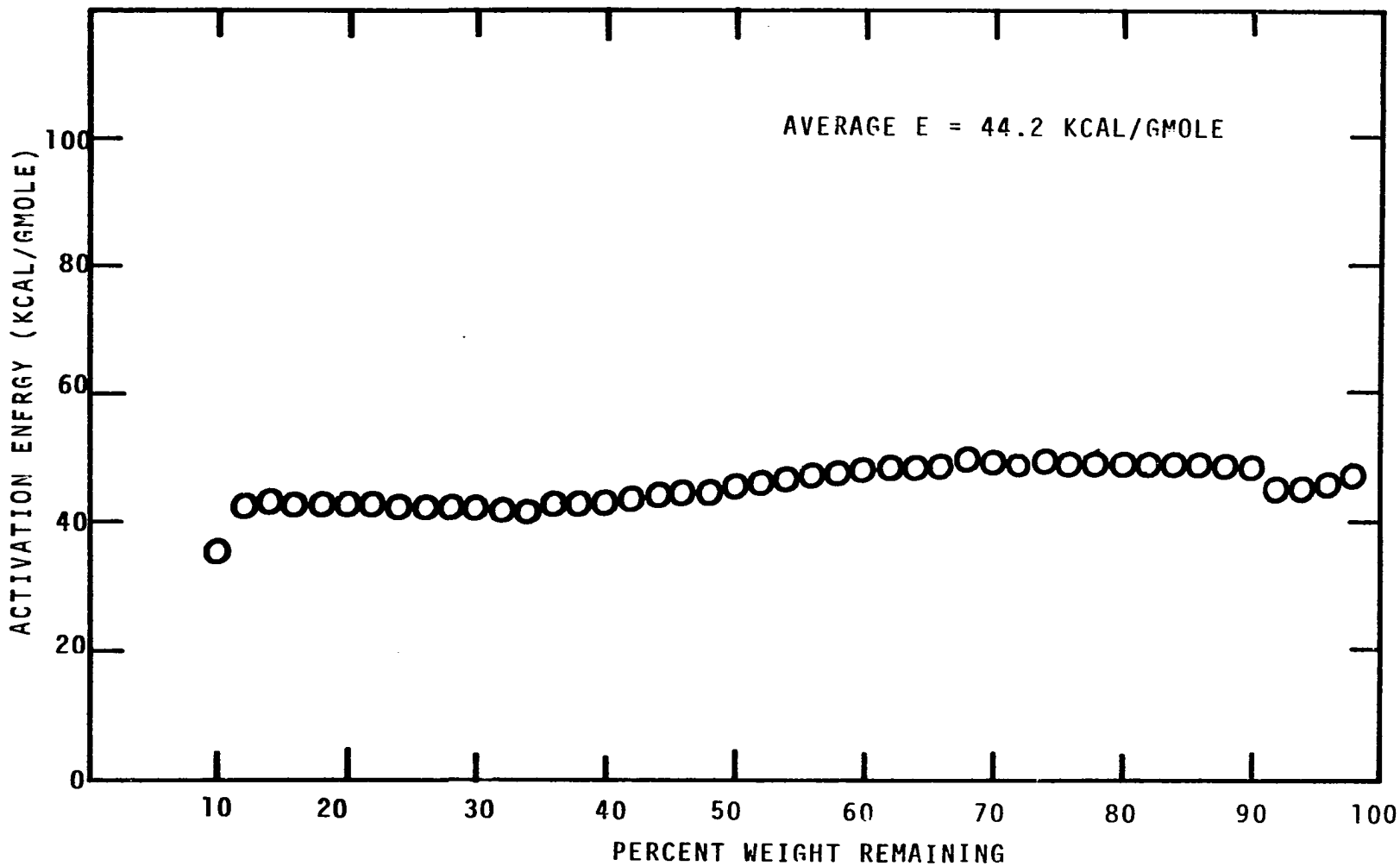

Figure III-19. Variation of Activation Energy with Conversion for the Weight Loss of Redwood.

$$\log k_o F(W) = \log k_o + \log F(W)$$

$$= \log \left[\frac{-1}{W_o - W_f} \frac{dW}{dt}\right]_H + \frac{E}{2.303\ R\ T_H} \qquad \text{(III-6)}$$

If it is assumed that $F(W)$ is of the form $[(W-W_f)/(W_o-W_f)]^n$, then

$$\log k_o F(W) = n \log \left[\frac{W - W_f}{W_o - W_f}\right] + \log k_o \qquad \text{(III-7)}$$

A plot of $\log k_o F(W)$, i.e., $\log [1/(W_o - W_f) \times dW/dt]_H + E/(2.303RT_H)$, versus $\log [(W-W_o)/(W_o - W_f)]$ should yield a straight line of slope n. Values of $\log k_o F(W)$ are calculated at each conversion for the various heating rates, and results are shown in Figures III-20 and III-21.

The kinetic parameters--activation energy, order and frequency factor--for the pyrolysis of spruce and redwood are summarized in Table III-2.

TABLE III-2

KINETIC PARAMETERS FOR PYROLYSIS OF SPRUCE AND REDWOOD

Wood	Weight Fraction Material Remaining	n	$k_o (sec^{-1})$
Spruce	0.54 - 1.00	1.1	2.71×10^{18}
E = 51,900 cal/g-mole	0.10 - 0.54	1.3	1.22×10^{16}
Redwood	0.54 - 1.00	1.3	5.51×10^{17}
E = 44,200 cal/g-mole	0.10 - 0.54	1.4	1.74×10^{14}

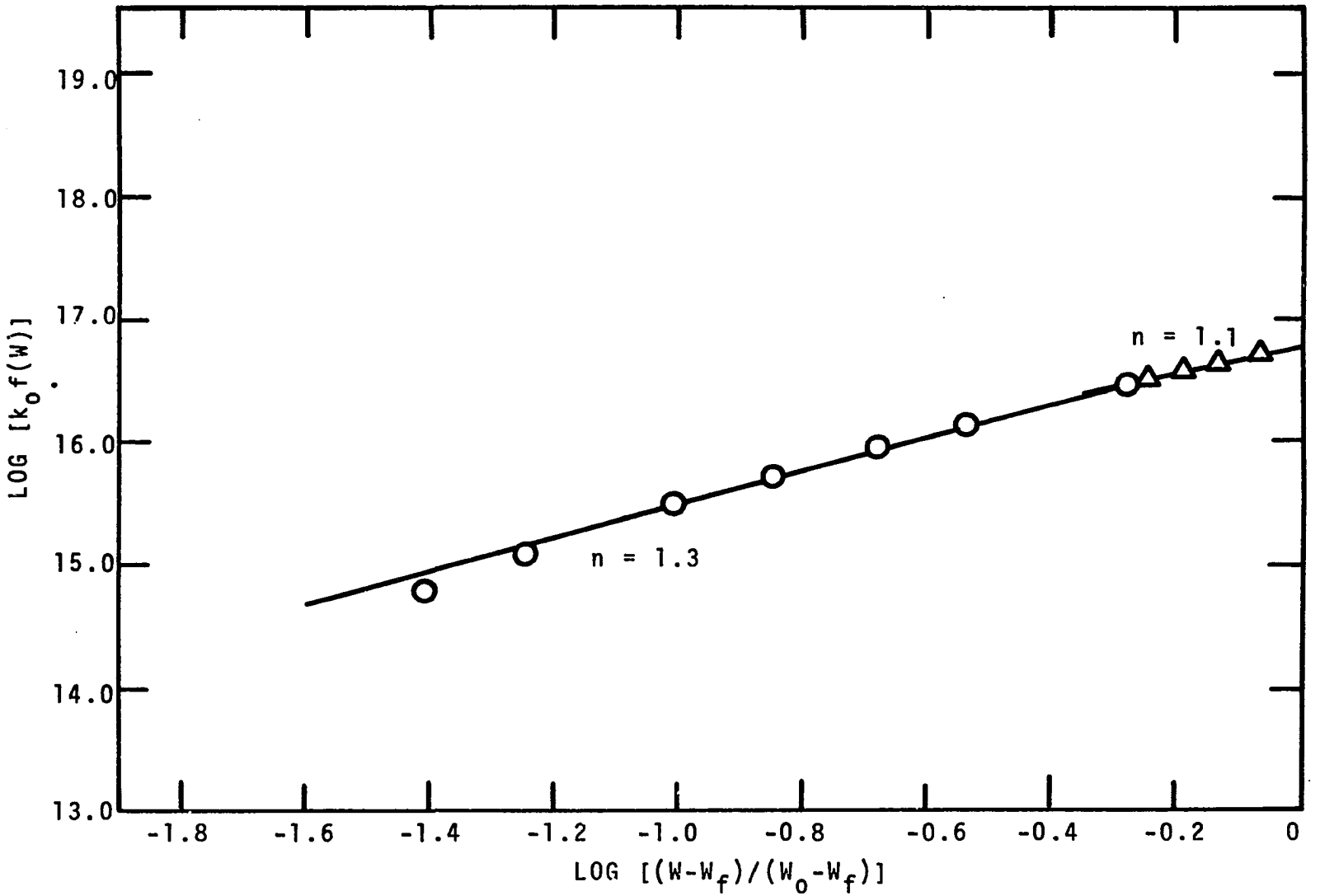

Figure III-20. Determination of the Order of Reaction and Frequency Factor for Spruce.

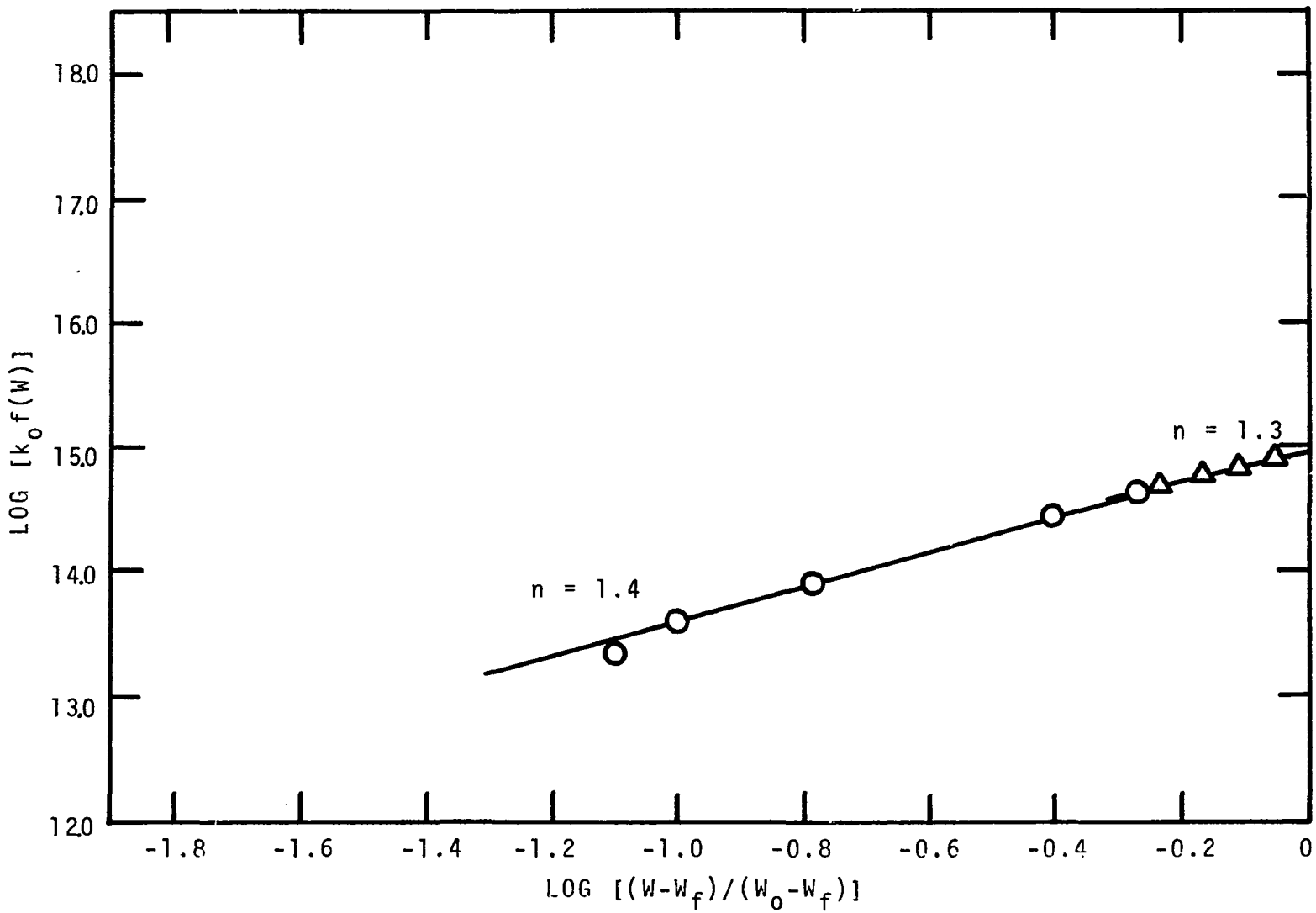

Figure III-21. Determination of the Order of Reaction and Frequency Factor for Redwood.

Measurement of "Energy Capacity" versus Temperature Relationship of Wood Using Differential Scanning Calorimetry

The DSC energy capacity technique was developed by Havens (18). He defined the energy capacity as the sum of the heat effects due to the sensible heat plus the heat generated or absorbed due to thermal decomposition; the energy capacity is assumed to be a function of temperature only. With this total heat effect lumped together, the number of parameters required to be specified is reduced and the problem of interaction of error in the specification of the data is minimized. This technique was used by Havens to measure the heat capacity of wood, and it was further demonstrated by Brown (7) at a heating rate of 20°C/min only. For providing data needed to solve the mathematical model, it is desired to extend the energy capacity measurements from 20°C/min to higher heating rates. The energy capacity of wood at heating rates higher than 20°C/min was not available before this study. The instrument used in this study was the Perkin-Elmer DSC-1B shown in Figure III-22. An excellent discussion on calorimetry in general, the relative merits of the DSC-1B as compared to similar instruments, and successful operation of the DSC-1B were presented by Havens (18), Brown (7), and Woodard (46). Only a brief and somewhat simplified description of the DSC-1B will be presented.

The DSC-1B sample holder assembly consists of two sample holders, one for the wood sample and one for the

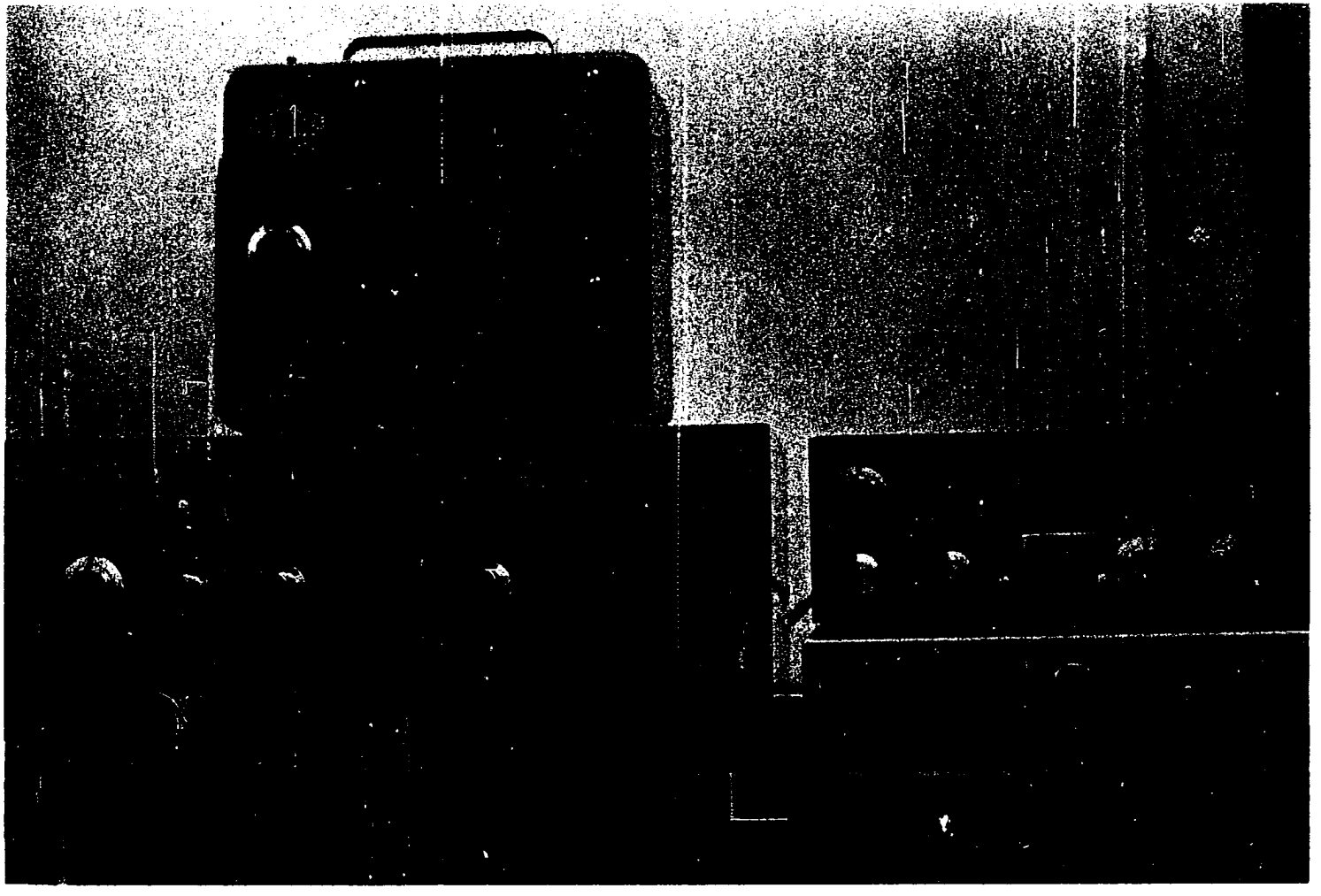

Figure III-22. Perkin-Elmer DSC-1B.

reference, and an inlet and exit line for the purge gas. Each sample holder has its own platinum resistance heater and temperature sensing element for temperature measurement and control. The electrical circuitry of the DSC-1B is designed for maintaining the two holders at the same temperature and measuring the difference in dissipated electrical energy required to maintain the two holders at the same temperature, while both the holders are being heated at a prescribed linear rate. The differential power requirement is dependent on three primary factors:

1. The heat capacity difference between the sample and reference holders.
2. The additional heat capacity of the sample.
3. The differences in heat losses from the sample holder and reference holder.

The only value of interest is the increment of differential power required to offset the additional heat capacity of the sample itself during a run. Ideally, if the two sample holders had exactly the same mass and heat capacity, and if the heat transfer characteristics of the two holders were identical with both holders empty, the amount of differential power required to maintain the two holders at the same temperature would be zero. Then, if a sample were placed in the sample holder and the reference holder left empty, the differential power required would reflect only the energy requirements of the sample. It is practically impossible to achieve

such conditions. However, this problem is partially overcome by running a "no sample" baseline, then running a sample under the same conditions and determining the differential power required by the sample by difference. In order to carry out this measurement, it has to be assured that the heat transfer characteristics of the two holders are the same during the sample and no-sample runs, independent of the contents of the sample holder. If there is a heat transfer property change, the differential energy supplied the two holders will reflect not only the energy requirements of the sample but also the energy requirements due to the change in this heat transfer property. This requirement can be checked on the instrument by simply allowing the recorder pen to reach its equilibrium position during isothermal operation at the beginning and end of the sample and no-sample runs, since at isothermal conditions the heat losses from the two sample holders should be the same regardless of the content of the holders. Thus, during isothermal operation at the beginning and end of the two runs, the sample line and the baseline should coincide. If the lines do not coincide the test is repeated because of the indication that the heat transfer characteristics have changed. This check on the reproducibility of heat losses from run to run is extremely important and without it there is no assurance that the change of differential energy corresponding to the heat capacity of the sample can be determined by difference.

By adjusting the flow pattern of the purge gas around the sample holders, covering the sample pan and contents with a thin aluminum disc, and placing of the radiation domes on the sample holders, several influential factors were reduced. There are two major influences, the temperature and emissivity of the radiation dome, which are difficult to control. The sensitivity of the DSC measurements due to changes in radiative heat transfer properties can be illustrated by a hypothetical heat capacity test. Suppose a sample weighing 10 mg with a specific heat of 0.35 cal/gm-°C is heated at 20°C/min in the DSC. Then the differential heat that must be supplied to offset the effect of sample heat capacity is

$$\frac{dq}{dt} = 10 \text{ mg } (0.35 \text{ mcal/gm-°C}) \left(\frac{20°C}{60 \text{ sec}}\right)$$

$$= 1.166 \text{ mcal/sec}$$

The surface area of the radiation dome is slightly greater than 1 cm^2, and if during a run the emissivity of the surface changes by 0.1 at 400°C, the differential heat which must be supplied to counteract the change in surface emissivity is:

$$\Delta\left(\frac{dq}{dt}\right) = 0.1\sigma AT^4$$

where σ = the Stefan-Boltzmann constant 1.355×10^{-9} (mcal/sec-cm^2-$°K^4$)

A = area of the radiation dome (cm^2)

T = temperature (°K)

Thus

$$\Delta\left(\frac{dq}{dt}\right) = 0.1(1.355 \times 10^{-9})(1)(673)^4 = 27 \text{ mcal/sec}$$

Obviously a small change in surface emissivity could become the dominant factor during a wood heat capacity measurement. Emissivity changes are due mainly to oxidation and condensation of the volatile products of decomposition on the dome surface. Proper conditioning of the radiation domes and adequate purging of the sample holder assembly will eliminate the problem of oxidation to a great extent. It is understood that the condensation of the volatile decomposition product on the dome influences the successful operation of the DSC to a large extent. Materials that produce a high percentage of light decomposition products will contribute much less error in the DSC operation than those materials that produce heavy, easily condensable products.

The DSC-1B requires three separate calibrations. These are power, temperature, and programmer calibrations.

A differential calibration is performed to ensure that both sample holders are at the same temperature as the temperature is programmed upward. In the DSC-1B this power calibration is normally accomplished using the heat of fusion of indium. The manufacturer suggested that the use of a calibration factor determined from the heat of fusion of indium, over the entire range of the instrument (0°-500°C) should not cause error in determinations of specific heat greater than

5 percent. Due to some unavoidable non-linearity in the control circuitry and to the inherent non-linearity of the platinum resistance temperature sensing elements, the temperature rise of the sample holders deviates from that indicated by the programmer as shown in Figure III-23. This difference in true temperature and programmer temperature was corrected by calibrating the programmer digital output against the melting points of indium (156.2°C), tin (231.9°C), lead (327.3°C) and zinc (419.5°C).

This non-linearity of the true heating rate can be eliminated by performing a specific heat type power calibration of the instrument. In this calibration the deflection of the instrument readout is measured from a no-sample baseline for an inert sample whose heat capacity as a function of temperature is accurately known. This deflection, Y', is equal to

$$Y' = \frac{m'C'}{K} \frac{dT}{dt} \qquad \text{(III-8)}$$

where Y' = pen deflection with standard material (cm)

K = calibration constant (cal/sec-cm)

$\frac{dT}{dt}$ = rate of temperature rise (°C/sec)

C' = heat capacity of standard (cal/gm-°C)

m' = mass of standard material (gm)

Likewise the deflection Y, obtained with the sample, is equal to

$$Y = \frac{mC}{K} \frac{dT}{dt} \qquad \text{(III-9)}$$

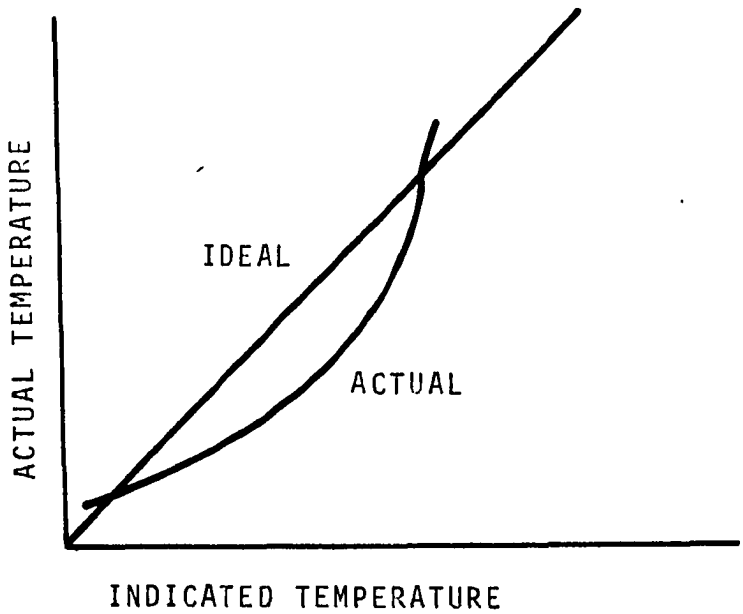

Figure III-23. Relation Between Programmed and Actual Temperatures in Perkin-Elmer DSC-1B Instrument.

where Y = pen deflection with sample (cm)

C = heat capacity of sample (cal/gm-°C)

m = mass of sample (gm)

This study used a small sapphire (Al_2O_3) disc of accurately known mass for such a specific heat calibration. Three runs were taken; one with empty holders, one with a sapphire standard, and one with the wood sample. The energy capacity of wood as a function of temperature was obtained by solving Equations III-8 and III-9.

$$C = \frac{Ym'}{Y'm} C' \qquad \text{(III-10)}$$

and the result is not affected by the non-linearity of the temperature program.

The energy capacity data obtained in this study for spruce and redwood are shown in Figures III-24 through III-29. The wood samples were prepared by grinding knot-free boards in a Wiley intermediate model laboratory mill. The fraction passing a 40-mesh screen was used for analysis. The samples were dried in the DSC-1B for 5 minutes at 100°C before beginning a run. The measurements were made at nominal heating rates of 20°, 40° and 80°C/min and a nitrogen purge flow rate of 100 ml/min.

The total energy as a function of temperature at the specified heating rate of two wood samples may be obtained directly from these figures by integration of the dE*/dt curves. The results of these integrations were used in the model. The

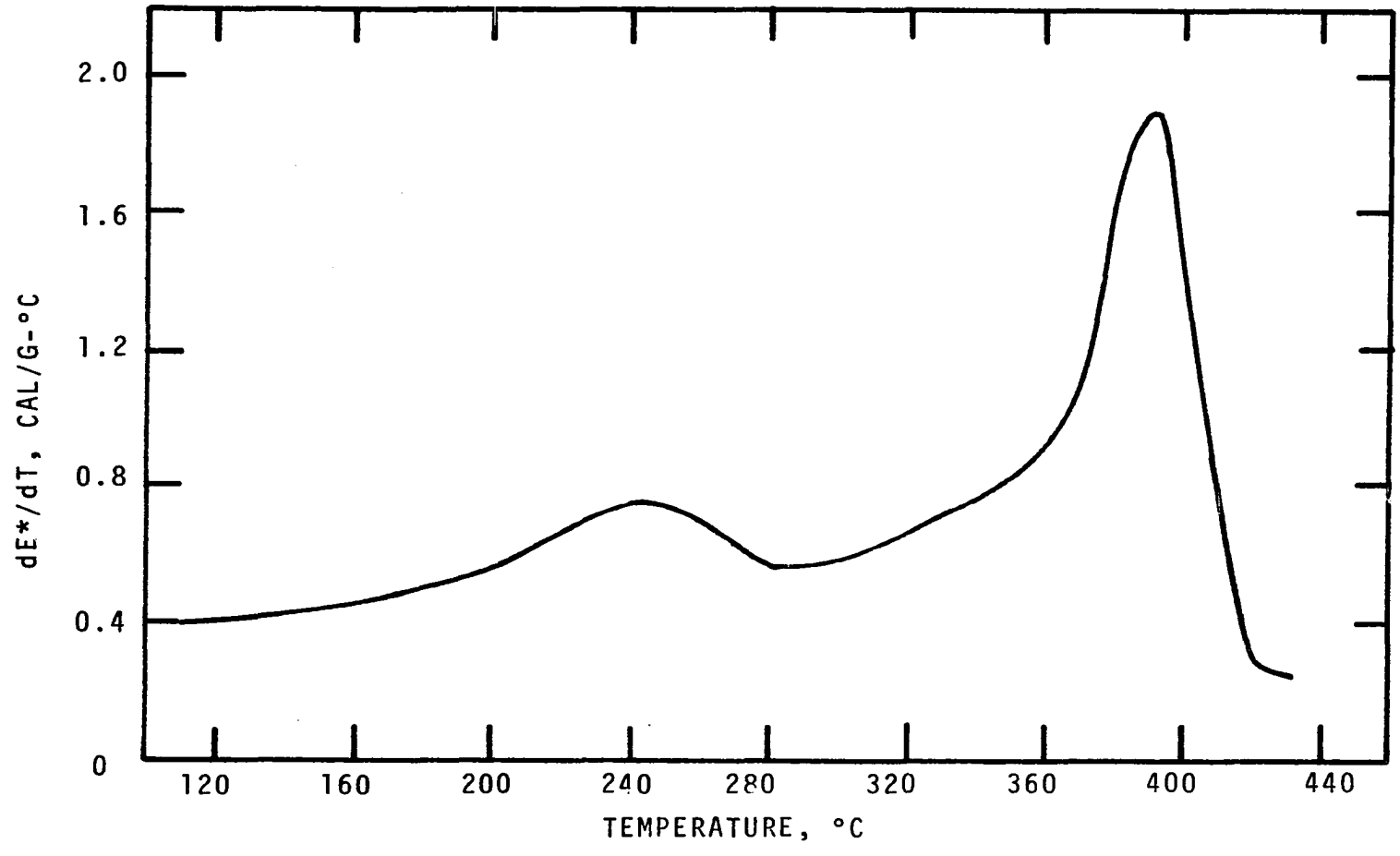

Figure III-24. Energy Capacity of Redwood as a Function of Temperature at a Nominal Heating Rate of 20°C/min (Based on Decomposable Weight).

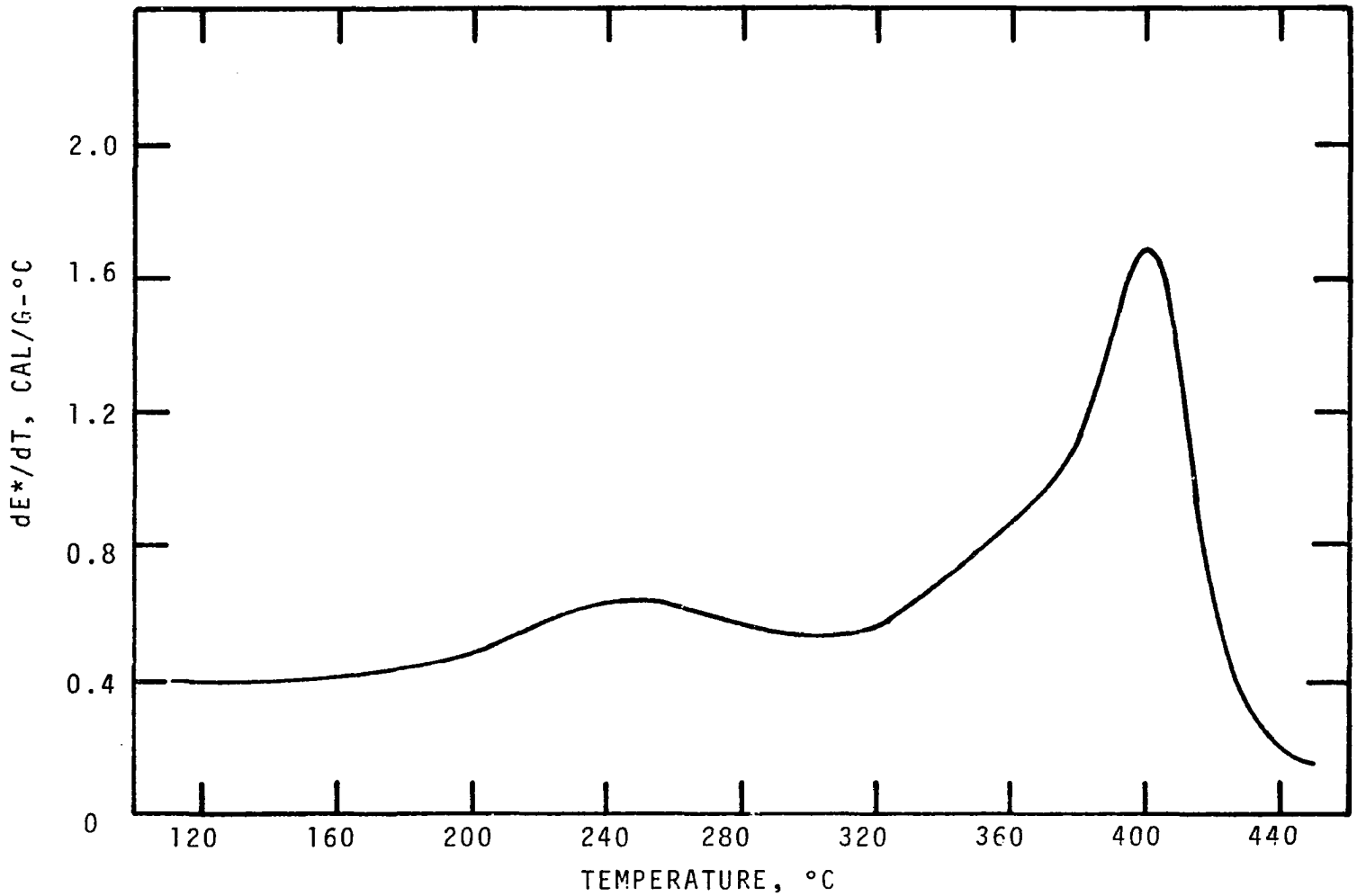

Figure III-25. Energy Capacity of Redwood as a Function of Temperature at a Nominal Heating Rate of 40°C/min (Based on Decomposable Weight).

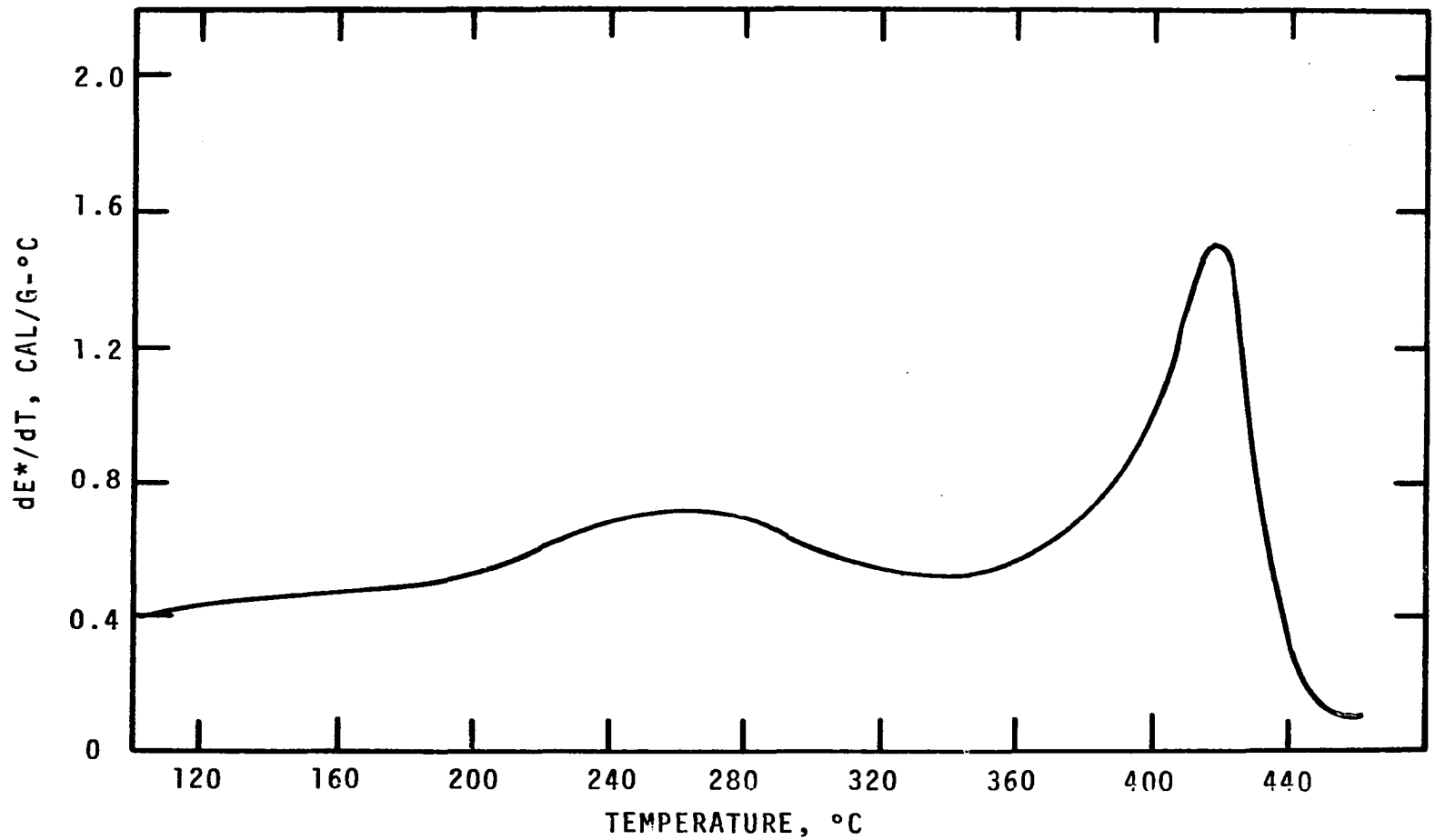

Figure III-26. Energy Capacity of Redwood as a Function of Temperature at a Nominal Heating Rate of 80°C/min (Based on Decomposable Weight).

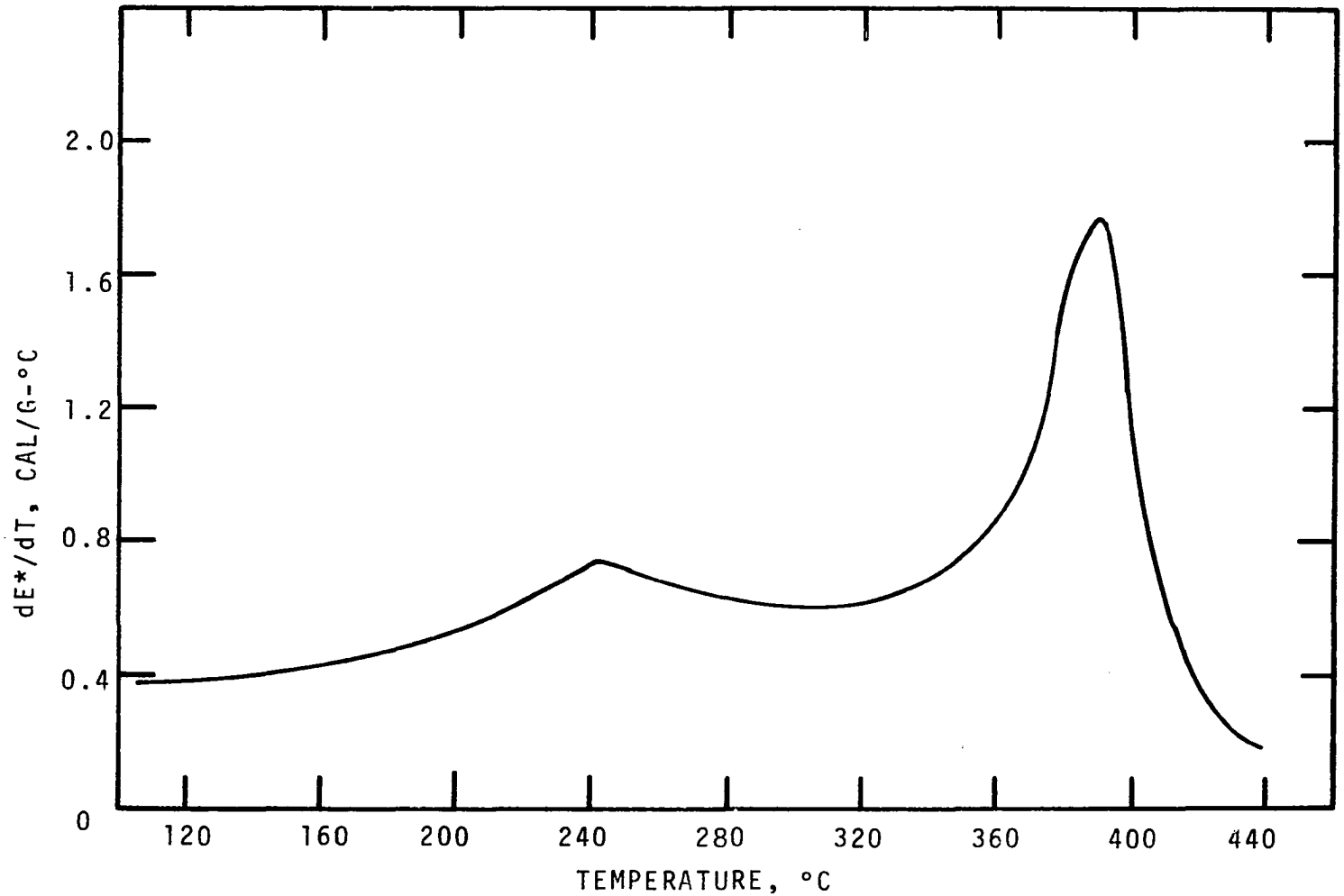

Figure III-27. Energy Capacity of Spruce as a Function of Temperature at a Nominal Heating Rate of 20°C/min (Based on Decomposable Weight).

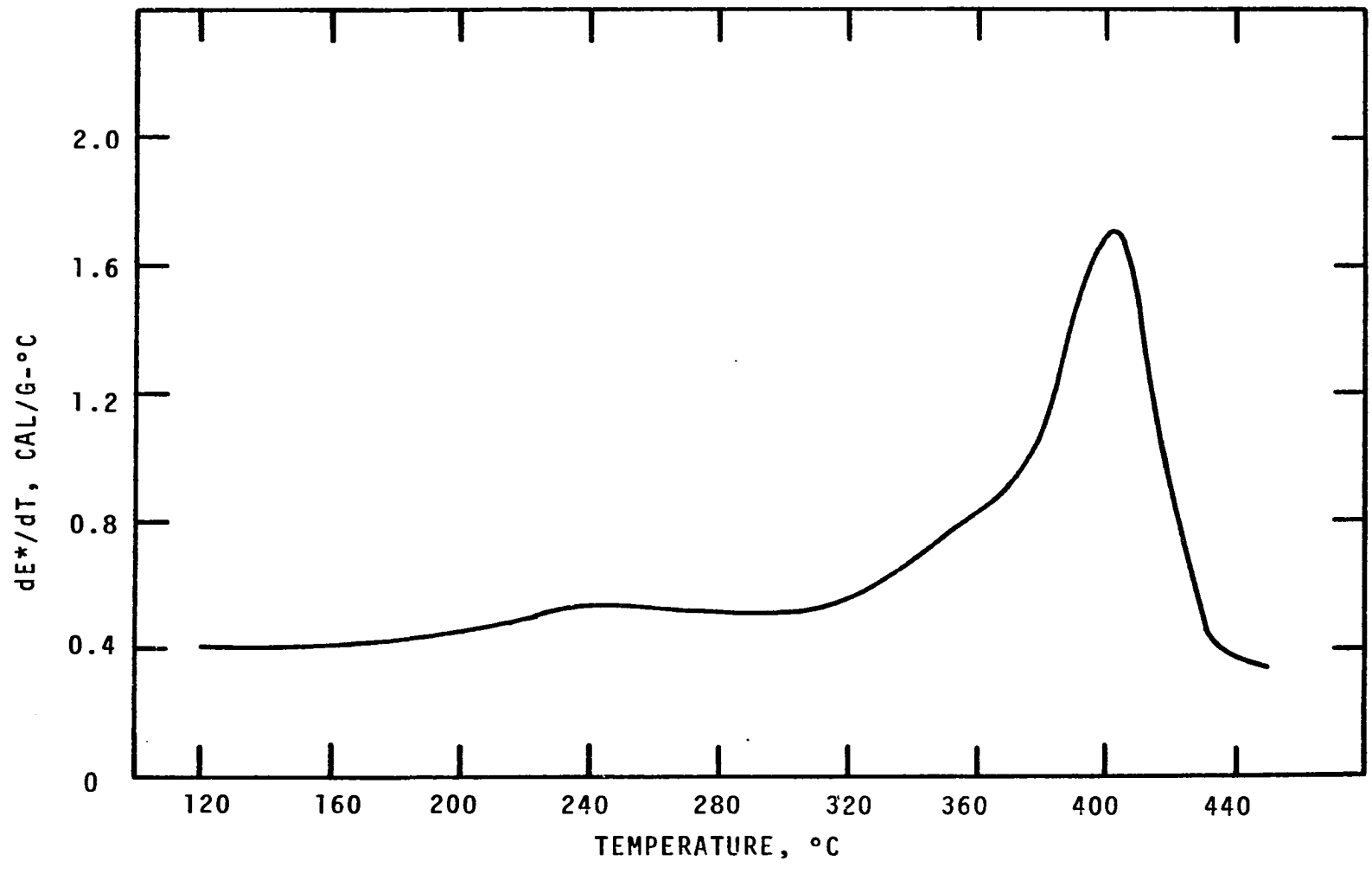

Figure III-28. Energy Capacity of Spruce as a Function of Temperature at a Nominal Heating Rate of 40°C/min (Based on Decomposable Weight).

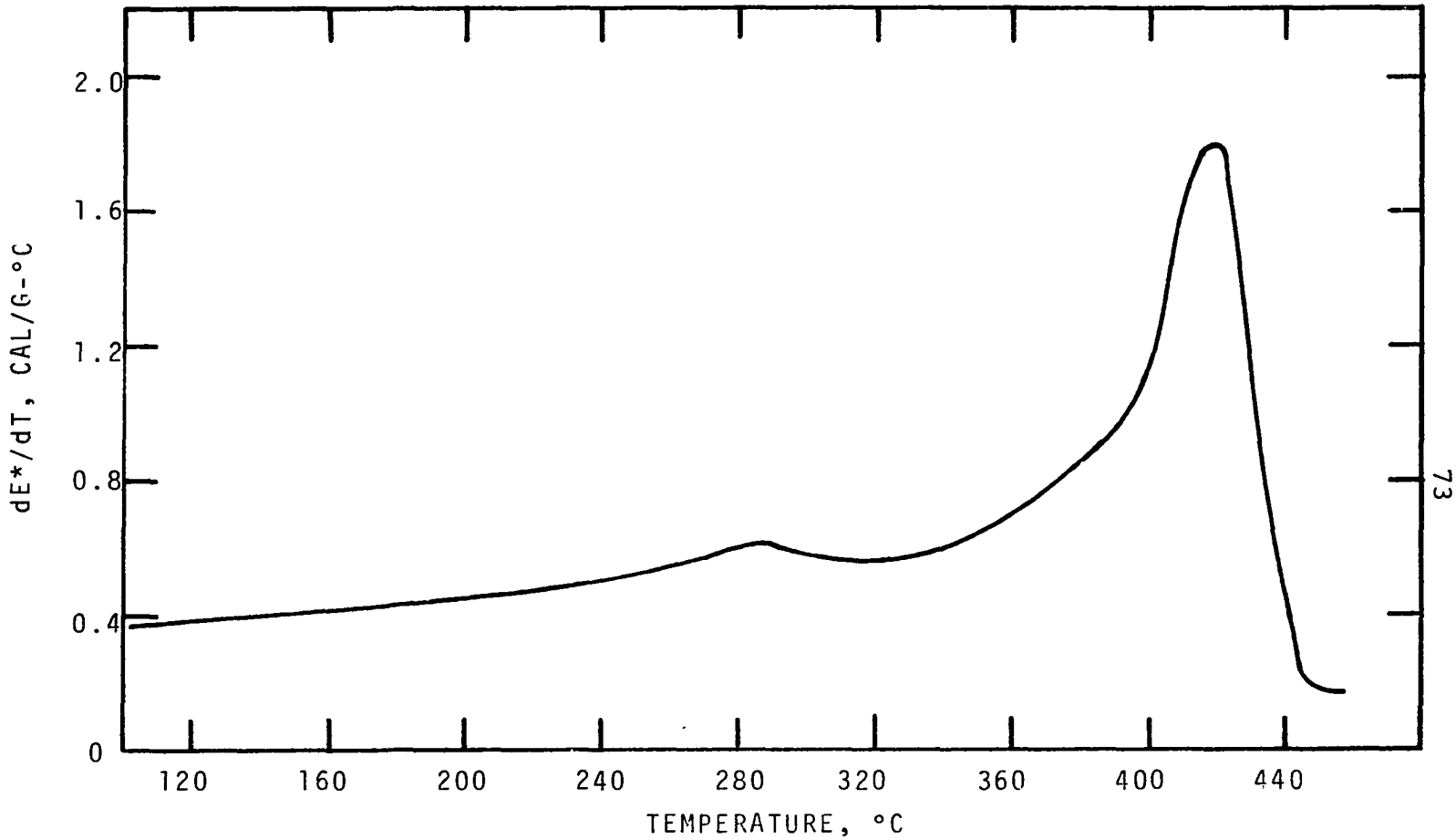

Figure III-29. Energy Capacity of Spruce as a Function of Temperature at a Nominal Heating Rate of 80°C/min (Based on Decomposable Weight).

shift in the dE*/dt curves with heating rate showed the corresponding features in the TG and DTG curves. These qualitative phenomena revealed that the pyrolysis mechanisms are consistant in both measurements. This aberration is a further indication that the degradation kinetics are not a function of heating rate.

CHAPTER IV

MATHEMATICAL MODEL

The prediction of ignition time based on a set of ignition criteria and measurements of pyrolysis parameters of wood samples requires the solution of the unsteady state transport equations for a heterogeneous medium in which phase changes and chemical reactions are occurring. The transport equation for a wood sample subjected to extensive radiation can be written, neglecting potential energy effects, kinetic energy effects and kinetic effects due to bulk flow, as follows

$$\frac{\partial}{\partial t}(\rho\bar{E}) = -\nabla\cdot\vec{q} - \nabla\cdot\vec{m}_f\bar{H}_f \qquad \text{(IV-1)}$$

where ρ = density of wood specimen (gm/cm^3)

$\bar{E}$ = specific internal energy of wood specimen (cal/gm)

$\vec{q}$ = heat flux vector ($cal/sec\text{-}cm^2$)

$\vec{m}_f$ = mass flux vector for fluid ($gm/cm^2\text{-}sec$)

$\bar{H}_f$ = specific enthalpy of fluid (cal/gm)

Combining Equation IV-1 with the equation of continuity

$$\nabla\cdot\vec{m}_f = -\partial\rho/\partial t \qquad \text{(IV-2)}$$

for a differential element gives

$$[\rho(\frac{\partial \bar{E}}{\partial t})_X + (\bar{E}-\bar{H}_f)(\frac{\partial \rho}{\partial t})_X] = -\nabla\cdot\vec{q} - \vec{m}_f\nabla\cdot\bar{H}_f \qquad \text{(IV-3)}$$

where x denotes the position vector.

If it is assumed that the dimensions of the sample remain constant, and if both the sample density and internal energy are functions of temperature and heating rate, i.e.,

$$\rho = f(T,\phi) \qquad \text{(IV-4)}$$

and

$$\bar{E} = q(T,\phi) \qquad \text{(IV-5)}$$

then Equation IV-3 becomes

$$\{\rho[(\frac{\partial \bar{E}}{\partial T})_\phi + (\frac{\partial \bar{E}}{\partial \phi})_T (\frac{\partial \phi}{\partial T})]_X + (\bar{E}-\bar{H}_f)[(\frac{\partial \rho}{\partial T})_\phi + (\frac{\partial \rho}{\partial \phi})_T (\frac{\partial \phi}{\partial T})]_X\}\frac{\partial T}{\partial t}$$

$$= -\nabla\cdot\vec{q} - \vec{m}_f\nabla\cdot\bar{H}_f \qquad \text{(IV-6)}$$

Equation IV-6 is exact for very small samples where temperature and density are uniform throughout the sample. The DSC measurements made in this study satisfy these criteria. Neglecting the bulk flow of gases, dividing Equation IV-6 by the initial mass of the sample, $m_o\rho_o v_o$, and integrating over the volume of the sample, the following equation is obtained

$$[\frac{\rho}{\rho_o}(\frac{\partial \bar{E}}{\partial T}) + (\bar{E}-\bar{H}_f)\frac{\partial(\rho/\rho_o)}{\partial T}]\frac{dT}{dt} = (-\int_V \nabla\cdot\vec{q}\,\frac{dv}{\rho_o v_o}) \qquad \text{(IV-7)}$$

where m_o = initial mass (gm)

ρ_o = initial density (gm/cm^3)

v_o = initial volume (cm^3)

The left side of Equation IV-7 consists of two terms; the first represents the sensible energy required to raise the temperature of the wood; the second represents the energy required to pyrolyze the wood to a fluid of enthalpy $\bar{H}_f$. If a small DSC test specimen is used such that locally isentropic properties can be assumed then the energy capacity measured using DSC is identical to the quantity represented by Equation IV-7.

The energy capacity measured using DSC at any specified heating rate can be applied to heat conduction in pyrolyzing wood as follows:

$$\left[\frac{\partial E^*}{\partial T}\ \frac{\partial T}{\partial t}\right]_y = \nabla \cdot k \nabla T \qquad \text{(IV-8)}$$

where $\partial E^*/\partial T = (\rho/\rho_o\ \partial\bar{E}/\partial T + (\bar{E} - \bar{H}_f)\partial(\rho/\rho_o)/\partial T]$

y = over the small element represented by the position vector y

This expression is the one proposed by Havens (18). However, dE*/dT had not been measured directly previously to Havens' work. Equation IV-8 with its boundary conditions

$$\partial T/\partial x = 0 \quad \text{for } x \to \infty \qquad \text{(IV-9)}$$

$$-k\ \partial T/\partial x\Big|_{x=0} = \bar{\alpha}H_i - h(T-T_\infty) - \bar{\varepsilon}\sigma T^4 \qquad \text{(IV-10)}$$

and initial condition

$$T = T_o \quad \text{for } t \leq 0 \qquad \text{(IV-11)}$$

is applicable for thermally thick, opaque samples, which covers most ignition tests using wood samples.

The numerical solution of this nonlinear boundary value problem has been developed by Hashemi (17) for predicting transient temperature profiles in frozen soil. In Hashemi's model, a region of interest is divided into a set of cells of finite dimensions, and a heat balance is written on each cell. The requirement of a heat balance for each cell can be guaranteed using this procedure even though the rates of heat transfer at the boundaries are approximate. Using this technique the problem in obtaining a consistent set of difference equations is avoided. Hashemi's technique is used in this study.

To illustrate the procedure for setting such a set of difference equations, consider a two-dimensional region in which a network of mesh points has been developed by the intersection of N_x lines parallel to the x-axis and N_y lines parallel to the y-axis. Let the intersection of the ith line parallel to the x-axis and j^{th} line parallel to the y-axis (the point x_i, y_j) be a mesh point, denoted as (i,j). Let the distance between mesh points (i,j) and (i-1,j) be h_i, $1 \leq i \leq N_x$, and the distance between mesh points (i,j) and (i,j-1) be k_j, $1 \leq j \leq N_y$. Let the rectangle defined by lines $x_i - 1/2\ h_i$, $x_i + 1/2\ h_{i+1}$, $y_j - 1/2\ k_j$, and $y_j + 1/2\ k_{j+1}$ be the mesh region

(i,j). Figure IV-1 shows one such mesh region and its adjacent mesh points.

Assume that for a two-dimensional locally isotropic medium the heat fluxes in the x and y directions obey Fourier's Law and are given by Equation IV-12.

$$j_x = -K \frac{\partial T}{\partial x} \simeq - \frac{T(x+\Delta x,y) - T(x,y)}{R\Delta x}$$

$$j_y = -K \frac{\partial T}{\partial y} \simeq - \frac{T(x, y+\Delta y) - T(x,y)}{R\Delta y} \qquad \text{(IV-12)}$$

where j_x, j_y = heat fluxes in x and y directions respectively (cal/cm^2-sec)

K = thermal conductivity (cal/cm^2-sec-°C/cm)

T = temperature (°C)

R = 1/K, the thermal resistivity (cm-sec-°C/cal)

Let the temperature T at a mesh point (i,j) be $T_{i,j}$ and the average value of the thermal resistivity, R, and the internal energy, E*, for a mesh region (i,j) be $R_{i,j}$ and $E^*_{i,j}$, respectively. Let the average values of $R_{i,j}$ and $E^*_{i,j}$ be those obtained at the temperature $T_{i,j}$ of the mesh point (i,j).

Let the rates at which heat is transferred by conduction into the mesh region (i,j) through sides 1, 2, 3 and 4 (see Figure IV-1) be q_1, q_2, q_3 and q_4, respectively. Then the heat balance around a mesh region (i,j) is

$$(q_1 - q_2) + (q_3 - q_4) = \Delta V_{i,j} \frac{dE^*_{i,j}}{dt} \qquad \text{(IV-13)}$$

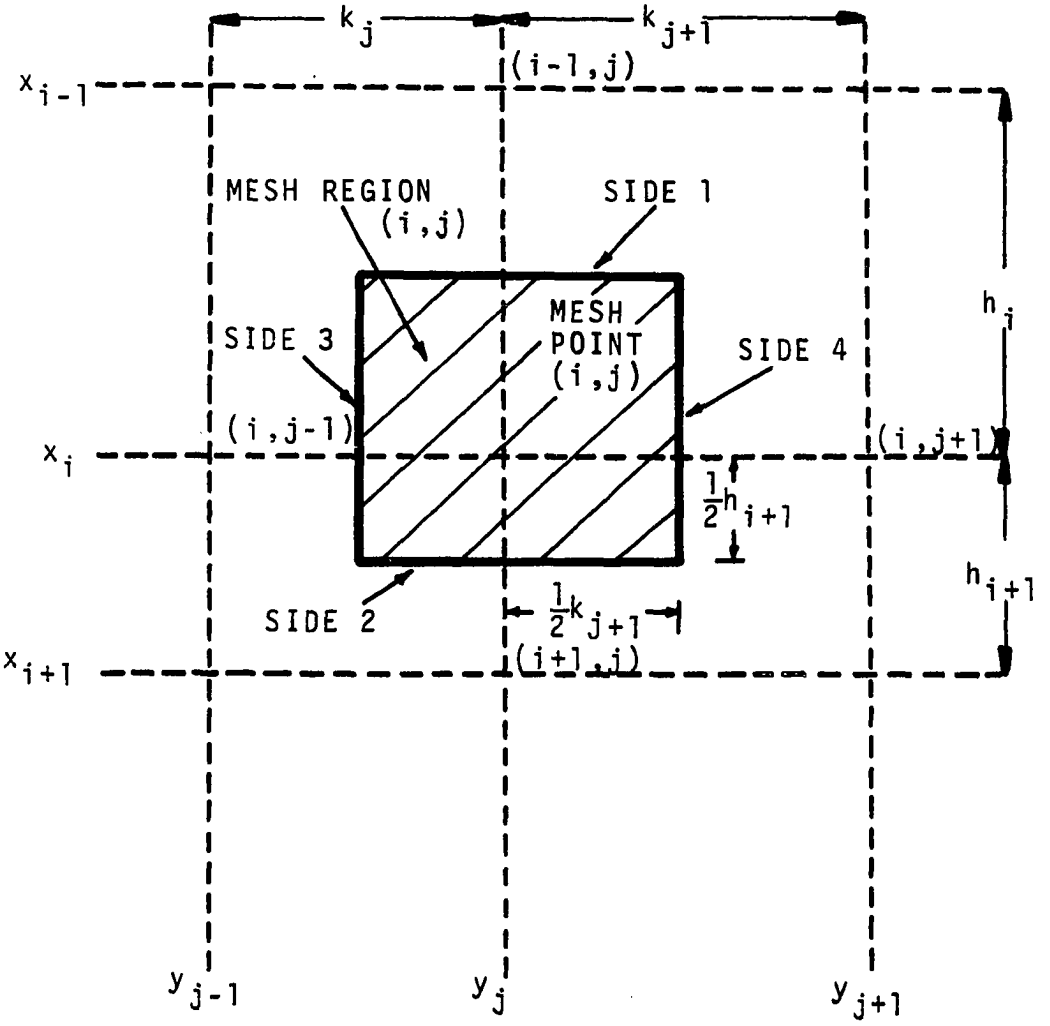

Figure IV-1. A Mesh Region (i,j) and Its Adjacent Mesh Points.

where $\Delta V_{i,j}$ is the volume of the mesh region (i,j) and is given by

$$\Delta V_{i,j} = \Delta z(1/2\ h_i + 1/2\ h_{i+1})(1/2\ h_j + 1/2\ h_{j+1}) \qquad \text{(IV-14)}$$

where Δz = the thickness of the region

q_1, q_2, q_3 and q_4 can be approximated with the aid of Equation IV-12 to obtain

$$q_1 = -1/2\ \Delta z(k_j + k_{j+1})(T_{i,j} - T_{i-1,j}) \div [1/2\ h_i(R_{i,j} + R_{i-1,j})]$$

$$q_2 = -1/2\ \Delta z(k_j + k_{j+1})(T_{i+1,j} - T_{i,j}) \div [1/2\ h_{i+1}(R_{i,j} + R_{i+1,j})]$$

$$q_3 = -1/2\ \Delta z(h_i + h_{i+1})(T_{i,j} - T_{i,j-1}) \div [1/2\ k_j(R_{i,j} + R_{i,j-1})]$$

$$q_4 = -1/2\ \Delta z(h_i + h_{i+1})(T_{i,j+1} - T_{i,j}) \div [1/2\ k_{j+1}(R_{i,j} + R_{i,j+1})] \qquad \text{(IV-15)}$$

Equations IV-15, when substituted in Equation IV-13, result in the desired difference equations. However, it is helpful to write the resulting difference equation in terms of dimensionless variables. To this end let

$$u_{i,j} = (T_{i,j} - T_1)/(T_2 - T_1)$$
$$r_{i,j} = 1/2\ K_o R_{i,j}$$

$$
\begin{aligned}
e_{i,j} &= E^{*}_{i,j}/[C_o(T_2 - T_1)] \\
\tau &= K_o t/(C_o h^2) \\
C_i &= 2h^2/h_i(h_i + h_{i+1}) \\
C_j &= 2h^2/k_j(k_j + k_{j+1}) \\
b_i &= 2h^2/h_{i+1}(h_i + h_{i+1}) \\
b_j &= 2h^2/k_{j+1}(k_j + k_{j+1})
\end{aligned}
\qquad \text{(IV-16)}
$$

Substituting Equations IV-15 into Equation IV-13, rearranging, and dividing by $K_o(T_2 - T_1)\Delta V_{i,j}/h^2$ gives

$$
\begin{aligned}
&\frac{-C_i u_{i-1,j}}{r_{i,j} + r_{i-1,j}} + \left(\frac{C_i}{r_{i,j} + r_{i-1,j}} + \frac{b_i}{r_{i,j} + r_{i+1,j}}\right) u_{i,j} \\
&- \frac{b_i u_{i+1,j}}{r_{i,j} + r_{i+1,j}} - \frac{C_j u_{i,j-1}}{r_{i,j} + r_{i,j-1}} + \left(\frac{C_j}{r_{i,j} + r_{i,j-1}}\right. \\
&\left. + \frac{b_i u_{i+1,j}}{r_{i,j} + r_{i,j+1}}\right) u_{i,j} - \frac{b_j u_{i,j+1}}{r_{i,j} + r_{i,j+1}} + \frac{de_{i,j}}{d\tau} = 0
\end{aligned}
\qquad \text{(IV-17)}
$$

where u = dimensionless temperature $(T-T_2)/(T_2-T_1)$

r = dimensionless thermal resistivity $(1/2\ K_o/K)$

K_o = reference state thermal conductivity (cal/cm^2-sec-°C/cm)

$E^{*}_{i,j}$ = internal energy (including sensible and decomposition heats) (cal/cm^3-°C)

$e_{i,j}$ = dimensionless internal energy

C_o = reference state specific heat (cal/cm^3-°C)

τ = dimensionless time

h = a geometrical scaling factor (cm)

c_i, c_j = dimensionless geometrical factors

b_i, b_j = dimensionless geometrical factors

For each mesh point at which the dimensionless temperature $u_{i,j}$ is unknown one obtains one equation such as Equation IV-17. For N mesh points one then has a set of N simultaneous equations to be solved for N unknowns.

The nonlinearity of the problem of heat conduction accompanied by decomposition is due to the strongly non-linear relation between $e_{i,j}$ and $u_{i,j}$, particularly in the range of temperatures where thermal decomposition occurs. If the internal energy $e_{i,j}$, which includes decomposition and sensible heat effects, is assumed to be an explicit function of temperature only, and not a function of the rate of change of temperature (in other words, if it is assumed to be independent of the rate of heating), one can write

$$\frac{de_{i,j}}{d\tau} = \frac{de_{i,j}}{du_{i,j}} \frac{du_{i,j}}{d\tau} = \phi_{i,j} \frac{du_{i,j}}{d\tau} \qquad \text{(IV-18)}$$

where $\phi_{i,j}$ can be thought of as an "energy capacity,"

Utilizing the relation given by Equation IV-18, the N simultaneous equations (Equation IV-17) for the N unknown values of $u_{i,j}$ can be expressed in matrix notation as

$$\Phi \frac{dU(\tau)}{d\tau} + (H + V)\, U(\tau) = S(\tau) \qquad \text{(IV-19)}$$

where Φ = an NxN diagonal matrix whose entries are the values of $\phi_{i,j}$

U = an N-dimensional vector whose entries are the unknown values of $u_{i,j}$

S = an N-dimensional source vector whose entries are zero when the mesh region (i,j) is not adjacent to the boundary, and contain information related to boundary conditions when the mesh region (i,j) is adjacent to the boundary

H and V are real NxN matrices with positive diagonal entries and non-positive off-diagonal entries, and both H and V have at most three non-zero entries per row. If one orders the mesh points by rows, i.e., from left to right, top to bottom, then H is the direct sum of tridiagonal matrices, i.e.,

$$H = \begin{bmatrix} H_1 & & & \\ & H_2 & & \\ & & \ddots & \\ & & & H_{Nx} \end{bmatrix}$$

where H_i, $1 \leq i \leq N_x$ are tridiagonal matrices whose diagonal entries are $[c_i/(r_{i,j} + r_{i-1,j}) + b_i/(r_{i,j} + r_{i+1,j})]$ and the off diagonal entries are $-c_i/(r_{i,j} + r_{i-1,j})$ and $-b_i/(r_{i,j} + r_{i+1,j})$. If instead, the mesh points are ordered by columns, i.e., from top to bottom, left to right, then V is the direct sum of tridiagonal matrices V_j, $1 \leq j \leq N_y$, i.e.,

$$V = \begin{bmatrix} V_1 & & & \\ & V_2 & & \\ & & \ddots & \\ & & & V_{Ny} \end{bmatrix}$$

where V_j, $1 \leq j \leq N_y$ are tridiagonal matrices whose diagonal entries are $[c_j/(r_{i,j} + r_{i,j-1}) + b_j/(r_{i,j} + r_{i,j+1})]$ and the off-diagonal entries are $-c_j/(r_{i,j} + r_{i,j-1})$ and $-b_j/(r_{i,j} + r_{i,j+1})$.

Equation IV-18 is applicable to all mesh regions of interest, including the mesh regions adjacent to the boundary surface. For example, if side 1 of a mesh region (i,j) is insulated, then one sets $r_{i-1,j} = \infty$ (in practice a very large number, say 10^6, would be used). If, instead, the temperature on side 1 of mesh region (i,j) (i.e., $u_{i-1,j}$) is prescribed, then one sets $r_{i\pm1,j} = 0$ and moves the expression $c_i u_{i-1,j}/r_{i,j}$ to the right side of Equation IV-17. Obviously one can use a similar method to specify a prescribed temperature on any other side or more than one side of any mesh region.

All natural boundary conditions fall into two categories: (1) the heat flux at the boundary is prescribed, or (2) the environment temperature is prescribed. When the heat flux is prescribed, the thermal resistivity of the external region is set equal to infinity and the prescribed value(s) of q_i, $1 \leq i \leq 4$, after being divided by K_o, $(T_2 - T_1)V_{i,j}/h^2$ is

added to the right hand side of Equation IV-17. When the temperature of the environment is prescribed, the value of thermal resistivity of the external mesh region is set equal to the heat transfer resistance at the boundary. When this resistance is zero, the boundary temperature is equal to the environment temperature.

Computer programs for solution of the temperature distribution in the region of interest (i.e., the solution of the system of first order, differential Equations IV-17) have been developed by Hashemi (17). The numerical procedure is based on a variant of the Peaceman-Rachford alternating direction, implicit iterative method which has been thoroughly discussed by Varga (40).

Havens, in applying the numerical technique of Hashemi, stated that if the "energy capacity" $de_{i,j}/du = \phi_{i,j} = f(u)$ (which includes heat effects due to decomposition as well as sensible heat effects), and the thermal conductivity K(u) can be specified, the transient temperature distribution of a wood sample undergoing pyrolysis can be computed.

The energy capacity data used by both Havens and Brown were obtained from DSC measurements of white pine and oak at a heating rate of 20°C/min. Due to the lack of experimental thermal conductivity for char, Havens used TG data obtained at a heating rate of 20°C/min to predict density and then used MacLean's thermal conductivity correlation to compute conductivity as a function of temperature. Brown (7) has

measured the values of char thermal conductivity which he found are approximately three times greater than that predicted by the density correlation. The dependency of thermal conductivity on temperature proposed by Brown is shown in Figure IV-2 and is used in the numerical solution of the model. It was developed based on the TG weight loss data obtained at a heating rate of 20°C/min. Thus at temperatures up to 280°C and above 420°C the thermal conductivity is the thermal conductivity for undecomposed and charred wood respectively. For the thermal conductivity of pyrolyzing wood a linear approximation has been made between the thermal conductivity of charred and uncharred wood and is shown as the dashed line between 280° and 420°C. At heating rates other than 20°C/min the thermal conductivity dependency on temperature was adjusted by assuming that the pyrolyzing wood totally charred at 2 percent weight remaining. The corresponding temperature at 2 percent weight remaining of the TG curve was chosen for the upper bound of the linear relationship between thermal conductivity and temperature.

Both Havens and Brown have demonstrated the validity of the model, the energy capacity data, and the weight loss data by comparing computed temperature profiles and mass losses with experimental data. This technique was used in this study to predict transient temperature profiles in the pyrolyzing wood. The surface temperature as a function of time was also estimated.

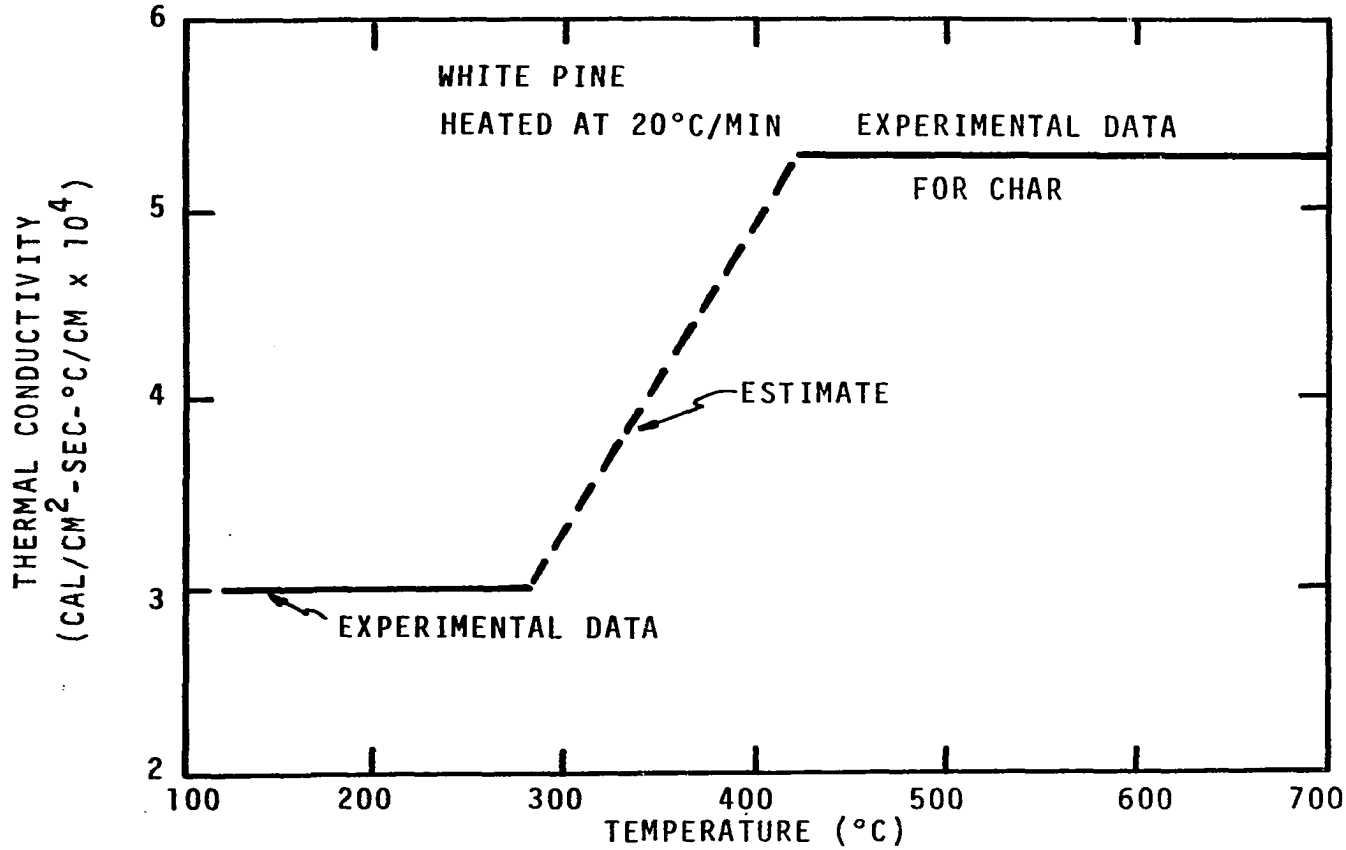

Figure IV-2. Thermal Conductivity of White Pine as a Function of Temperature.

The "energy capacity" for wood samples was not measured previous to Havens' work. However, both Havens and Brown only measured the energy capacity for wood at a heating rate of 20°C/min. Brown extended the energy capacity curve obtained at 20°C/min as a reference and applied a temperature correction to that data to define the energy capacity data at other heating rates. In this study, the energy capacities for spruce and redwood were measured at heating rates of 20°C/min, 40°C/min and 80°C/min as shown in Figures IV-3 and IV-4. It should be more reliable to predict the ignition time if the effect of heating rate on energy capacity can be measured directly at any specific heating rate for the ignition test. The highest heating rate of the Perkin-Elmer DSC-1B is 80°C/min. However, it is justified that the set of energy capacity data measured at 20°, 40° and 80°C/min can be extrapolated to the higher heating rate desired if the detailed chemical mechanism for wood pyrolysis is independent of heating rate.

It has been shown in the previous chapter that at heating rates up to 160°C/min the overall pyrolysis chemistry for spruce and redwood is independent of heating rate. The only effect of heating rate is to displace the weight loss curve. The consistent fact can be examined from Figures IV-3 and IV-4 which show that the total energy required to raise the temperature where the wood is totally charred is the same regardless of the path by which the heating was accomplished.

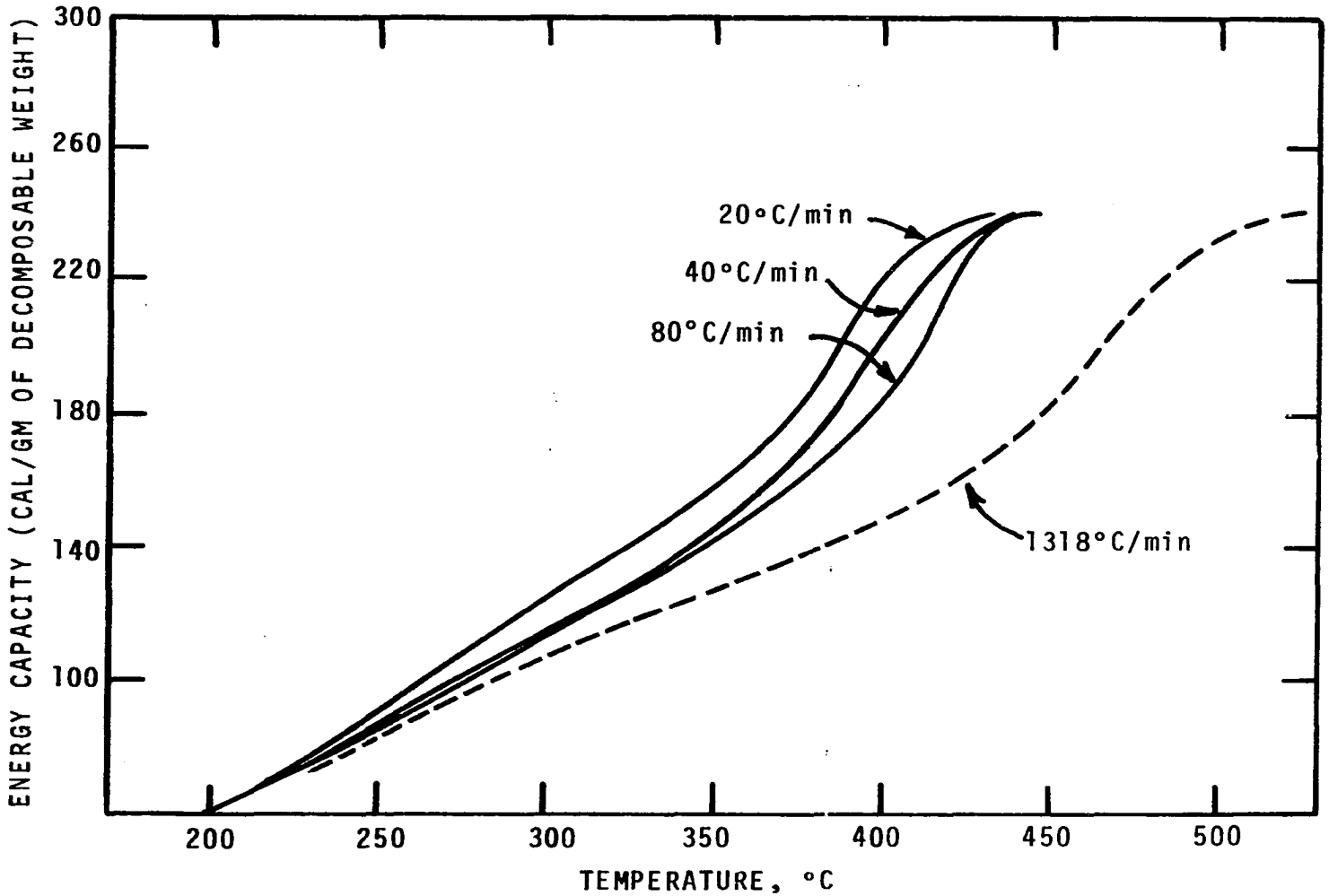

Figure IV-3. Estimate of Effect of Heating Rate on Heat of Pyrolysis for Spruce.

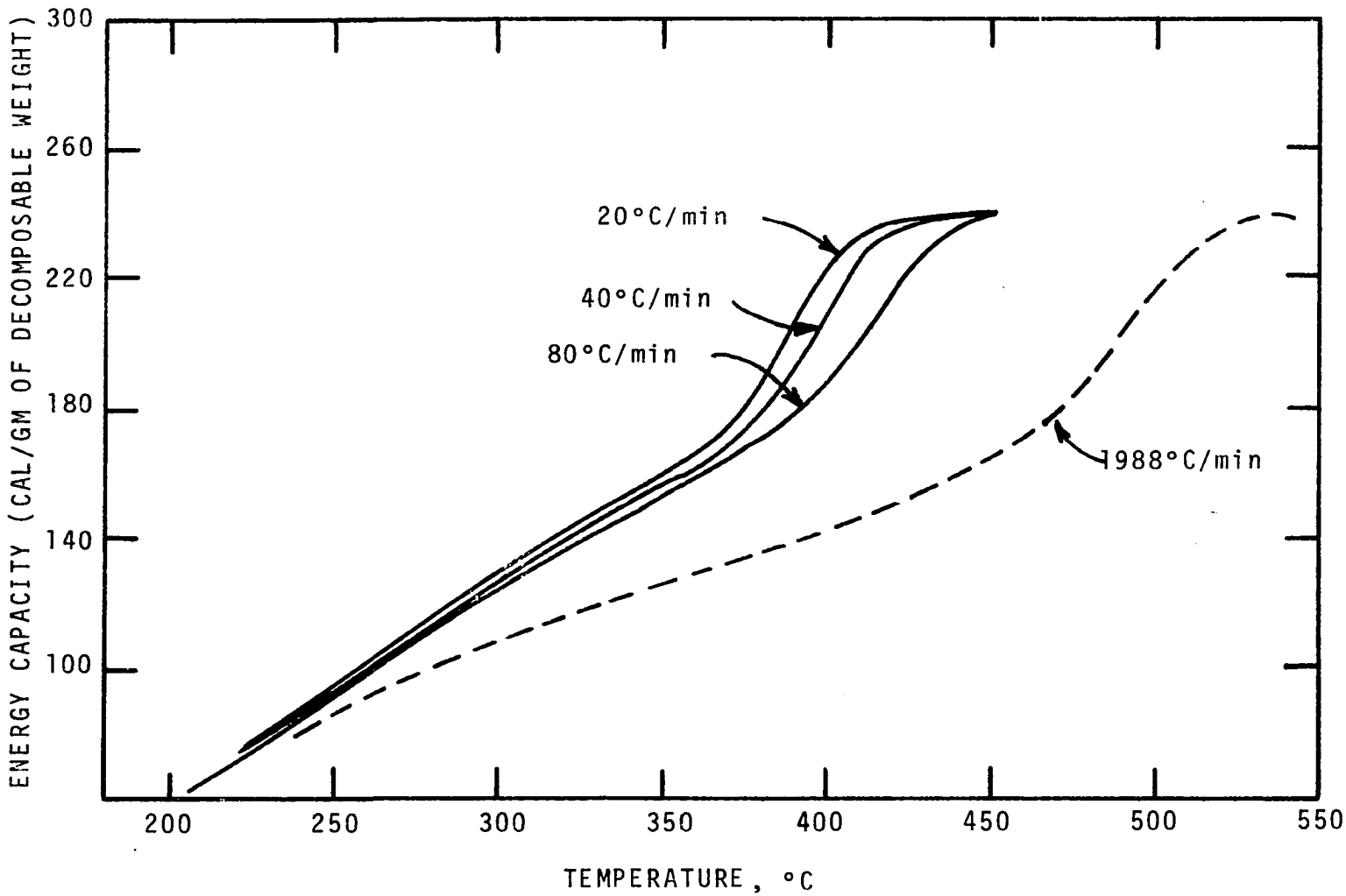

Figure IV-4. Estimate of Effect of Heating Rate on Heat of Pyrolysis for Redwood.

Extrapolations of energy capacity against temperature at higher heating rates are shown as dotted curves in Figures IV-3 and IV-4. As the effect of heating rate on energy capacity, weight loss and thermal conductivity can be quantitatively expressed as a function of temperature at any specified heating rate, the numerical solution of Equation IV-8 with its non-linear boundary conditions will give the heating history of the sample subjected to an ignition test. Criteria for ignition have yet to be established before the ignition time can be predicted. In this study, the criterion for ignition has been set as follows: Ignition is assumed to occur at the temperature at which the maximum rate of weight loss occurs.

In order to estimate the peak temperature where maximum rate of weight loss occurs, it is necessary to back calculate the weight loss curve using the TG parameters obtained for the wood sample. To accomplish this Equation III-2 is given in integral form.

$$- \frac{1}{W_o - W_f} \int_{W_o}^{W} \frac{dW}{[(W-W_f)/(W_o-W_f)]^n} = A \int_{T_o}^{T} e^{-E/RT}\, dt \qquad \text{(IV-20)}$$

The temperature is given by

$$T = T_o + \beta t \qquad \text{(IV-21)}$$

where T_o is the initial temperature and β is the heating rate

$$\beta = dT/dt \qquad \text{(IV-22)}$$

Substituting Equation IV-22 into IV-20 gives

$$\frac{-1}{W_o - W_f} \int_{W_o}^{W_f} \frac{dW}{[(W-W_f)/(W_o-W_f)]^n} = \frac{A}{\beta} \int_{T_o}^{T} e^{-E/RT}\, dT \qquad \text{(IV-23)}$$

Integrating the left side of Equation IV-23 for $n \neq 1$

$$(1-n)\left[1 - \left(\frac{W - W_f}{W_o - W_f}\right)^{1-n}\right] = \frac{A}{\beta} \int_{T_o}^{T} e^{-E/RT}\, dT \qquad \text{(IV-24)}$$

For any specified heating rate, the weight loss curve can be obtained by numerical computation of the above equation. Knowing the weight loss as a function of temperature, the rate of weight loss may be calculated. Thus plots of peak temperature against heating rate can be made. These plots are shown in Figure IV-5. The mathematical model then computes the time required for the irradiated surface to reach the peak temperature corresponding to the heating rate under question.

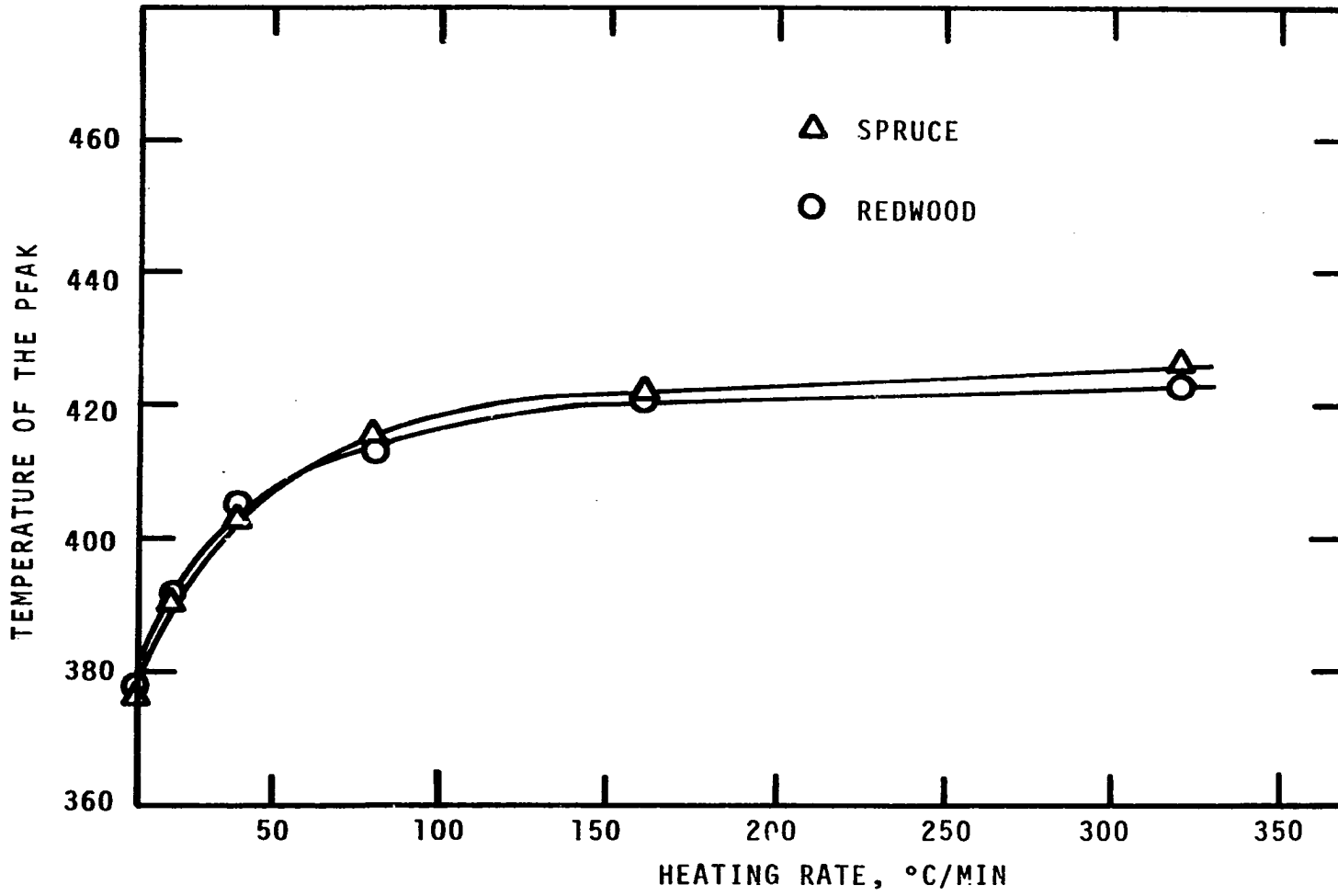

Figure IV-5. Relation Between T_{peak} and Heating Rate for Spruce and Redwood.

CHAPTER V

DISCUSSION OF RESULTS

The mathematical model developed in Chapter IV is exact for very small samples where temperature and density are uniform throughout the sample. The DSC and TG measurements in Chapter III were made on very small sawdust samples to satisfy the criteria by minimizing sample geometry and heat transfer effects on the experimental data. Thus, the experimental results should represent the physical and thermal properties of the woods studied.

The energy capacity data shown in Figures III-24 through III-29 provide the basis for heating rates other than 20°C/min. For ignition tests, surface heating rates as high as 1500°C/min are not uncommon. The energy capacity data at such high heating rates are not available from any experimental study. Brown (7) has extended the energy capacity curve obtained at 20°C/min as a reference and applied a temperature correction to those data to define the energy capacity data at other heating rates. Because of the difficulty of reproducing isothermal heat loss for higher heating rates than 20°C/min the extension is indispensable for mathematical modeling.

However, deliberate efforts have made it possible in this study to measure energy capacity at heating rates of 40°C/min and 80°C/min with reproducible isothermal heat losses. These data can then be extrapolated to the higher heating rates required for ignition modeling.

The basis for extending thermal energy capacity data obtained at 20°C/min, 40°C/min and 80°C/min to any specified heating rate is dependent on demonstrating the effect of heating rate on the chemistry of wood pyrolysis. It has been shown in the TG data of this study that the overall chemistry of wood pyrolysis is independent of heating rate over the range of heating rates studied. An examination of Figures IV-3 and IV-4 shows that the energy required to raise the temperature where the wood is totally charred is the same regardless of the path by which the heating was accomplished. This observation further supports the supposition that the energy of wood pyrolysis is independent of heating rate. The shift of the DSC curves to higher temperature with increased heating rate shows consistency relative to the DTG curves. The effect of an increasing heating rate on the TG curves has been explained in Chapter III. Thus, the extrapolated energy capacity data at any heating rate can be incorporated into the mathematical model.

The energy capacity data shown in Figures IV-3 and IV-4 provide a complete accounting for the energy required to heat spruce and redwood sawdust from 25°C to 450°C. Both

sensible and decomposition heat effects are included in the data. The relation between total energy and temperature are needed to solve the mathematical analogs described in Chapter IV.

The predicted results are obtained by incorporating the microanalytical data, DSC, TG and DTG into the mathematical model. Typical surface temperature histories of the pyrolyzing wood for each set of input conditions are shown in Figures V-1 and V-2 for spruce and redwood, respectively.

The relation between T_{peak} (the temperature at which rate of weight loss is maximum) against heating rate was shown in Figure IV-5 for spruce and redwood. The prediction of T_{peak} versus heating rate was based on the TG parameters analytically obtained from the experimental data in Chapter III. Goldfarb's (15) technique was used for obtaining these parameters. It has been shown by Brown (7) that Goldfarb's analysis is successful in modeling the weight loss kinetics of woods. Table V-1 shows some peak temperatures and heating rates calculated using the parameters given in Table III-2.

It is assumed that surface temperature at ignition is the temperature at which the maximum weight loss rate occurs. Thus, ignition time can be obtained from the T_{peak} versus heating rate plot and $T_{surface}$ versus time plot.

Figures V-1 and V-2 both show the non-linear rate of surface temperature rise for ignition tests. This nonlinearity is because of the non-linear rate of heat loss from the surface

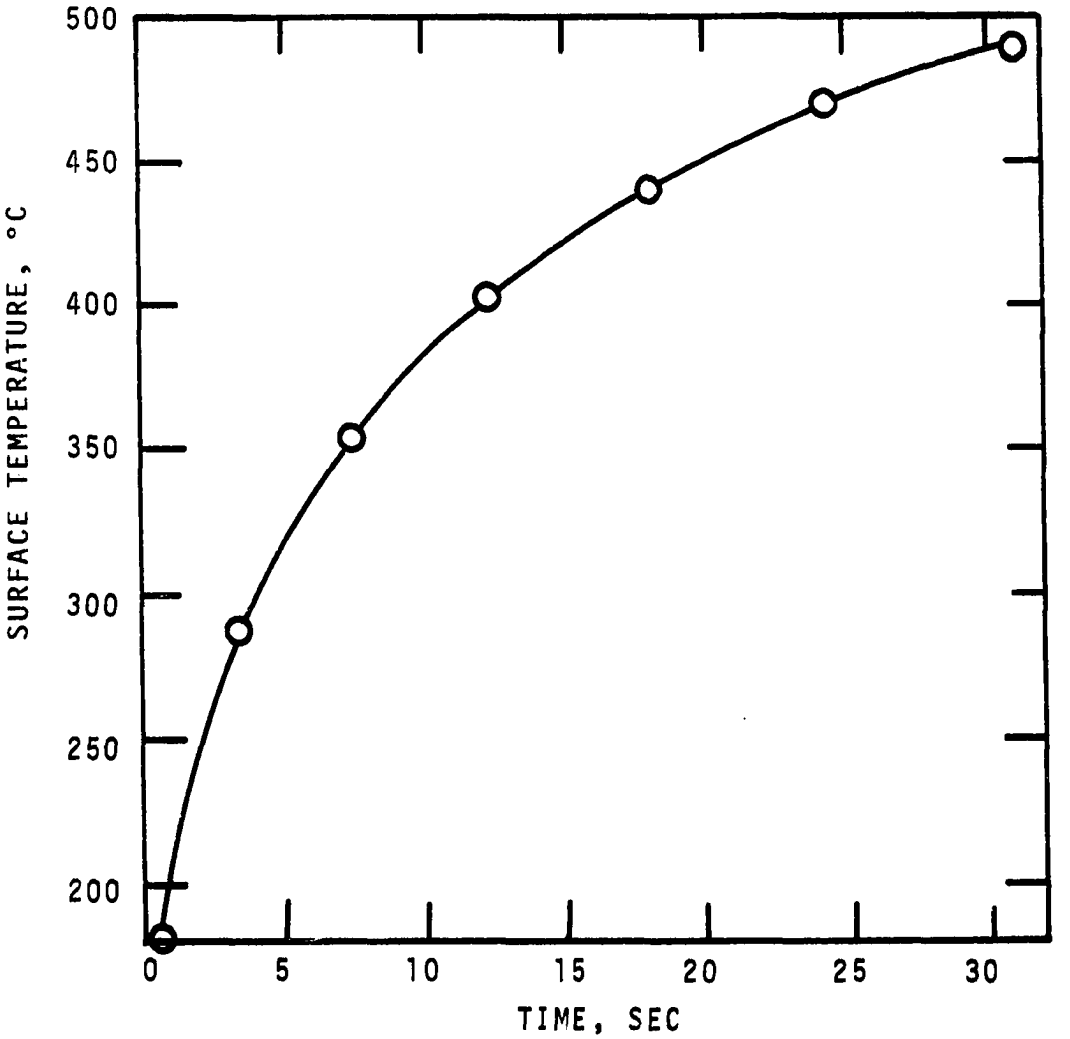

Figure V-1. Surface Temperature History of Spruce at H_i = 1.08 cal/cm^2-sec.

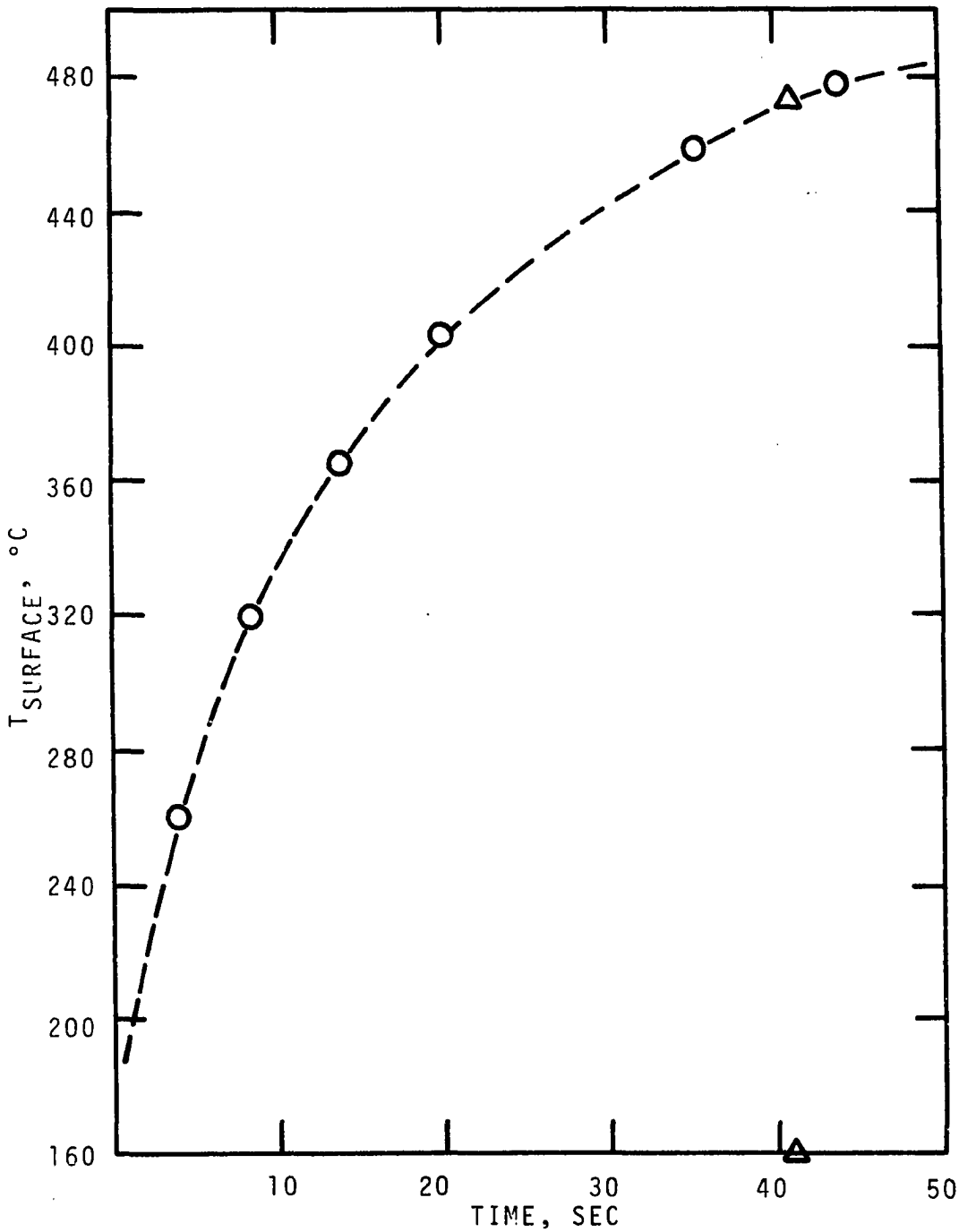

Figure V-2. Surface Temperature History of Redwood at H_i = 0.88 cal/cm^2-sec.

TABLE V-1

T_{peak} VS HEATING RATE FOR SPRUCE AND REDWOOD

Sample	Heating Rate °C/min	T_{peak}, °C
Spruce	1028.0	475.5
	1781.0	482.0
	2196.0	486.6
Redwood	1017.0	473.0
	2243.0	494.0
	2705.0	497.5

which describes most ignition tests using wood samples. The ignition temperature rises as the heating rate rises because T_{peak} rises. Table V-1 shows that ignition occurs over some temperature range for the various heating conditions, not at a fixed surface temperature as postulated by prior investigators (33). Koohyar (22) has reported that ignition does not occur at a fixed surface temperature. Welker (44) refers to ignition as the appearance of a flame in the volatile gas stream evolved from a material undergoing pyrolysis. At the maximum rate of weight loss, the pyrolyzing wood has been heated to such a point that both the temperature and amount of evolved volatiles near the surface of the solid are high enough for ignition to occur. Bamford, et al. (4) reported a minimum rate of weight loss as a criterion for ignition and burning based partly on a mathematical analysis. Koohyar (21) reported rates of evolution of volatiles from wood samples at

the time of ignition may be less than that proposed by Bamford, et al., but could not specify an absolute minimum rate from his experimental data.

Figures V-3 and V-4 show the ignition time predicted by the mathematical model versus heating rate for spruce and redwood, respectively. Plots are made on logarithmic coordinates. A linear relation between ignition time and heating rate is obtained. Wesson's (45) and Vyas' (42) correlations of ignition data suggested a linear relation between ignition time and heating rate when plotted on logarithmic coordinates. For the objective of comparison, data predicted in the present study and data obtained experimentally by Wesson are plotted on the same figure. An examination of Figures V-3 and V-4 shows that the agreement between measured and predicted ignition times is very good. At worst, the predicted ignition times are 10 percent high. This situation happens at incident irradiance greater than 2 cal/cm^2-sec. The reason for this may be due to the lower average absorptance used for higher incident irradiance. At higher heating rate the surface characteristics of the wood sample change rapidly with time; for instance, the surface becomes blackened faster than that subjected to lower heating rates. Thus the average absorptance values should be higher as reported by Wesson (45). If this factor is considered, more energy is absorbed as compared to that using a lower average absorptance. For incident irradiance lower than 2 cal/cm^2-sec, an average absorptance factor of 0.82 was used for both spruce and redwood.

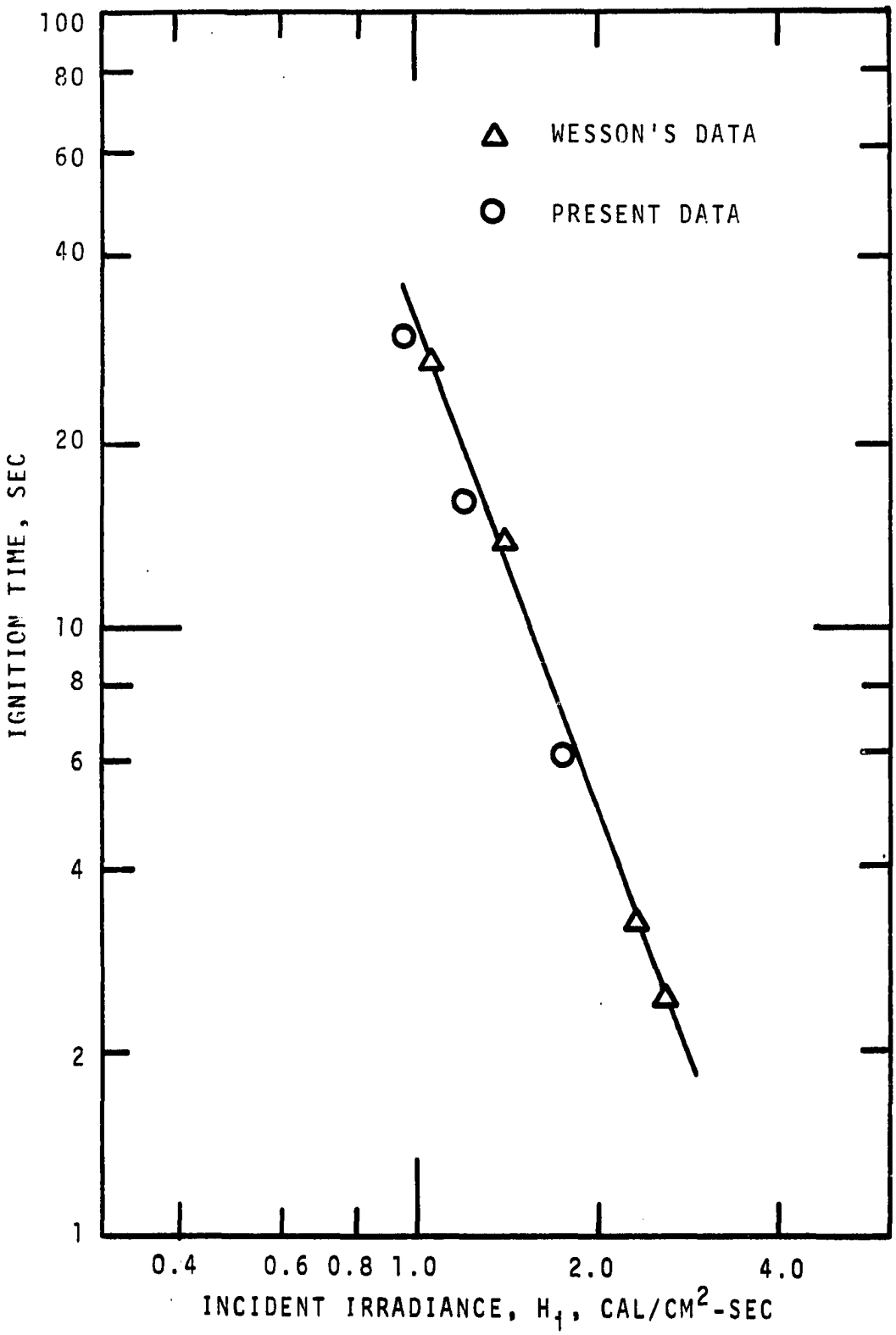

Figure V-3. Ignition Time of Spruce versus Incident Irradiance.

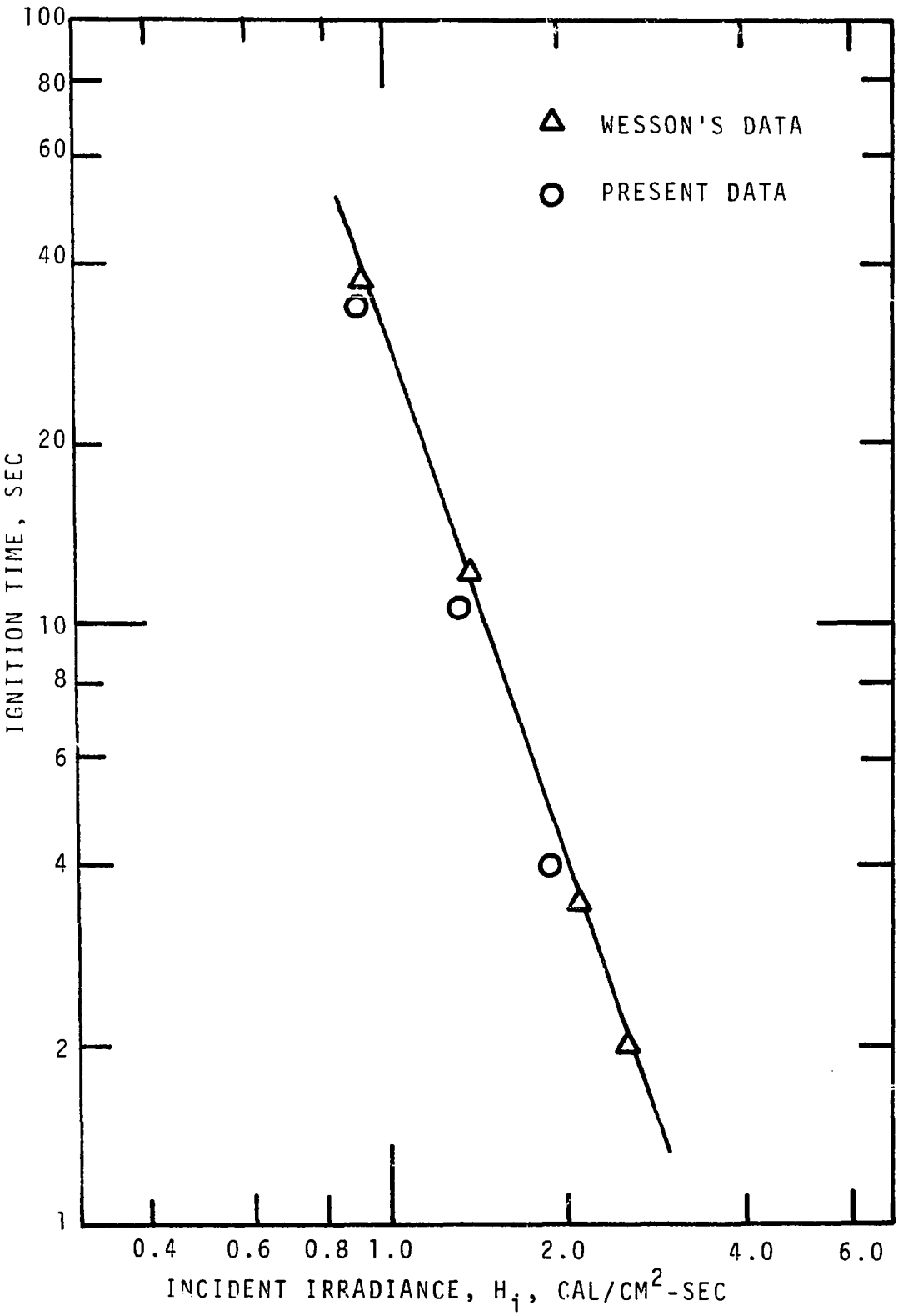

Figure V-4. Ignition Time of Redwood versus Incident Irradiance.

CHAPTER VI

CONCLUSIONS

The thermal degradation kinetics of spruce and redwood, as revealed by weight and energy changes during pyrolysis, were studied using thermogravimetric analysis and differential scanning calorimetry. The weight loss data fit an Arrhenius kinetic expression, and the kinetic parameters for the Arrhenius equation adequately model the effect of heating rate on the rate of decomposition. The kinetic parameters can then be used to extend the weight loss data to higher heating rates where physical measurements cannot be made directly. The thermal properties can likewise be extrapolated based on the measured values at experimental heating rates.

Once the thermal and decomposition parameters are extrapolated to higher heating rates, the ignition time can be predicted for wood samples through a heat transfer model and the assumption of an ignition criterion. Comparison of calculated and measured ignition times showed close agreement.

BIBLIOGRAPHY

1. Akita, K. "Studies on the Mechanism of Ignition of Wood." Fire Research Abs. and Rev., 4, 109 (1962).

2. Alvares, N. J. "Measurement of the Temperature of the Thermally Irradiated Surface of Alpha Cellulose." USNRDL-TR-735 (1964).

3. Alvares, N. J.; Blackshear, P. L.; and Kanury, A. M. "The Influence of Free Convection on the Ignition of Vertical Cellulosic Panels by Thermal Radiation." Comb. Sci. and Tech., 1, 407 (1970).

4. Bamford, C. H.; Crank, J.; and Malan, D. H. "The Combustion of Wood--Part I." Proc. of Cambridge Philos. Soc., 42, 166 (1946).

5. Broido, A. "Thermogravimetric and Differential Thermal Analysis of Potassium Bicarbonate Contaminated Cellulose." WSCI Paper No. 66-20, Western States Section, Spring Meeting, Combustion Institute (April, 1966).

6. Brown, C. R. "Determination of the Ignition Temperatures of Solid Materials." Fuel, 14, 14 (1935).

7. Brown, L. E. "An Experimental and Analytic Study of Wood Pyrolysis." Ph.D. dissertation. University of Oklahoma, Norman, Oklahoma, 1972.

8. Buschman, A. J., Jr. "Ignition of Some Woods Exposed to Low Level Thermal Radiation." NBS Project No. 1002-11-10427, Tech. Report No. 1 (1961).

9. Butler, C. P.; Martin, S. B.; and Lai, W. "Thermal Radiation Damage to Cellulosic Materials--Part II--Ignition of Alpha Cellulose by Square Wave Exposure." U.S. Naval Radiological Defense Lab., Tech. Report USNRDL-TR-135, NS-081-001, AFSWP-906 (1956).

10. Carslaw, H. S., and Jaeger, J. C. Conduction of Heat in Solids. 2nd ed. London: Oxford University Press, 1959.

11. Deverall, L. I., and Lai, W. "A Criterion for Thermal Ignition of Cellulosic Materials." Comb. and Flame, 13, 8 (1969).

12. Duvvuri, M. S. "Ignition Characteristics of Wet Wood by Thermal Radiation." M.S. thesis. University of Oklahoma, Norman, Oklahoma, 1970.

13. Freeman, E. S., and Carroll, B. "The Application of Thermoanalytical Techniques to Reaction Kinetics." J. of Physical Chemistry, 62, 394 (1958).

14. Fons, W. L. "Heating and Ignition of Small Wood Cylinders." Ind. & Eng. Chem., 42, 2130 (1950).

15. Goldfarb, I. J.; McGuchan, R.; and Meeks, A. C. "Kinetic Analysis of Thermogravimetry. Part II. Programmed Temperature." Air Force Materials Laboratory, Wright-Patterson Air Force Base, Ohio, AFML-TR-68-181, Part #2 (1968).

16. Hallman, J. R. "Ignition Characteristics of Plastics and Rubber." Ph.D. dissertation. University of Oklahoma, Norman, Oklahoma, 1971.

17. Hashemi, H. T. "Heat Conduction with Phase Change." Ph.D. dissertation. University of Oklahoma, Norman, Oklahoma, 1965.

18. Havens, J. A. "Thermal Decomposition of Wood." Ph.D. dissertation. University of Oklahoma, Norman, Oklahoma, 1969.

19. Heinrich, H. J., and Kaesche-Krischer, B. "Contributions to the Explanation of Self-Ignition of Wood." Brennstoft Chemie, 43, 5, 142-148 (1962).

20. Kanury, A. M. "Ignition of Cellulosic Solids--A Review." Tech. Report, FMRC Serial No. 19721-7, November 1971.

21. Koohyar, A. N.; Welker, J. R.; and Sliepcevich, C. M. "The Irradiation and Ignition of Wood by Flame." Fire Technology, 4, 284 (1968).

22. Koohyar, A. N. "Ignition of Wood by Flame Radiation." Ph.D. dissertation. University of Oklahoma, Norman, Oklahoma, 1967.

23. Lawson, D. I., and Simms, D. L. "The Ignition of Wood by Radiation." Brit. J. Appl. Phys., 3, 288 (1952).

24. Lee, B. T.; and Alvares, J. J. "The Effect of Irradiance on the Ignition and Rate of Fire Spread Along Composite Cellulosic Materials." Spring meeting, Western States Section, The Combustion Institute, La Jolla, Calif., April 1967.

25. Martin, S. B. "The Mechanism of Ignition of Cellulosic Materials by Intense Thermal Radiation." USNRDL-TR-102, NS-081-001, AFSWP-779 (1956).

26. Martin, S. B. "Diffusion Controlled Ignition of Cellulosic Materials by Intense Radiant Energy." Tenth Symposium (International) on Combustion, 877 (1965).

27. Muir, W. E. "Studies of Fire Spread Between Buildings." Ph.D. dissertation. University of Saskatchwan (1967).

28. Ryan, L. R.; Penzias, G. J.; and Tourin, R. H. "An Atlas of Infrared Spectra of Flames. Part I. Infrared Spectra of Hydrocarbon Flames in the 1-5μ Region." Scientific Report No. 1, Contract AF 19(604)-6106, July 1961.

29. Roberts, A. F., and Clough, G. "Thermal Decomposition of Wood in an Inert Atmosphere." Ninth Symposium (International) on Combustion. New York: Academic Press, 1963

30. Simms, D. L. "Damage to Cellulosic Solids by Thermal Radiation." Comb. and Flame, 6, 303 (1962).

31. Simms, D. L. "The Correlation of Ignition Time with the Physical Properties of Materials." Fire Research Note No. 319 (1958).

32. Simms, D. L. "Ignition of Cellulosic Materials by Radiation." Comb. and Flame, 4, 293 (1960).

33. Simms, D. L. "On the Piloted Ignition of Wood by Radiation." Comb. and Flame, 7, 253 (1963).

34. Simms, D. L. "Ignition of Cellulosic Materials by Radiation." Comb. and Flame, 4, 293 (1960).

35. Smith, W. K. "Ignition of Materials by Radiant Heat." Naval Weapons Center Tech. Note 40604-8 (1968).

36. Smith, W. K. "Ignition of Materials by Radiant Heat." Technical Note 40604-8, Naval Weapons Center, China Lake, California (1968).

37. Smith, W. K., and Schilberg, L. E. "Surface Temperature History of Materials During Radiant Heating to Ignition." Tech. Note 40604-9, Naval Weapons Center, China Lake, California (20 June 1969).

38. Tang, W. K. "Study of the Effect of Chemical Treatment on the Thermal Decomposition of Wood." Forest Products Laboratory Report, 1960.

39. Thomas, P. H.; Simms, D. L.; and Law, M. "The Effects of Moisture Content on the Spontaneous Ignition of Wood by Radiation." Fire Research Note No. 280, Joint Fire Research Organisation, England (1956).

40. Varga, R. S. Matrix Iterative Analysis. Englewood Cliffs, N.J.: Prentice-Hall, 1962.

41. Varma, A., and Steward, F. R. "Spontaneous Ignition of High Voidage Cellulosic Materials." J. Fire and Flammability, 1, 154 (1970).

42. Vyas, R. J. "End-Grain Piloted Ignition of Wood by Flame Radiation." M.S. thesis. University of Oklahoma, Norman, Oklahoma, 1973.

43. Welker, J. R.; Wesson, J. R.; and Sliepcevich, C. M. "Ignition of Alpha-Cellulose and Cotton Fabric by Flame Radiation."" Fire Technology, 5, 59 (1969).

44. Welker, J. R. "The Pyrolysis and Ignition of Cellulosic Materials: A Literature Review." J. Fire and Flammability, 1, 12 (1970).

45. Wesson, H. R. "The Piloted Ignition of Wood by Radiant Heat." D.Engr. dissertation. University of Oklahoma, Norman, Oklahoma, 1970.

46. Woodard, W. M. "Thermal Decomposition of Synthetic Polymers." Ph.D. dissertation. University of Oklahoma, Norman, Oklahoma, 1973.